



# EUROPEAN SOUTHERN OBSERVATORY

Organisation Européenne pour des Recherches Astronomiques dans l'Hémisphère Austral  
Europäische Organisation für astronomische Forschung in der südlichen Hemisphäre

ESO - European Southern Observatory  
Karl-Schwarzschild Str. 2, D-85748 Garching bei München

---

## Very Large Telescope Paranal Science Operations VISIR User Manual

Doc. No. VLT-MAN-ESO-14300-3514

Issue 102.1, Date 01/07/2018

W.J. de Wit & the VISIR IOT

Prepared .....  
Date Signature

S. Mieske

Approved .....  
Date Signature

A. Kaufer

Released .....  
Date Signature

This page was intentionally left blank

**Change Record**

Issue/ Rev.	Date	Section/Parag. affected	Reason/Initiation/Documents/Remarks
v1.0	04/09/04	creation	First release for science verification in P74 and OT proposals in P75.
v1.1	10/12/04	2.4, 3.2, 6.2, 6.3, 7, 8	update for P75 Phase2
v76.1	01/02/05	all	update for P76 CfP
v76.2	06/07/05	all	update for P76 Phase 2
v76.3	14/07/05	4.8.1	Corrected Legend Fig 17
v76.4	14/07/05	Cover pages	Corrected typos
v77.1	04/09/05	3.5-7,4.1,4.3,4.8.1,7,8.1,10	update for P77 CfP
v77.2	05/09/05	4.6	match imager overhead of CfP
v77.3	20/12/05	1,2,3.4,3.6,4.2-4.4,4.7,7,8	update for P77 Phase2
v78.1	27/02/06	3.6, 3.10	update for P78 CfP
v78	19/06/06	cover, 2.2, 3.2, 4.3.1	P78 release
v79	30/11/06	4.8	P79 release
v80	28/02/07	3.1, 4.2.1, 5.1, 6.2, 8.2	P80 release, burst mode included
v81	31/08/07	3.1, 4.2.1, 4.3.2	P81 release, new filters included
v87	22/09/10	4.3.2, 8.2, 8.3	P87 release, Exclusion of <i>K</i> -band in science imaging templates
		3.2.5	P87 release, update of HR allowed $\lambda_c$
		8.2	P87 release, non-availability of <i>jitter</i> with <i>IMG – GenericChopNod</i>
v88	22/02/11	4.1	P88 release, upper limit of 5 filters in a single service mode OB
		4.4	P88 release, UCAC3 substituting USNO for guide stars selections.
v89	31/08/11	all	P89 release, removing most references to the old DRS detector, and reporting the first properties of AQUARIUS detector.
v90	26/02/12	1	Update new schedule of VISIR upgrade.
v90	17/08/12	all	New updates after the commissioning#1.
v95.1	27/08/14	all	P95 release, updates after 07/2014 tests.
v95.2	01/02/15	all	Release for P95 phase 2
v96.1	28/02/15	all	Release for P96 phase 1
v96.2	04/07/15	all	Release for P96 phase 2
v97.1	26/08/15	3.5	Release for P97 phase 1
v97.2	20/12/15	3.5, 4.2	Release for P97 phase 2, sensitivities updated
v98.1	01/03/16	all	Release for P98 phase 1, SAM & burst mode
v99.1	01/09/16	all	Release for P99 phase 1, multiple changes.
v101.0	01/12/17	all	Release for P101 phase 2
v102.0	01/03/18	3.1, 4.1	Release for P102 phase 1
v102.1	04/07/18		Release for P102 phase 2, removed P2PP references

v1.0, v1.1, v76.1: edited by R. Siebenmorgen, E. Pantin, M. Sterzik

v76.2 – 4, v77.1 – 3, updated by A. Smette.

v78 – 80, updated by L. Vanzi.

v87 – 90, updated by Y. Momany.

v95.1 updated by Y. Momany, V.D. Ivanov, et al.

v95.2-100.0, updated by K. Tristram, et al.

v101.0 and onwards, updated by W.J. de Wit, et al.

# Contents

<b>1</b>	<b>Introduction</b>	<b>1</b>
<b>2</b>	<b>Observing in the mid-infrared from the ground</b>	<b>1</b>
2.1	The Earth's Atmosphere . . . . .	1
2.2	Precipitable Water Vapour . . . . .	2
2.3	Spatial Resolution . . . . .	3
2.4	MIR background . . . . .	3
2.5	Chopping and nodding . . . . .	5
2.6	Sensitivity . . . . .	5
2.6.1	Imaging . . . . .	5
2.6.2	Spectroscopy . . . . .	7
<b>3</b>	<b>Instrument description and offered observing modes</b>	<b>9</b>
3.1	Imager . . . . .	9
3.1.1	Regular imaging . . . . .	9
3.1.2	Burst mode . . . . .	10
3.1.3	Coronagraphy . . . . .	10
3.1.4	Sparse Aperture Masking . . . . .	12
3.2	Spectrometer . . . . .	12
3.2.1	Description . . . . .	12
3.2.2	Offered spectroscopic modes . . . . .	14
3.3	Calibration unit . . . . .	16
3.4	Detectors . . . . .	16
3.4.1	Detector Architecture . . . . .	17
3.4.2	Detector Readout . . . . .	17
3.4.3	Detector Dark Current . . . . .	18
3.4.4	Excess Low frequency Noise . . . . .	18
3.4.5	Detector Linearity . . . . .	18
3.4.6	Detector Cosmetics . . . . .	19
3.5	Data acquisition system . . . . .	19
<b>4</b>	<b>Observing with VISIR at the VLT</b>	<b>22</b>
4.1	Tools for the preparation of proposals and observations . . . . .	22
4.2	Observing Parameters . . . . .	23
4.2.1	Instrument orientation on the sky . . . . .	23
4.2.2	Chopping parameters . . . . .	25
4.2.3	Nodding parameters . . . . .	25
4.3	Target acquisition . . . . .	26
4.3.1	Introduction . . . . .	26
4.3.2	Acquisition Templates . . . . .	26

4.4	Guide stars	29
4.5	Brightness Limitations	30
4.6	Overheads	30
4.7	Calibration Observations	30
4.8	Observing constraints and OB Classification	32
<b>5</b>	<b>VISIR data</b>	<b>33</b>
5.1	Data format and orientation	33
5.2	Pipeline	34
5.3	Spectrometer data	35
<b>6</b>	<b>Description of VISIR templates</b>	<b>37</b>
6.1	Acquisition	37
6.2	Observing with the imager	37
6.3	Observing with the spectrometer	39
6.4	Calibration	40
<b>7</b>	<b>Checklist</b>	<b>41</b>
7.1	Phase 1	41
7.2	Phase 2	41
<b>8</b>	<b>Appendix: VISIR template parameters</b>	<b>43</b>
<b>9</b>	<b>Appendix: Filter transmission curves</b>	<b>64</b>
<b>10</b>	<b>Appendix: Sensitivities in various spectroscopic settings</b>	<b>67</b>

## List of acronyms

AGPM	Annular Groove Phase Mask
BIB	Blocked impurity band
BLIP	Background limited performance
BOB	Broker of observation blocks
DIT	Detector integration time
ETC	Exposure time calculator
FWHM	Full width at half maximum
ICS	Instrument control software
IR	Infrared
IRACE	InfraRed Array Control Electronics
MIR	Mid infrared
NGC	New General detector Controller
OB	Observing block
PAE	Preliminary acceptance in Europe
pfov	pixel field of view
PSF	Point spread function
PWV	Precipitable Water Vapor
SAM	Sparse Aperture Masking
S/N	Signal-to-noise ratio
TCS	Telescope control system
TMA	Three mirrors anastigmatic
UT	Unit Telescope
VISIR	VLT imager and spectrometer for the mid infrared
WCU	Warm calibration unit

# 1 Introduction

The VLT spectrometer and imager for the mid-infrared (VISIR), built by CEA/DAPNIA/SAP and NFRA/ASTRON, aims to provide diffraction-limited imaging at high sensitivity in three mid-infrared (MIR) atmospheric windows: the M-band at  $5\ \mu\text{m}$ , the N-band between 8 and  $13\ \mu\text{m}$  and the Q-band between 17 and  $20\ \mu\text{m}$ . In addition, it offers a slit spectrometer with a range of spectral resolutions between 150 and 30 000.

The MIR provides invaluable information about warm dust and gas in the Universe. Micron sized particles such as silicates, silicon carbide, carbon, coals, aluminum oxides or polycyclic aromatic hydrocarbon (PAH) molecules are major contributors to the thermal MIR emission. The gaseous phase emits through a large number of ionic and atomic lines. Examples are NeII ( $12.8\ \mu\text{m}$ ) and the rotational transitions of molecular hydrogen at 8.02, 9.66, 12.27 and  $17.03\ \mu\text{m}$ .

Because of the very high background emission from the ambient atmosphere and telescope, the sensitivity of ground-based MIR instruments cannot compete with that of space-born ones. However, ground based instruments mounted on large telescopes offer superior spatial resolution. For example VISIR at the VLT provides diffraction limited images at  $\sim 0''.3$  (FWHM) in the N-band. In comparison, this is an order of magnitude higher than what could be reached by the Spitzer Space Telescope (SST).

This VISIR user manual is structured as follows: Basic observing techniques of ground-based MIR instruments are summarized in § 2. § 3 provides a technical description of VISIR and its offered observing modes. An overview on how to observe with VISIR at the VLT can be found in § 4. A description of the structure of the imaging and spectroscopic data files is given in § 5. A checklist to help the preparation of OBs is available in § 7. Acquisition, observing and calibration templates are explained in § 6.

We strongly recommend to consult <http://www.eso.org/instruments/visir/> for additional information and updates. For support during proposal preparation and OB submission, please contact ESO's User Support Department at [usd-help@eso.org](mailto:usd-help@eso.org).

## 2 Observing in the mid-infrared from the ground

### 2.1 The Earth's Atmosphere

Our atmosphere absorbs the majority of the MIR radiation from astronomical sources. The main absorbing molecules are  $\text{H}_2\text{O}$ ,  $\text{CH}_4$ ,  $\text{CO}_2$ ,  $\text{CO}$ ,  $\text{O}_2$ ,  $\text{O}_3$ . However, the atmosphere is quite transparent for mid-IR radiation in the so-called M, N, and Q atmospheric windows. These windows are centered on roughly 5, 10 and  $19.0\ \mu\text{m}$ , respectively. The transmission in the N-band is fairly good at a dry site and becomes close-to transparent in the wavelength range between 10.5 and  $12.0\ \mu\text{m}$ . The transmission in the Q-band decreases rapidly with wavelength and can be viewed as the superposition of many sub-bands having a typical spectral coverage of  $\Delta\lambda = 1\ \mu\text{m}$  at an average transmission of about 60%. Observations in this band require a low atmospheric water vapor content. The atmospheric transmission in the M-, N- and Q-bands is displayed in Fig. 1. A detailed modelling of both atmospheric transmission and emission can be done using ESO's SKYCALC Sky Model Calculator<sup>1</sup>.

---

<sup>1</sup>The SKYCALC Sky Model Calculator can be found at <https://www.eso.org/observing/etc/bin/gen/form?INS.MODE=swspectr+INS.NAME=SKYCALC>.



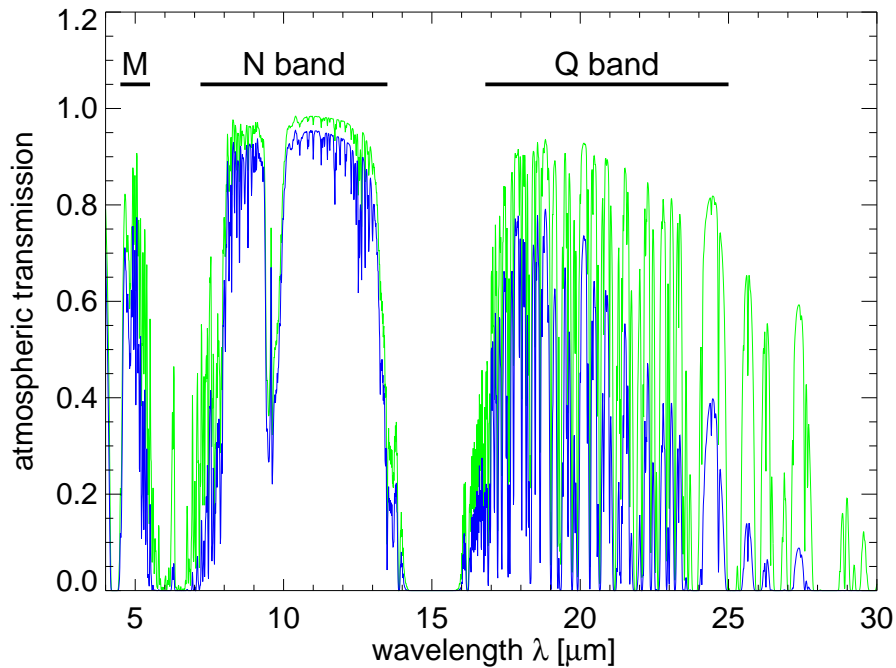


Figure 1: MIR atmospheric transmission at Paranal computed with ATRAN (Lord 1992, NASA Tech. Mem. 103957) for an altitude of 2600 m: in green for 1 mm of precipitable water vapor (PWV) at zenith (airmass = 1); in blue for 3 mm of PWV and airmass = 1.5. The largest changes are in the M- and Q-band and at the edges of the N-band.

## 2.2 Precipitable Water Vapour

The amount of Precipitable Water Vapor (PWV) in the Earth’s atmosphere, usually measured in millimeters, has an impact on the atmospheric transmission in a wavelength dependent way. Whereas a PWV column of 3 mm or larger is still acceptable for performing quality observations in the N-band, Q-band observations must be carried out with PWV columns below the value of 3 mm.

For efficient night-time operations, up-to-date knowledge of the PWV column is a requirement for successful mid-IR observations. Paranal performs real-time PWV monitoring via a RPG L-HATPRO radiometer (in use since the VISIR upgrade project in 2012). The autonomous radiometer provides the following information:

- PWV range 0.5 – 9.0 mm
- PWV precision: ca. 30  $\mu\text{m}$
- PWV accuracy: ca. 0.1 mm
- High time resolution (sec)
- All sky pointing, 2D capability

The median PWV over Paranal is 2.1 mm with strong seasonal variations (see Fig. 2). The fraction of time in which the PWV contents over Paranal is lower than 1 mm is about 10%. For observations conducted in service mode, the PWV value is a user-defined constraint parameter.

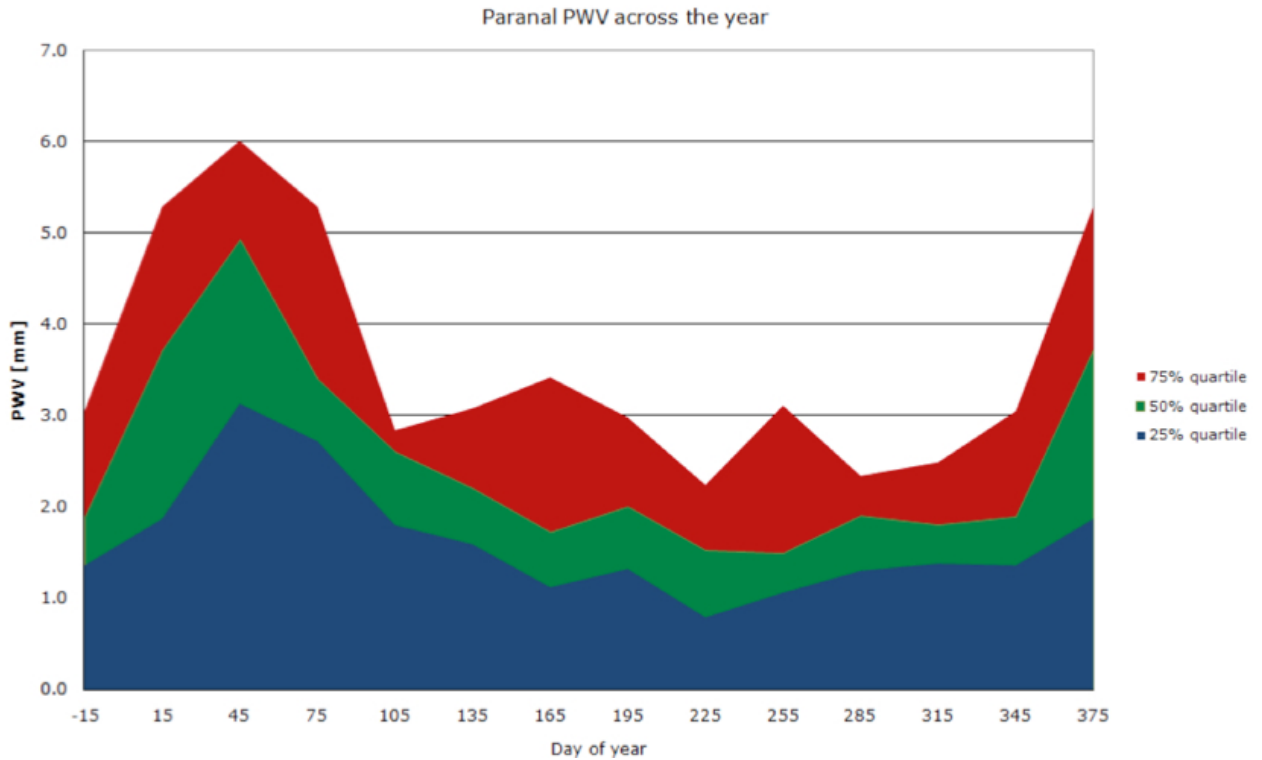


Figure 2: PWV (in mm) over Paranal. The best conditions occur during the southern winter season.

### 2.3 Spatial Resolution

The spatial resolution of an instrument is ultimately limited either by the diffraction of the telescope or the atmospheric seeing. The diffraction limit as measured by the diameter of the first Airy ring increases with wavelength as  $1.22 \lambda/D$ , where  $\lambda$  is the observing wavelength and  $D$  the diameter of the telescope mirror (see solid line in Fig. 3). The wavelength dependence of the seeing can be derived by studying the spatial coherence radius of the atmosphere in the telescope beam and is to first order approximated by the Roddier formula, where the seeing is  $\propto \lambda^{-0.2}$  (see dot-dashed lines in Fig. 3). However, initial results from VISIR data indicate that this formula overestimates the measured MIR seeing at Paranal by 20–50%, as the size of a UT mirror is comparable to the turbulence outer scale. As a result, VISIR data are close to diffraction limited for optical seeing below  $0.6''$ . The results of measurements obtained in 2005 are shown in Fig. 4.

### 2.4 MIR background

The Earth’s atmosphere absorbs the mid-IR photons from astrophysical targets and emits black-body radiation of approximately 253 K (Kirchhoff’s law). Additionally, the telescope itself provides a strong mid-IR background radiation field. The VLT telescopes emit at  $\sim 283$  K with a preliminary emissivity estimate of  $< 15\%$  in the N-band. The VISIR instrument is cooled to avoid internal background contamination. The detectors are at  $\sim 9$  K and the interior of the cryostat at  $\sim 29$  K. The total background radiation at  $10\mu\text{m}$  is typically  $m_N = -5 \text{ mag/arcsec}^2$  ( $3700 \text{ Jy/arcsec}^2$ ) and at  $20\mu\text{m}$   $m_Q = -7.3 \text{ mag/arcsec}^2$  ( $8300 \text{ Jy/arcsec}^2$ ).

Consequently, the number of photons reaching the detector is huge, often more than  $10^8$

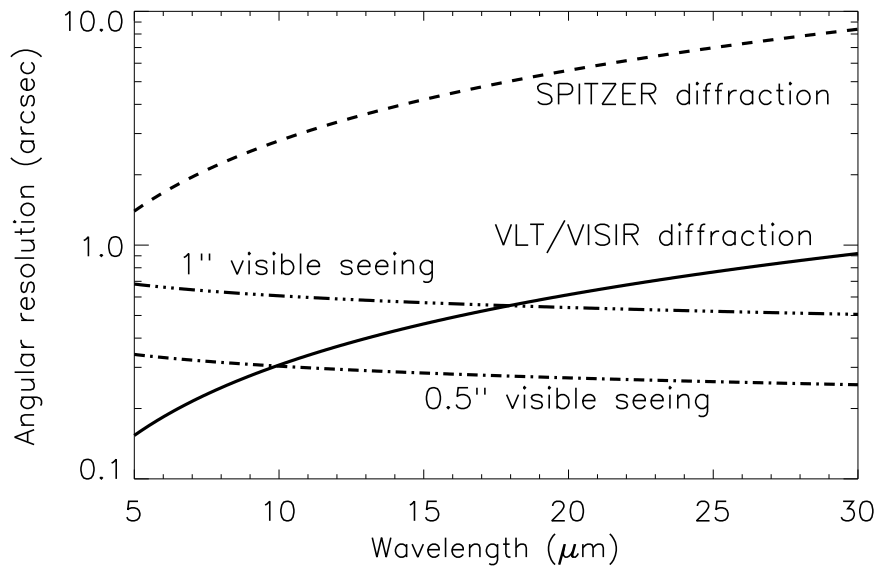


Figure 3: VLT diffraction limit (full line) versus seeing. The Spitzer Space Telescope diffraction limits (dashed) are shown for comparison. The Roddier dependence is shown for two optical seeings (dashed-dot).

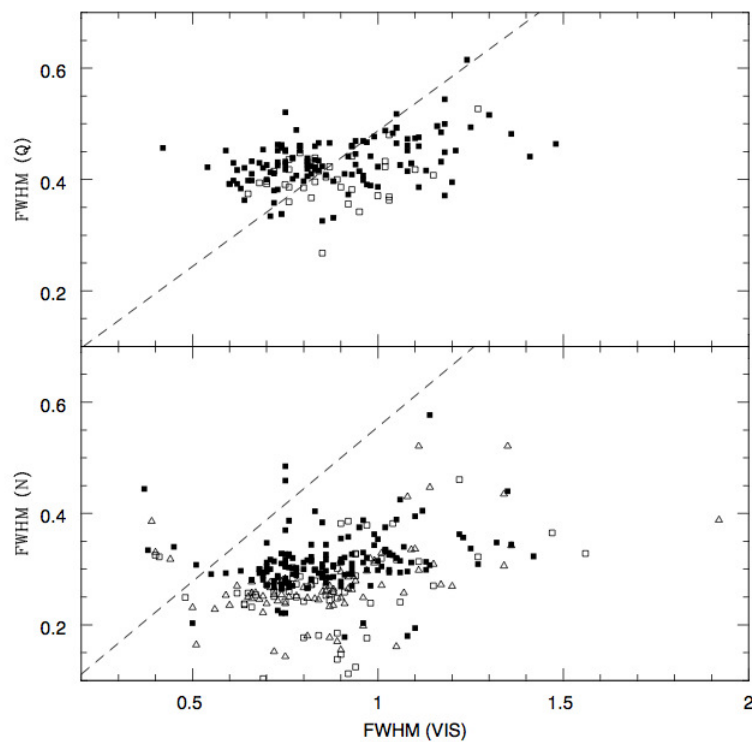


Figure 4: Measures of the VISIR image quality versus optical seeing obtained during 2005. The dashed lines indicates the prediction of Roddier's formula.

photons/s. Therefore, the exposure time of an individual integration – the Detector Integration Time (DIT) – is short, of the order of a few tens of milli-seconds in imaging mode.

## 2.5 Chopping and nodding

The basic idea to suppress the MIR background is to perform differential observations, using the chopping/nodding technique.

In the chopping technique two observations are performed. One set of exposures on–source, include the background and the astronomical source. A second set of off–source exposures measures the pure background. The on– and off–source observations have to be alternated at a rate faster than the rate of the background fluctuations. In practice, this is achieved by moving the secondary mirror of the telescope. As the background fluctuations have typical time-scales of several seconds, chopping frequencies of a fraction of a Hz are sufficient to reduce the background. Additionally, the excess low frequency noise (ELFN) of the AQUARIUS detectors can be reduced effectively by chopping (see § 3.4.4). For this, chopping rates of more than 1 Hz are required. Thus, chopping frequencies between 2 and 4 Hz are used for imaging observations, such that the signal-to-noise within a certain observing time, including chopping overheads, is maximized (see § 3.5). Spectroscopic observations on the other hand can be performed with lower chopper frequencies, at 0.3 Hz or less, as the number of background photons per spectral bin decreases with increasing spectral resolution.

The chopping technique cancels most of the background. However, the optical path is not exactly the same in both chopper positions. Therefore a residual background remains. It is varying at a time-scale which is long compared to that of the sky. This residual is suppressed by nodding, where the telescope itself is moved off–source and the same chopping observations as in the on–source position is repeated.

An illustration of the chopping and nodding technique is shown on Fig. 5. Depending on the choice of chopping and nodding amplitudes and directions, up to 4 images of the source can be seen on the frame and used for scientific analysis. Of course, the *free* field- of- view on the chop/nod images can be severely reduced depending on the particular chopping and nodding parameters chosen.

## 2.6 Sensitivity

### 2.6.1 Imaging

Measurements of VISIR sensitivities are based on observations of mid-infrared calibration standard stars (Cohen et al. 1999, AJ 117, 1864). In imaging mode, the stars are recorded using perpendicular chopping and nodding patterns with throws of  $13''^2$ . Calibrators are frequently observed during the night (§ 4.7). Flux and noise levels are extracted by multi-aperture photometry using the curve-of-growth method: the aperture used for all 4 beams in a given frame is the one for which the flux to noise ratio is the largest. By combining all 4 beams, the sensitivity in a given filter is defined as the limiting flux of a point-source detected with a S/N of 10 in one hour of on–source integration. This does not correspond to the S/N of the peak flux above the background, which depends much stronger on the achieved image quality.

---

<sup>2</sup>With the old DRS detector, standards were also recorded using the intermediate field ( $0.076''$ ) and  $8''$  chopping.

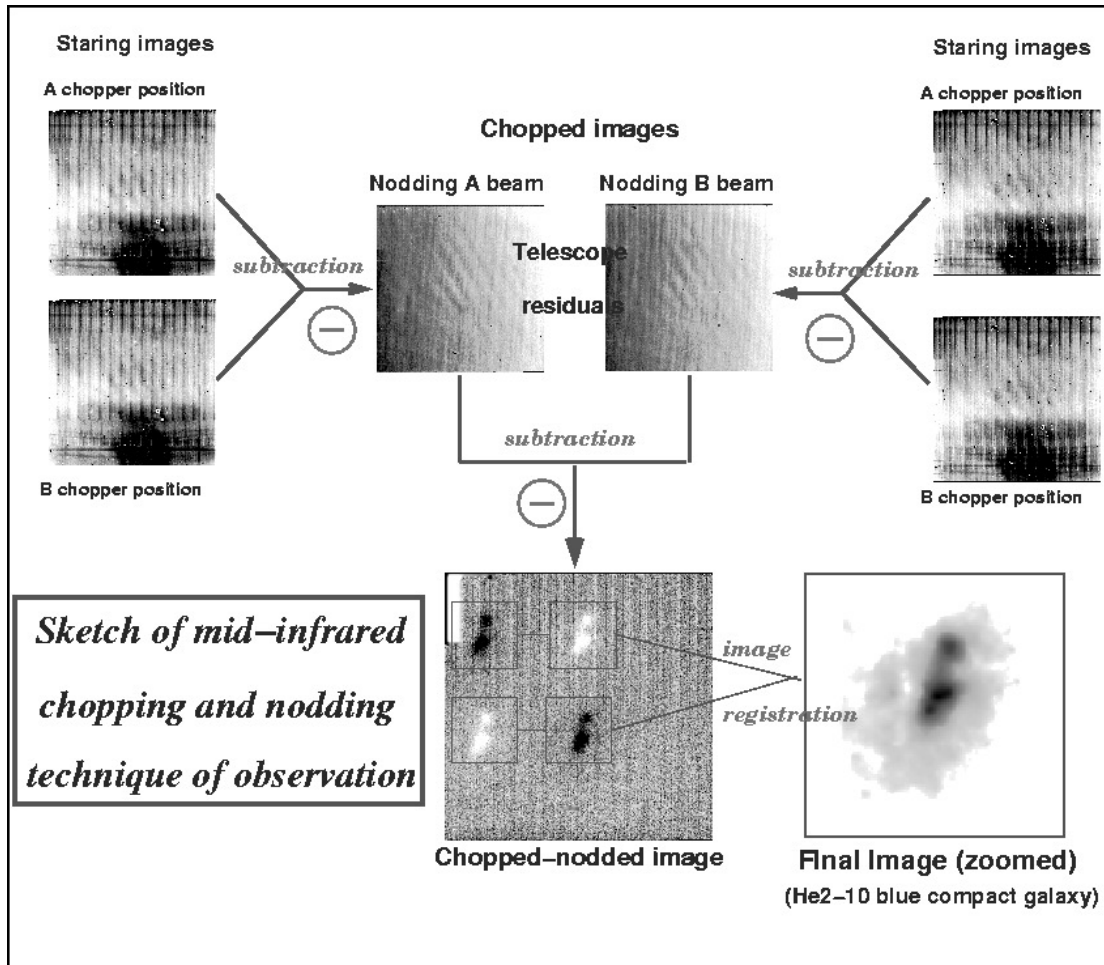


Figure 5: Illustration of the chopping and nodding technique on observations of the blue compact galaxy He2-10. The galaxy only appears after chopping and nodding (courtesy VISIR commissioning team, June 2004).

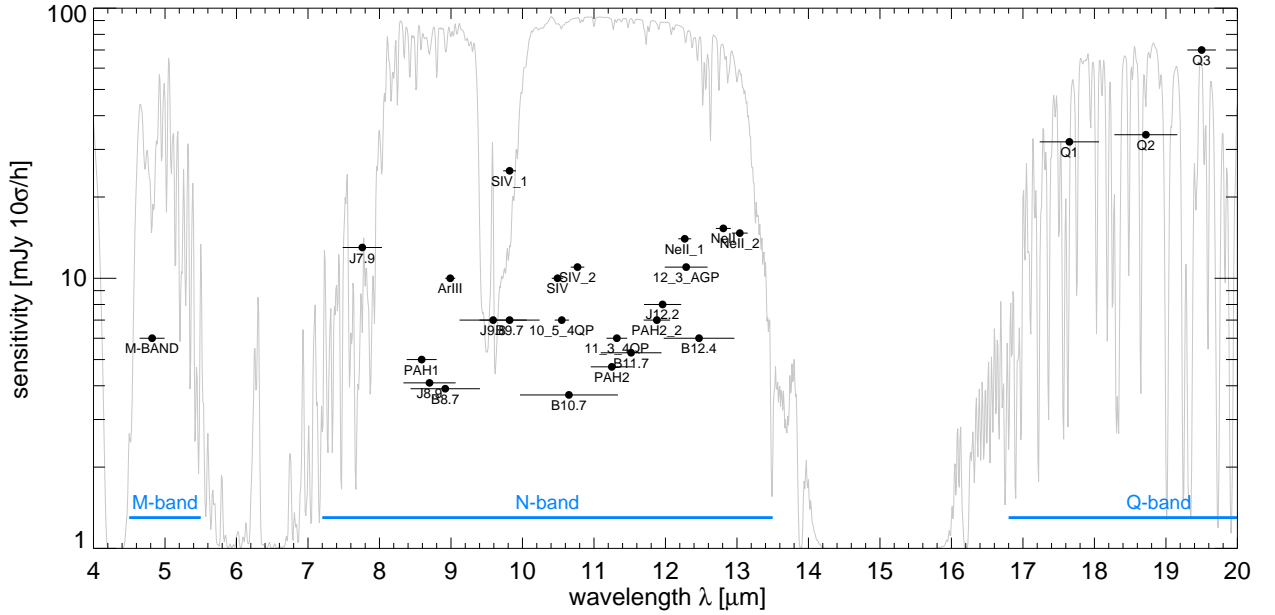


Figure 6: Sensitivities for the VISIR imager in various filters in the M-, N- and Q-bands determined with the new AQUARIUS detector. The atmospheric transparency spectrum for PWV = 1 mm at an airmass of 1 is plotted in the background.

For details see the VISIR Pipeline User Manual<sup>3</sup>. The values of the sensitivity for each filter are given in Table 1 and refer to the median of the observations since the re-commissioning of the instrument. A graphical compilation is presented in Fig. 6.

### 2.6.2 Spectroscopy

Sensitivity estimates for the VISIR spectroscopy observing modes are obtained in a similar way. However, in this case, chopping and nodding are performed in parallel. Consequently, only 3 beams are obtained, with the central one containing twice as much flux as the two other ones. Table 2 lists typical sensitivities measured in high resolution spectroscopy away from strong sky emission lines for the wavelength ranges currently offered for this mode. Figures 20 to 26 in the Appendix (§ 10) show the dependence of sensitivity on wavelength for the high resolution mode using the old DRS detector. As of P101, the HR (and the HRX) mode will use FOWLER read-out scheme as the standard. This has proven to deliver an increase in sensitivity with a factor  $\sim 2$  for negligible overhead increase. The sensitivity values mentioned in table 2 are the updates ones, applicable as of P101.

The median sensitivities are the reference for classification of VISIR service mode observations, and the basis to assess the feasibility of an observing programme. In particular, *classification* of service mode OBs will be based on sensitivity measurements made at zenith. Calibrations will be provided following the guidelines given in § 4.7. For up to date information, please consult the VISIR [public pages](#). The use of the VISIR [exposure time calculator](#) (ETC) is strongly recommended in order to estimate the on-source integration time.

<sup>3</sup>The VISIR Pipeline User Manual is downloadable at <http://www.eso.org/sci/software/pipelines/>

Filter	$\lambda_c$ ( $\mu\text{m}$ )	filter width FWHM ( $\mu\text{m}$ )	max. trans- mission (%)	detector windowing (SF) [px]	detector windowing (IF) [px]	sensitivity (SF), $10\sigma/1\text{h}$ (mJy)		
						theory BLIP	median	effective
M-BAND	4.82	0.35		900	512		6	9
J7.9	7.78	0.55		900	512		13	17
PAH1	8.59	0.42	77	900	900	1.6	5	7
J8.9	8.70	0.73		900	512		4	6
B8.7	8.92	0.97		512	256		4	6
ArIII	8.99	0.14	72	900	900	4.1	10	16
J9.8	9.59	0.94		900	512		7	10
SIV_1	9.82 <sup>1</sup>	0.18	72	900	900	4.0	25	31
B9.7	9.82	0.84		512	256		7	10
SIV	10.49	0.16	70	900	900	4.5	10	14
10.5_4QP <sup>2</sup>	10.55	0.20	87	800	800		7	10
10.5_SAM <sup>3</sup>	10.50			900	900		–	–
B10.7	10.65	1.37		900	512		4	6
SIV_2	10.77 <sup>1</sup>	0.19	70	900	900	4.6	11	14
PAH2	11.25	0.59	75	900	512	2.3	5	7
11.3_4QP <sup>2</sup>	11.32	0.29	87	800	800		6	9
11.3_SAM <sup>3</sup>	11.30			900	900		–	–
B11.7	11.52	0.85		900	512		5	7
PAH2_2	11.88 <sup>1</sup>	0.37	58	900	900	4.1	7	11
J12.2	11.96	0.52		900	512		8	12
NeII.1	12.27 <sup>1</sup>	0.18	51	900	900	6.9	14	18
12.3_AGP <sup>2</sup>	12.29	0.60	90	800	512		11	15
B12.4	12.47	0.99		512	256		6	9
NeII	12.81	0.21	64	900	900	6.1	15	19
NeII.2	13.04	0.22	68	900	900	6.3	15	19
Q1	17.65	0.83	59	512	256	11.1	32	42
Q2	18.72	0.88	49	512	256	13.6	34	45
Q3	19.50	0.40	50	900	512	41.7	70	97

Table 1: Filter characteristics for the VISIR imager, following the manufacturer specifications, except for the central wavelengths noted with <sup>1</sup> which were re-determined with the monochromator of the WCU because they deviate from their original specifications. The last 3 columns give, respectively, the theoretical expectations under BLIP and excellent weather conditions, the median and effective sensitivities obtained in various weather conditions since the re-commissioning of VISIR. The median sensitivities only take into account the pure integration time ( $t_{\text{src}}$ ), while the effective sensitivities include overheads due to chopping and nodding ( $t_{\text{tot}}$ , see § 3.5). The sensitivities were obtained using the curve-of-growth method on data obtained in perpendicular chopping/nodding directions (4 beams). The three coronagraphic filters are marked by <sup>2</sup>. These three filters are the only filters with Lyot stops attached. The filters for Sparse Aperture Masking are marked by <sup>3</sup>. Detector windows in Small and Intermediate Fields are listed (see § 3.1.1).

mode	$\lambda_c$ ( $\mu\text{m}$ )	$\Delta\lambda$ ( $\mu\text{m}$ )	line	order	R	dispersion (pixels/ $\mu\text{m}$ )	sensitivity Jy $10\sigma/1\text{h}$
HR	7.800 – 8.100	<b>0.055</b>	[H2_S4]	17B	32000	17573	$\sim 1.5$
HR	12.738 – 12.882	0.03571	[Ne II]	11A	17000	11908	$\sim 0.4$
HR	16.800 – 17.200	0.05156	[H2_S1]	8B	14000	8250	$< 5$

Table 2: Characteristics of the VISIR high resolution long-slit (HR) mode. The second column gives the minimum and maximum allowed values for the central wavelength ( $\lambda_c$ ) in the given setting. The wavelength range per setting is given in the 3rd column ( $\Delta\lambda$ ).  $R$  is the theoretical spectral resolution. Offered slits have widths of 0.40, 0.75 and 1.00". The dispersion is given in the 7th column, and has been estimated for the new AQUARIUS detector pixel size. Sensitivities refer to FOWLER read-out, which is the standard read-out for HR(X) spectroscopy since P101.

### 3 Instrument description and offered observing modes

The VISIR imager and the VISIR spectrometer are two independent sub-instruments integrated in one instrument. They have separate light paths, optics and detectors. VISIR offers one single spatial scale in imaging and several spectral resolution modes in slit spectroscopy. The cryogenic optical bench is enclosed in a vacuum vessel. The vessel is a cylinder, 1.2 m long and 1.5 m in diameter. Standard Gifford-McMahon closed-cycle coolers are used to maintain the required temperatures:  $\sim 29$  K for most of the structure and optics and  $< 15$  K for the parts near the detector. The detectors are cooled down to  $\sim 9$  K.

#### 3.1 Imager

The imager is based on an all-reflective design. The optical design is shown in Fig. 7. It consists of two parts:

- A collimator, which provides an 18 mm diameter cold stop pupil in parallel light: As generally designed for IR instruments, the pupil of the telescope is imaged on a cold stop mask to avoid straylight and excessive background emission. The collimator mirror (M1) is a concave aspherical mirror. It is followed by a folding flat mirror (M2) which eases the mechanical implementation.
- A set of three objectives mounted on a wheel: “small field” (SF), “intermediate field” (IF), and “large field” (LF). Each objective is based on a three mirror anastigmatic (TMA) system. Each of the TMA’s is made of three conic mirrors.

##### 3.1.1 Regular imaging

The Small Field objective is the standard set-up in regular imaging. The AQUARIUS detector provides a field of view of  $38''.0 \times 38''.0$  with a pixel scale of  $0''.045$ . Because the detector is slightly larger than the area of sky imaged by the VISIR optics, a part of the detector has been masked and only the pixel between  $x = 20 \dots 880$  and  $y = 75 \dots 945$  receive light from the sky. The cosmetic quality of the AQUARIUS detector is proven to be excellent. The regions of masked pixels and stripes, which were characteristic for the old DRS detector, are not present anymore.



In addition to the SF mode, also the Intermediate Field with a field of view of  $1' \times 1'$  (pixel scale  $0''.076$ ) can be used in service mode. The larger pixel scale results in increased background levels compared to the SF. The background is reduced by adopting half the SF DIT values. For broad-band filters, the IF DITs are shorter than the detector's minimum DIT and windowing is necessary (see Table 1), losing the advantage of a larger field of view. There is little point to observe with VISIR in IF when the detector needs windowing. Those programs are done better with the SF objective. See 1 for the filters that need windowing. IF waiver requests for Q-band will be rejected as experience shows that the background becomes too high.

Users who would like to use the IF need to submit a waiver which can only be accepted for imaging with the narrow band filters, i.e. any filters centered on lines. Waiver requests will be rejected for filters needing smaller detector windowing in IF than in SF (see Table 1), as well as any of the coronagraphic and SAM filters.

### 3.1.2 Burst mode

The burst read-out mode allows the user to save every single DIT frame (or several averaged DITs) of the exposure. In this way it is possible to follow rapidly evolving events or to improve the spatial resolution by taking short enough exposures to freeze the atmospheric turbulence. Because of the typically relatively short exposure times of a few milliseconds, each frame contains the instantaneous PSF corresponding to the momentary atmospheric turbulence. This allows to shift and add the images, to perform lucky imaging or to apply speckle techniques in order to reach the diffraction limit of the telescopes. This mode can be used only for objects bright enough to provide a S/N high enough in a single elementary exposure. Typical flux limits are of the order of 5 Jy in N and 10 Jy in Q. Some compromise between sensitivity and time resolution can be reached by averaging a number of elementary frames. The same setups and filters as for regular imaging are available in Burst Mode. Combining the burst read-out with coronagraphy or SAM (see below) is not possible due to the design of the observing template.

For solar system objects with differential speeds exceeding  $0.15''$  per second, a exceptional telescope set-up can be used in burst-mode to avoid problems of chopping at high differential speeds. This is achieved by leaving the telescope only in tracking and switching off the auto-guiding while chopping and nodding. Experience shows that objects up to  $0.4''/s$  can be observed in this way. A waiver request and (delegated) visitor mode is mandatory.

### 3.1.3 Coronagraphy

Since the upgrade, VISIR includes an Annular Groove Phase Mask (AGPM) coronagraph. The AGPM consists of a vector vortex induced by a rotationally symmetric subwavelength grating and allows for coronagraphic imaging of the close environment of stars, especially enabling the search for exoplanets and circumstellar disks<sup>4</sup>. The AGPM was designed for an optimal performance between  $10.0$  and  $13.2 \mu\text{m}$  without any significant loss in sensitivity; at other wavelengths the total rejection is expected to decrease significantly. Additionally, the coronagraph requires an appropriate Lyot stop to function properly. Only the three coronagraphic filters (10\_5\_4QP, 11\_3\_4QP and 12\_3\_AGP) are equipped with such a Lyot stop, including a central stop. Although the VISIR cold stop acts as a non-optimised Lyot stop, currently only the three coronagraphic filters are officially offered for the coronagraphic mode. A

---

<sup>4</sup>A detailed description of the AGPM can be found in [Delacroix et al. 2012, SPIE Vol. 8446, 84468K](#).

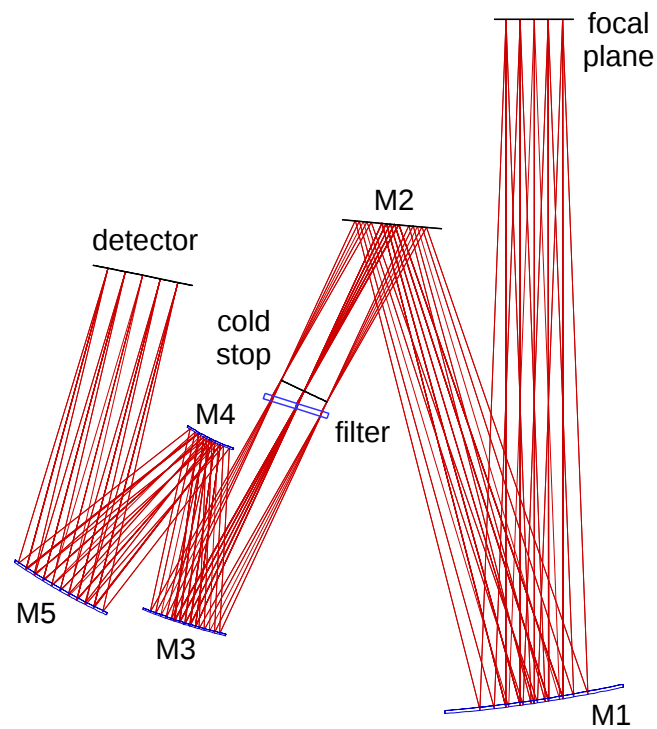


Figure 7: The optical path of the imager with a pixel scale of  $0''.045$  is shown from the focal plane down to the detector.

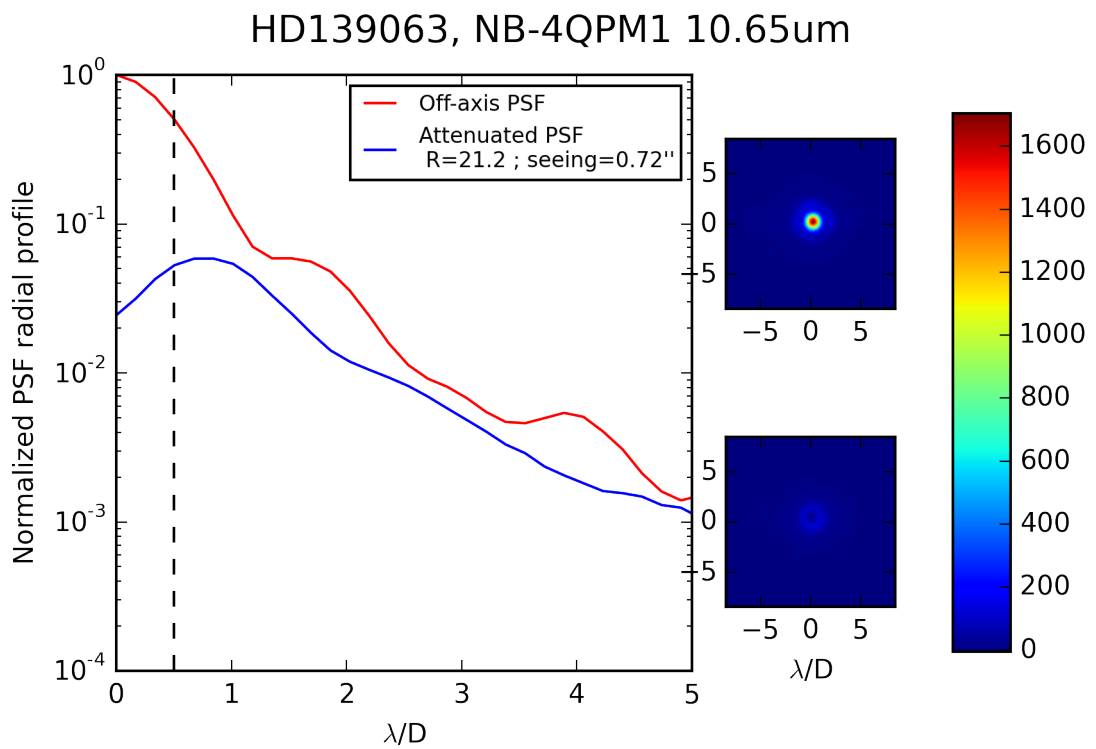


Figure 8: Coronagraphic (blue) PSF profile compared to the non-conographic PSF profile for HD139063 observed during commissioning in 2015.

comparison of the radial profile of the coronagraphic PSF compared to the non-coronagraphic PSF is shown in Fig. 8. The guaranteed total rejection under normal atmospheric conditions (optical seeing better than 0.9 arcsec) in the 12\_3\_AGP filter is 4. During commissioning, a peak attenuation of 1:20 and an attenuation in the wing by a factor of 2 to 4 was achieved routinely. A more detailed analysis of the performance is still under way. The coronagraphic mode is currently only offered in visitor mode.

### 3.1.4 Sparse Aperture Masking

While mid-infrared imaging with 8m class telescopes is often considered "diffraction-limited", precise measurements of partially resolved objects are difficult due to changes in seeing between observing a target object and a point-spread function (PSF) calibrator (Monnier et al. 2009, ApJ, 700, 491). SAM observations are driven by programs that need "extreme" PSF stability in order to identify marginally resolved objects. A better contrast close to bright point sources can be obtained as the Airy rings in straight imaging can become a problem because they may show asymmetries and instabilities. SAM is more forgiving for the true PSF of the telescope than straight imaging. Performing SAM in the mid-IR when compared to the near-IR, thanks to the back-ground noise limited performance regime, throwing away photons in SAM is less of a problem in terms of loss of sensitivity compared to K-band.

The VISIR filters are located in a pupil plane. Taking advantage of this geometry, two filters are equipped with a Sparse Aperture Mask (SAM). The filters are 10\_5\_SAM and 11\_3\_SAM. Hence only these two filters can be used in the SAM mode. There are seven sub-apertures yielding 21 non-redundant baselines. In normal operation, i.e. rotating VISIR to compensate for field rotation, the spiders of the telescope would rotate relative to the SAM-pattern and vignette the SAM pattern systematically. For that reason SAM can only be used in pupil tracking mode. As VISIR is a Cassegrain instrument this is equivalent to observing with a fixed parallactic angle and full field rotation. This angle cannot be chosen but is set by the template to keep the spiders in the obscured part of the pupil.

The SAM mode is vignetted equivalent to a reduced transmission of 11%. Given that VISIR operates in the Background Noise Limited Performance (BLIP) regime this transforms, comparing to normal filters, into a loss of S/N for point sources of a factor of three, or to maintain S/N a factor of 10 in integration time.

The actual size of the telescope pupil defined by M2, when imaged onto the VISIR cold pupil stop, is 17.67 mm. The mask hexagons have side lengths of 1.4 mm corresponding to 0.64 m in the telescope pupil of 8.115 m.

Users of this mode should be aware that the reduction of SAM data is not integrated into the VISIR data reduction pipeline.

## 3.2 Spectrometer

### 3.2.1 Description

The VISIR spectrometer is capable of performing spectroscopy at three different spectral resolutions with a pixel scale of  $0''.076$ . They provide a spectral resolving power of  $R \sim 300$ ,  $R \sim 3000$  and  $R \sim 15000$ , respectively. This is obtained by means of two arms, one with a prism and low order gratings for the low and medium spectral resolution, the other with large echelle gratings providing high spectral resolution. Currently, VISIR is offered to the

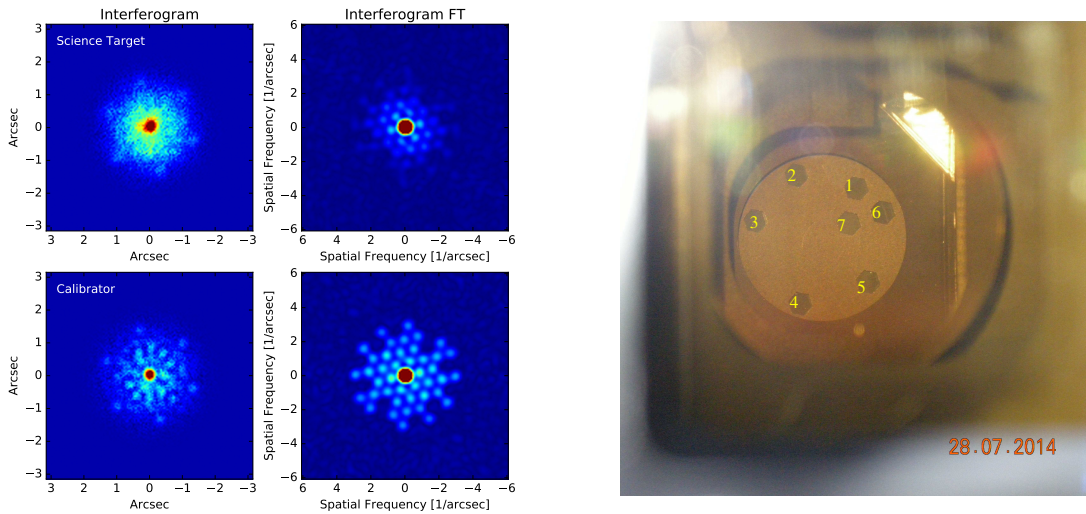


Figure 9: Interferograms at 10.5 micron obtained with SAM. *Left*: VISIR observations and the corresponding Fourier Transform which are directly related to the object visibilities. Note the lower contrast in the science target indicating that it is spatially resolved. *Right*: SAM mask as seen from the telescope side.

Hole	x (mm)	y (mm)
1	-5.707	-2.885
2	-5.834	3.804
3	0.099	7.271
4	7.989	0.422
5	3.989	-6.481
6	-3.790	-6.481
7	-1.928	-2.974

Table 3: Sub-aperture hole positions. For hole numbering see Fig. 9

community in two spectral settings, *viz.* the low and high resolution.

The long slits have a length of  $34''$ . The short slits, only used in high resolution cross-dispersed mode, have a length of  $4''$ . The all-reflective optical design of the spectrometer uses two TMA systems in double pass (pass 1: collimator, pass 2: camera). A schematic layout of the VISIR spectrometer design is shown in Fig. 10. The 3-mirror system of the low and medium resolution arm gives a 53 mm (diameter) collimated beam; the collimated beam diameter in the high resolution arm is 125 mm. Both subsystems image the spectrum onto the same detector; selection between the two spectrometer arms is done by two pairs of folding flat mirrors. In front of the actual spectrometer subsystems is a reflective re-imager consisting of two off-axis paraboloids and three folding flats. The re-imager provides a 16 mm diameter cold-stop pupil in parallel light and transforms the incoming VLT Cassegrain beam of F:13.4 to an F:10 beam at the spectrometer entrance.

Three different slit widths ( $0.4''$ ,  $0.75''$  and  $1''$ ) are offered for all spectral settings. For oversized widths (e.g. for the  $1''$  slit with respect to the diffraction limit around  $10\mu\text{m}$ ), the user should be aware that the spectral resolution obtained for a point-source is better than the sky spectrum. The zero-point of the wavelength calibration will be affected by an incorrect centering of the object within the slit. The spectrometer slit wheel is also equipped with a

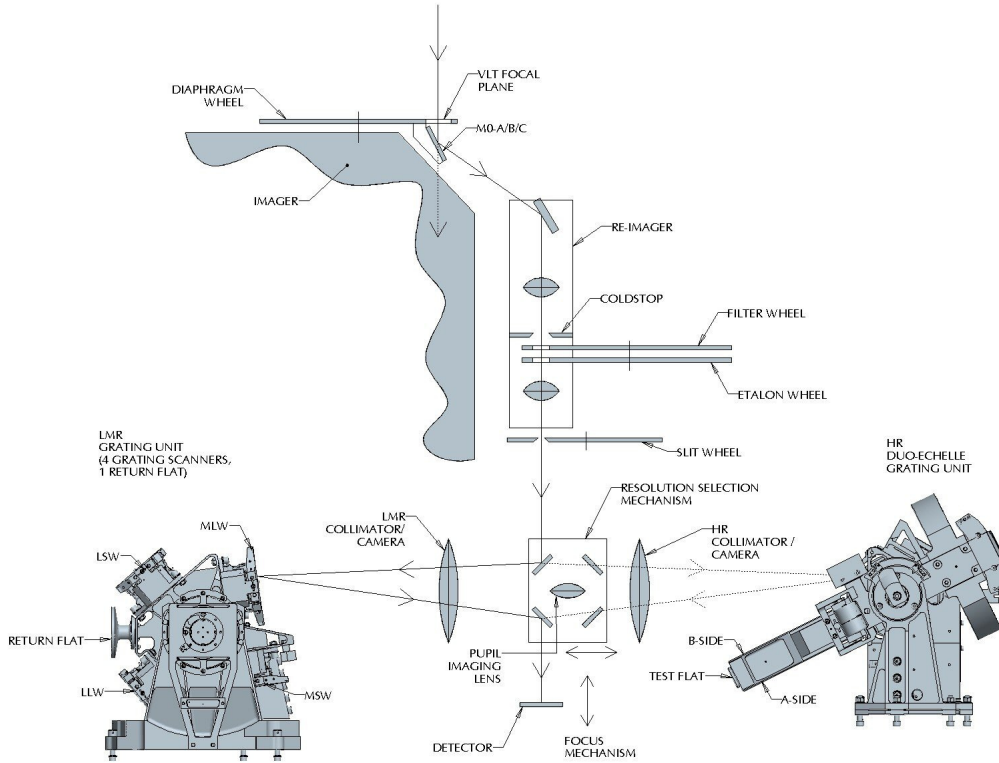


Figure 10: Schematic layout of the design of the VISIR spectrometer.

Filter	$\lambda_c$ ( $\mu\text{m}$ )	half-band width ( $\mu\text{m}$ )	sensitivity, $10\sigma/1\text{h}$ (mJy)
ArIII	8.94	0.11	200
NeII_2	12.81	0.10	50

Table 4: VISIR spectrometer filter characteristics. The sensitivities correspond to those obtained with the old DRS detector. New sensitivities will be made public on the VISIR webpage as soon as they become available.

very wide slit ( $14''$ ). It gives the possibility to make imaging with the spectrometer detector and is used for object acquisition and centering on the detector.

There are only two filters available for target acquisition with the spectrometer: ArIII and NeII.2. Their measured band-passes and approximate sensitivities for acquisition are listed in Table 4. For faint sources, the VISIR imager can be utilized for target acquisition in a first step before switching the beam to the spectrometer. In this way the user has a larger choice of filters to acquire faint targets (see 4.3.2).

### 3.2.2 Offered spectroscopic modes

#### Low resolution

The low resolution (LR) setting provides a resolving power of  $\sim 300$ . Since the VISIR-upgrade project, LR spectroscopy delivers in a single exposure the entire  $8 - 13\mu\text{m}$  wavelength range. This is achieved by replacing the former grisms by a new prism (with  $R \simeq 300$ ) The sensitivity currently offered in this setup is 70 mJy at  $10\sigma/1\text{h}$  in the clean regions of the spectrum. The largest gain, however, comes from the possibility to obtain the spectrum in the entire N-band

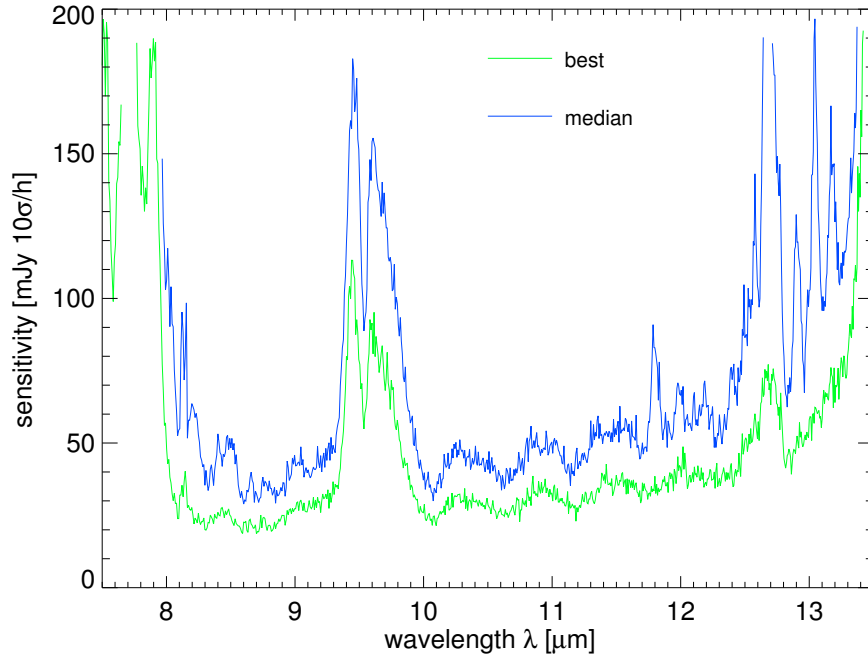


Figure 11: Median and best low resolution sensitivities [mJy/10 $\sigma$ /h] observed during commissioning 2 under mediocre atmospheric conditions.

in one shot, reducing the observing time by a factor of four. The median and minimum low resolution sensitivities observed during re-commissioning are shown in Fig. 11. Offered slits have widths of 0.4", 0.75" and 1".

### Medium resolution

The medium resolution (MR) setting is not offered yet.

### High resolution

The high resolution setting provides a resolving power of  $\sim 15\,000$ . VISIR offers a long slit and a cross-dispersed mode.

The regular long-slit mode (HR) is available in three passbands centred on the transitions of the [H2\_S4], [NeII] and [H2\_S1] lines using order-sorting filters. Table 2 lists the details of wavelength ranges covered as well as sensitivities. A minimum flux in an emission line below  $10^{-16}$  W/m<sup>2</sup>/arcsec<sup>2</sup> can be achieved with the 1" slit. This value corresponds to an approximate sensitivity limit around 1 Jy in the continuum. It is foreseen that additional filters will be commissioned for the high resolution long-slit mode in the future. The high resolution cross-dispersed mode (HRX) accesses the entire wavelength range between 7.7 and 24.0  $\mu\text{m}$  using a short 4" "long" slit.

We would like to make the user aware that the ESO ETC offers the possibility to take into account the earth motion to predict the observed wavelength of a given line depending on the foreseen date and time of observations. In particular, this feature allows to determine the dates when the emission line under study would appear at the same wavelength as a sky line. A more detailed analysis can be done using ESO's SKYCALC Sky Model Calculator<sup>5</sup>.

<sup>5</sup>The SKYCALC Sky Model Calculator can be found at <https://www.eso.org/observing/etc/bin/gen/>

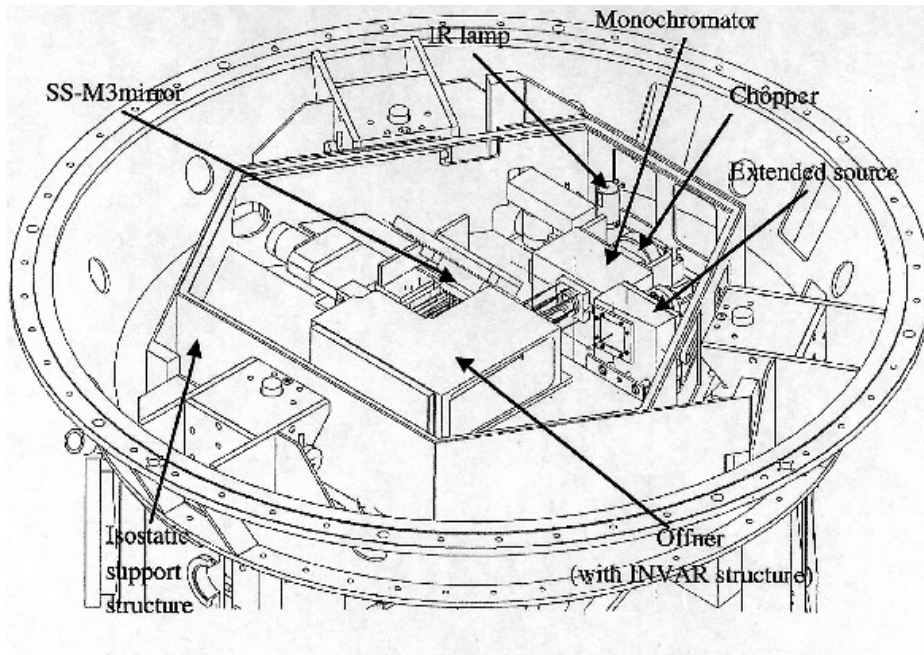


Figure 12: Schematic drawing of the warm calibration unit on top of the VISIR vessel.

### 3.3 Calibration unit

A warm calibration unit (WCU) is located on top of the VISIR vacuum enclosure. The WCU is also called star simulator. It simulates either a monochromatic point source with adjustable wavelength or an extended black-body source with adjustable temperature. A selection mirror allows to switch from the telescope to the simulator beam. It can be used for calibration and tests, also during daytime. Fig. 12 shows the unit on top of the enclosure.

### 3.4 Detectors

Following the upgrade of VISIR, the imager and spectrometer are equipped with two AQUARIUS  $1k \times 1k$  detectors, with a pixel size of  $30 \mu\text{m}^2$ . In principle, this provides a field of view that is four times larger in area than that offered by the old DRS  $256 \times 256$  detector. However, the unvignetted and usable part of the AQUARIUS detector of the imager is smaller than the entire detector. Only a region of approximately  $860 \times 860$  pixels<sup>2</sup> is illuminated by the sky, providing a field of view of  $38'' \times 38''$  with a pixel scale of  $0''.045$ . Similarly, onla a region of  $190 \times 450$  pixels<sup>2</sup> is illuminated by the sky using the imaging capability of the spectrometer (i.e. the wide slit), providing a field of view of  $14'' \times 34''$  with a pixel scale of  $0''.076$ .

The AQUARIUS array was developed at Raytheon Vision Systems at Santa Barbara USA. The development was funded by ESO to upgrade the VISIR instrument at VLT, for next generation VLTI instruments, and for the future mid-IR candidate instrument (METIS) at the E-ELT. For a detailed presentation of the AQUARIUS detector we refer the reader to Ives et al. (Proc. SPIE 8453-38), in the following we will highlight on the major properties of the detector.

To properly operate in the mid-IR window, the AQUARIUS detector is designed to deliver low thermal background, high quantum efficiency, and high sensitivity. With respect to con-

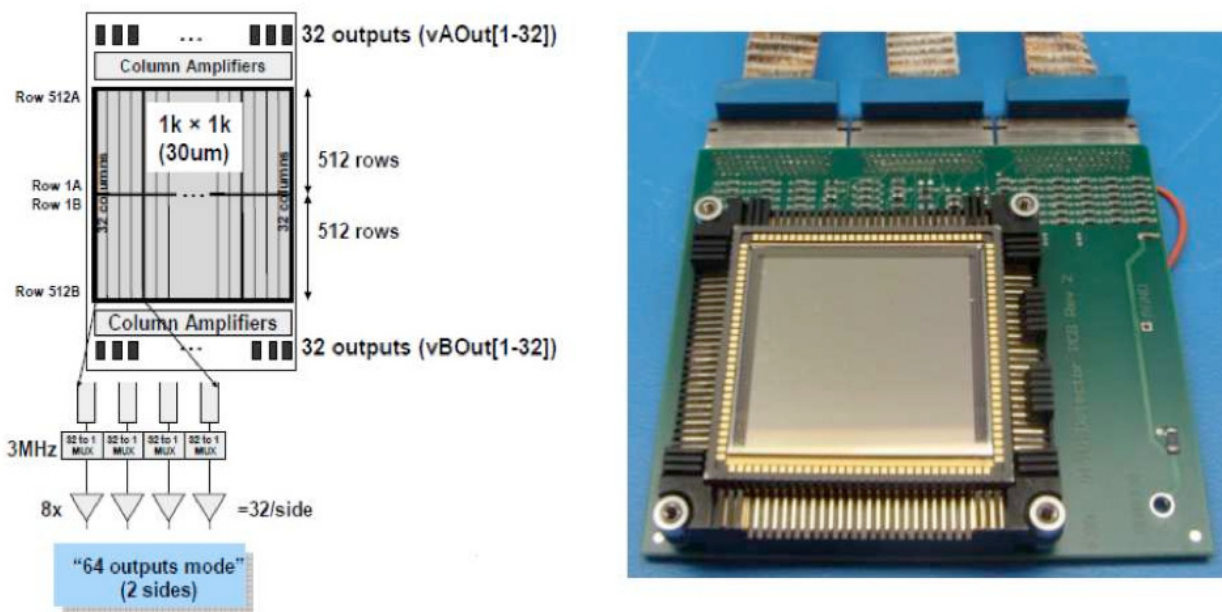


Figure 13: Left panel shows the AQUARIUS multiplexing readout scheme. Right panel shows the detector mounted in its socket.

ventional ones, these goals have been achieved by the introduction of a new class of photo-conductors, called the Impurity Band Conduction (IBC, Raytheon designation). Their Si:As IBC design achieved higher sensitivities by decreasing the thickness of the photo-conductor and increasing the doping of the Si:As diodes.

### 3.4.1 Detector Architecture

Figure 13 displays the architecture of the AQUARIUS detector. It is split into two perpendicular areas; each made of 512 rows and 1024 columns. Each area has 32 outputs, such that, each output is configured to read out 32 x 512 pixels, all 64 outputs from the two areas being read in parallel. This readout scheme also allows for 16 outputs rather than 64 to simplify the system design for low background applications. With this multiplexer configuration it is possible to read-out the full detector at 110 Hz (9 milli-seconds) frame rates, each output operational at 3 MHz pixel rates.

### 3.4.2 Detector Readout

For imaging with detector integration times of a few milliseconds, the detector is read-out in “rolling mode”. In this mode, a row is read then immediately reset, then the next row is read and reset and so forth, for a programmable row time which can overlap the read of the next row. For the high resolution Echelle mode with significantly longer intergration times, the detector is read-out using “correlated double sampling”.

It is possible to read out only a part of the detector, i.e. the detector is “windowed”. A number of rows can be selected to be read out (from the center outwards) with the remaining rows reset automatically. For example, a 1024 x 150 sized window, centered in the middle of the device, can be readout at 1 kHz (0.001 milli-seconds) frame rates. There is no advantage in read-out speed to windowing in the column direction since all outputs run in parallel. To reach sufficiently short exposure times and prevent the detector from saturating, the detector



has to be windowed for several filters: for B8.7, Q1 and Q2, the detector is windowed to 512 pixels in  $y$ -direction (corresponding to  $\sim 23''$ ), for the SIC the detector is windowed to 256 pixels  $y$ -direction (corresponding to  $\sim 11''$ ). The detector windows for all filters are given in Table 1 and on the VISIR website.

### 3.4.3 Detector Dark Current

Mid-IR detectors operate at a temperature range that is set by the Closed Cycle Coolers; typically 6 – 9 K. Lower operating temperatures allow to minimize the leakage and, most importantly, the dark current. Laboratory experiments showed that the dark current ranged between  $\sim 2200$  and  $0.56 e/pixel/s$  at 10.0 and 5.6 K, respectively. The upgrade operational goals aimed at reaching a  $\sim 1.0 e/pixel/s$  and this was achieved for a temperature of 7 K.

### 3.4.4 Excess Low frequency Noise

The AQUARIUS detectors by Raytheon suffer from excess low frequency noise (ELFN) which is the result of a design optimized for operations in a low background environment such as space applications. The ELFN is a form of correlated noise caused by fluctuations in the space charge induced by ionization/recombination in the blocking layer. It manifests itself as a memory of photons in subsequent frames. This correlation can be broken by modulating the scene seen by the detector (sources and background) at sufficiently high speed. Chopping has been demonstrated in the lab and on-sky to significantly reduce the impact of ELFN with increasing chopping frequencies. Therefore, VISIR is now operated at much higher chopping frequencies as before, up to 4 Hz in imaging. The chopping frequencies are predefined and chosen such that the signal-to-noise is maximised.

### 3.4.5 Detector Linearity

The AQUARIUS detector linearity was derived for both the high gain and the low gain configurations. The left panel of Fig. 14 displays the measured signal level as a function of exposure time. Typically these data are taken in a non-destructive read mode such that many hundreds of frames are taken between the signal detector starvation level up to its saturation level. A linear fit was applied to the data points between 15 000–40 000 DN, and the differences between the fit and the data points is plotted for the high gain setup (right panel of Fig. 14). Over this signal range the detector shows an excellent linearity of the order of  $\pm 0.5\%$ . For this particular detector, the gain and therefore the detector saturation level and read noise can be changed by a factor of approximately eight.

At the operating temperature of the detector ( $\sim 9$  K), the dark current, which is the signal obtained when the detector receives no photons, is negligible compared to the background generated by the photons emitted by the telescope and the atmosphere. The dark current is removed by the observation technique (chopping and nodding).

The detectors have a switchable pixel (“well”) capacity. The large capacity is used for broad-band imaging and the small capacity for narrow-band imaging and spectroscopy. Detector saturation due to the enormous MIR background is avoided by a storage capacity of  $0.6 \times 10^6 e^-$  in small and  $6.0 \times 10^6 e^-$  in large capacity modes, respectively. The detector integration time (DIT) is a few milli-seconds in broad-band imaging and may increase to several seconds in high resolution spectroscopy.

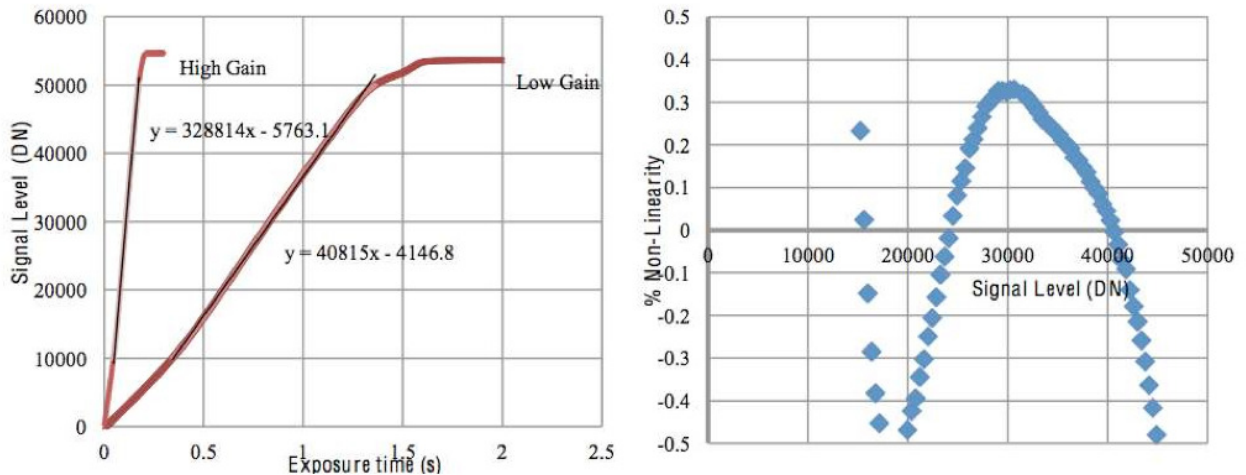


Figure 14: Left panel displays the measured AQUARIUS detector linearity for both high and low gain read modes. Right panel displays the non-linearity as a function of the signal level, as computed for the high gain setup.

The actual DIT used for each filter or setup is predefined in the instrument software in order to ensure that the detector is operated at a reasonable 30% (approximately 20 000 counts) of the potential well and that the combination of DIT and chopping frequency lead to the highest observing efficiency. It is hence not a parameter to be chosen by the observer.

### 3.4.6 Detector Cosmetics

The new AQUARIUS detector cosmetic testing shows that it does not show the high fraction of bad pixels seen in the old DRS detector. Moreover, the AQUARIUS detector can be considered free from striping effects which were visible when observing bright sources with the old VISIR detector (see Fig. 15). For bright sources falling on the edge between two detector outputs there is, however, a memory effect which can lead to the appearance of bright stripes in horizontal direction ( $x$ -direction) in the two outputs affected. This “bleeding”-effect is currently still under investigation, but it seems that it is not caused by a redistribution of flux. For accurate photometry, the flux in the feature should therefore not be added to the flux of the source, i.e. it has to be subtracted before doing e.g. aperture photometry. Also, it is recommended not to use the blind preset (template `VISIR_img_acq.Preset`) if looking for faint emission around a bright object, so that the object can be manually centred by the night astronomer into the middle of one of the detector outputs. Moreover, due to the new spectroscopic/imaging detectors readout structure (from the center outwards) it is now recommended that the scientific/standard stars targets are not placed in the very center of the detectors, but slightly offset by few arcseconds, either above or below the central division of the detectors.

It is advised to observe only sources fainter than 500 Jy in N and 2500 Jy in Q. Due to the low flux levels, eventual detector artifacts are less important in spectroscopy.

## 3.5 Data acquisition system

The AQUARIUS detectors are controlled by the New General Detector Controller (NGC). In imaging, the DIT depends on the filter, and the minimum DIT to read out the full frame of

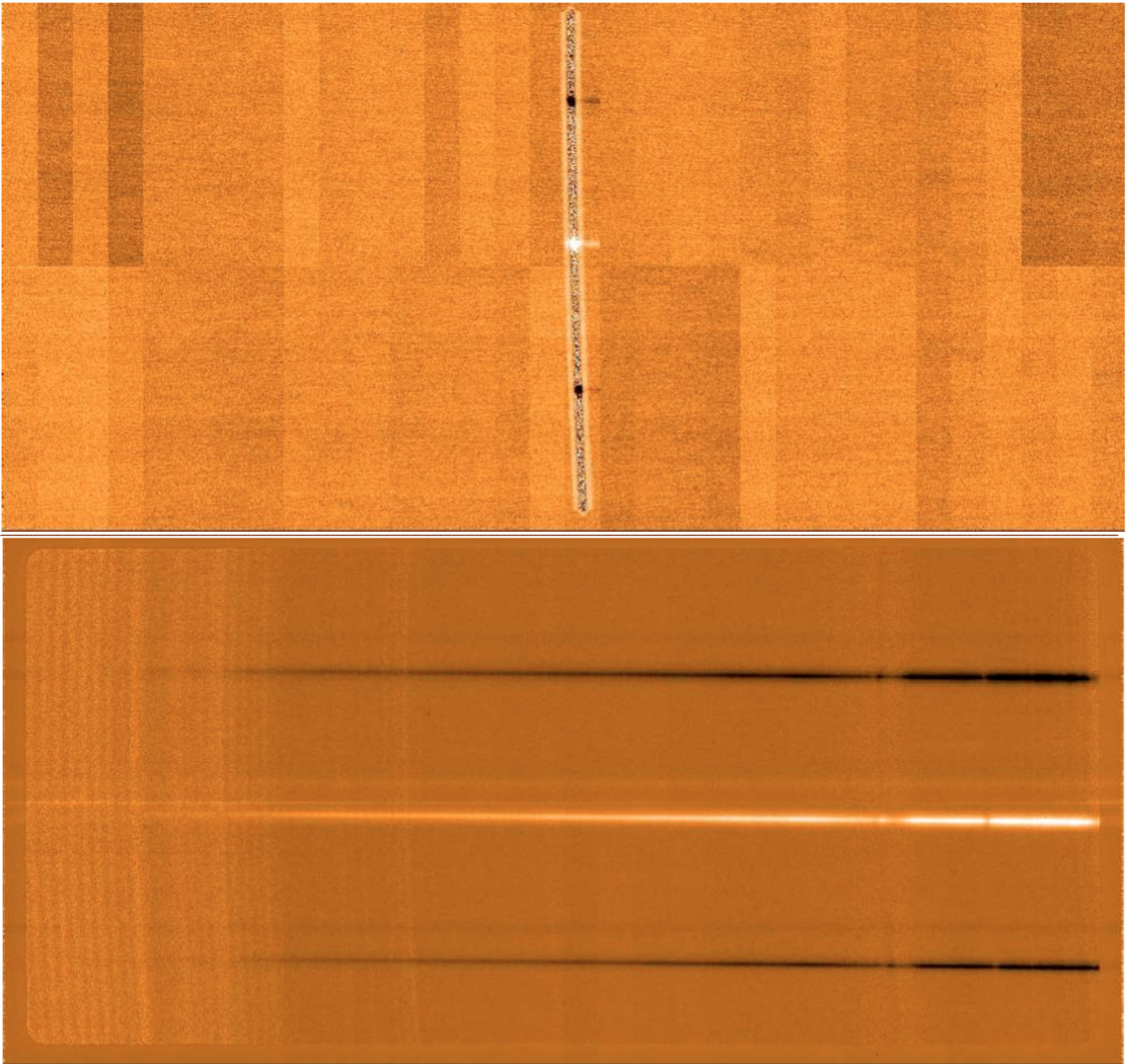


Figure 15: Upper panel: An example of the good cosmetics on the new AQUARIUS detector, used for the acquisition of a Cohen standard in the  $1''.0$  slit. Note the central division of the detector due to the intrinsic central-outward readout, and how the target was placed slightly above. Lower panel: A sequence of chop/nod, reduced spectra obtained in the low resolution mode, covering the entire N-band with a single exposure. The `TEL.CHOP.THROW` was set to  $10''$ .

1024 × 1024 pixels is 9 ms. In normal imaging, the pixels are coded with 4 bytes (long integer), leading to one full frame having a size of 4096 KB. In order to increase performance, only 2 bytes per pixel are used in burst mode where every DIT is saved. Windowing of the detector further decreases the data rate. Note that although windowing in principle allows smaller DITs, the latter are fixed for each filter in order to stay in the linear range of the detector.

Normally, the NGC by default sums up all frames for each of the two chopping positions during the whole stay in one nodding position (nodding half-cycle), and only saves its average. Alternatively, one frame per chopping position (chopping half-cycle) can be saved. This is the default for coronagraphy and SAM. For more details, see §5.

The number of useful individual exposures per chopping half-cycle depends on DET.DIT and on the chopping frequency  $f_{\text{chop}}$  and is given by

$$\text{NDIT} = (2 \cdot \text{DIT} \cdot f_{\text{chop}})^{-1} - \text{NDITSKIP}. \quad (1)$$

Here, NDITSKIP specifies the number of read-outs at the beginning of each chopping half-cycle, which are rejected during the stabilization of the secondary mirror, i.e. during the first 25 ms of each chopping half-cycle. Both DIT and  $f_{\text{chop}}$  are predefined for each filter / spectral setup (except in the high-resolution cross-dispersed mode) by the instrument software in order to achieve the highest sensitivity per unit of time. They are hence not changeable by the observer. The observing efficiency  $e_{\text{chop}}$  due to chopping is hence

$$e_{\text{chop}} = \frac{\text{NDIT}}{(2 \cdot \text{DIT} \cdot f_{\text{chop}})^{-1}} = 1 - 2 \cdot \text{NDITSKIP} \cdot \text{DIT} \cdot f_{\text{chop}}$$

The total integration time on source,  $t_{\text{src}}$ , is specified by the user through the parameter SEQ.TIME, i.e.  $t_{\text{src}} := \text{SEQ.TIME}$ . With this the integration time including the overheads due to chopping, but without nodding, is  $t_{\text{raw}} = t_{\text{src}}/e_{\text{chop}}$ . The number of nodding cycles during the entire integration period is set by the user-defined parameter NODNCYCLES so that the time spend observing in one nodding half-cycle is

$$\begin{aligned} t_{\text{nod}} &= \frac{1}{2} \frac{t_{\text{raw}}}{\text{NODNCYCLES}} + t_{\text{nodset}} \\ &= \frac{t_{\text{src}}}{2 \cdot \text{NODNCYCLES}} \cdot (1 - 2 \cdot \text{NDITSKIP} \cdot \text{DIT} \cdot f_{\text{chop}})^{-1} + t_{\text{nodset}} \end{aligned}$$

where  $t_{\text{nodset}} = 6$  sec is the nodding settling time required to move the telescope. Typically, NODNCYCLES should be chosen such that the entire nodding cycle takes  $\sim 90$  s. Thus,

$$\text{NODNCYCLES} \approx t_{\text{src}}/90 \text{ s to the first order.}$$

The total integration time then is

$$\begin{aligned} t_{\text{tot}} &= \text{NODNCYCLES} \cdot 2 \cdot t_{\text{nod}} \\ &= \frac{t_{\text{src}}}{1 - 2 \cdot \text{NDITSKIP} \cdot \text{DIT} \cdot f_{\text{chop}}} + 2 \cdot \text{NODNCYCLES} \cdot t_{\text{nodset}}, \end{aligned}$$

accounting for all overheads due to chopping and nodding. The algorithm described above ensures that the integration time on source requested by the observer using SEQ.TIME will actually also be the true integration time on source.

Typical duty cycles ( $t_{\text{src}}/t_{\text{tot}}$ ) are between 70 and 90%.

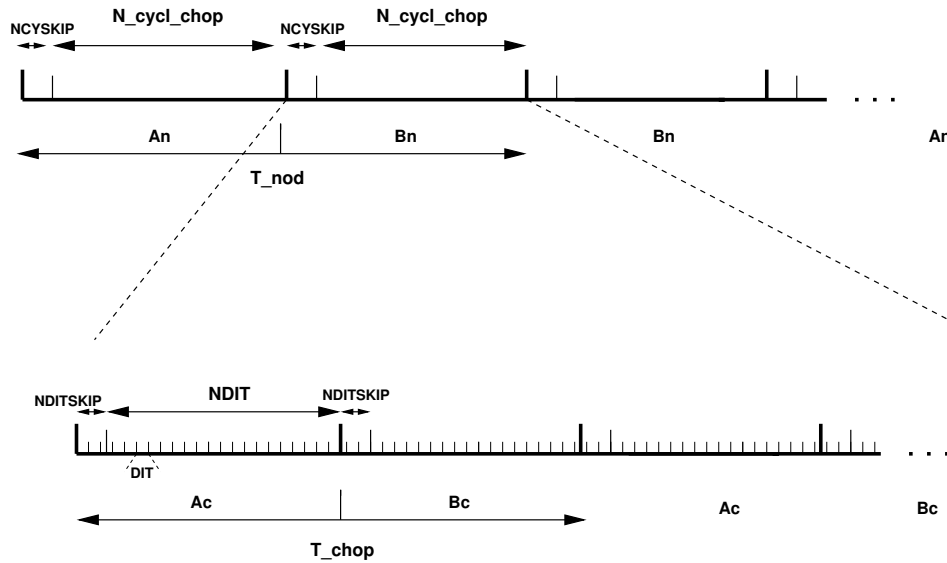


Figure 16: Data timing in VISIR.  $A_c$  and  $B_c$  refer to the two chopper positions,  $A_n$  and  $B_n$  refer to the two nodding (telescope) positions. Note the  $A_n B_n B_n A_n$  cycle sequence for the nodding to save observing time.

## 4 Observing with VISIR at the VLT

### 4.1 Tools for the preparation of proposals and observations

Tools are available to prepare the observations, either during phase 1 (call for proposals), or during phase 2 (creation of observing blocks by the observer):

- The *exposure time calculator* (ETC, available at <http://www.eso.org/observing/etc/>) may be used to estimate the integration time needed to obtain the required S/N for a given instrument setting and set of atmospheric conditions. Because of the numerous sky absorption lines, (see Fig. 20 and following), it is recommended to display the S/N as a function of wavelength when using the spectrograph ETC in order to ensure that the correct S/N is reached for the targeted line emission or absorption. The ETC also allows to carry out a detailed assessment of the effect of different PWV values on the sensitivity for specific observations and predicts the achieved image quality for a given optical seeing.
- Astronomers with granted VISIR telescope time in Service and Visitor mode prepare their observations using the web-based tool [p2](#). Acquisitions, observations and calibrations are coded via observing templates. One or more templates build up an observing block (OB). They contain all the information necessary for the execution of a complete observing sequence. An overview of the currently offered VISIR templates and their parameters is given in §6 of this manual.
- It is mandatory to check that a guide star brighter than  $V=13.5$  within a field of 7.5 arcmin radius around the science target is available. This is best done by using the *GuideCamTool* (see § 4.4).
- For each science template, the user has to provide a finding chart so that the target can be acquired. In addition to the general instruction on how to create these finding charts

(see <http://www.eso.org/sci/observing/phase2/SMGuidelines.html>) the following VISIR requirements apply:

- All finding charts have to be made using existing infrared (K-band or longer wavelength) images. Typically, 2MASS or DENIS K-band images are acceptable, although higher spatial resolution is preferred, especially if the object has a complex structure.
- If the wavelength at which the finding chart has been taken is different from that of the science observation, e.g. a K-band finding chart for a  $10\mu\text{m}$  spectroscopic template, the user has to describe clearly how to identify the target at the observing wavelength in the README section of the programme description. Adequate examples of such comments are:
  - \* The target will be the brightest source in the field of view at  $10\mu\text{m}$  .
  - \* At  $10\mu\text{m}$  , there will be two bright sources in the VISIR field of view. The science target is the southernmost of these two.
- For high resolution cross-dispersed spectroscopy the finding chart should include a copy of the output spectrum of the ETC at the requested wavelength including and indication of the exact position of the emission line. This is required, so that the DIT can be adjusted manually depending on the atmospheric conditions in order to ensure the optimal S/N.

Note that observations close to zenith during meridian crossing should be avoided, because of fast tracking speeds that do not allow proper background cancelation through nodding.

Questions related to the VISIR Phase1 and Phase 2 observing preparation should be directed to the User Support Department ([usd-help@eso.org](mailto:usd-help@eso.org)).

## 4.2 Observing Parameters

### 4.2.1 Instrument orientation on the sky

By default, the imager orientation is such that North is at the top and East is to the left. Since VISIR is mounted on a rotator at the Cassegrain focus of Melipal, it is possible to change the default orientation of VISIR on the sky. The parameter `TEL.ROT.OFFANGLE`, defaulted to  $0^\circ$ , is used for this purpose. A positive value rotates the VISIR field of view clockwise (from North to West).

For the spectrometer, the default orientation is mirrored along the North-South axis ( $y$ -axis) respective to the imager, so that East is to the right, with the slit orientation along the North-South direction. Figure 17 summarises the situation.

Similar to the imager, it is possible to change the default orientation of VISIR on the sky, for example, to obtain the spectra of two objects, A and B, at once. If PA represents the actual position angle of object B relative to A, measured on the sky east of north (i.e., counted positively from north to east) within the range  $0^\circ$  to  $360^\circ$ , then setting

$$\text{TEL.ROT.OFFANGLE} = 360^\circ - \text{PA}$$

allows one to have both A and B objects on the slit. To chop along the slit, one has to set `TEL.ROT.OFFANGLE = TEL.CHOP.POSANG` (see next section).

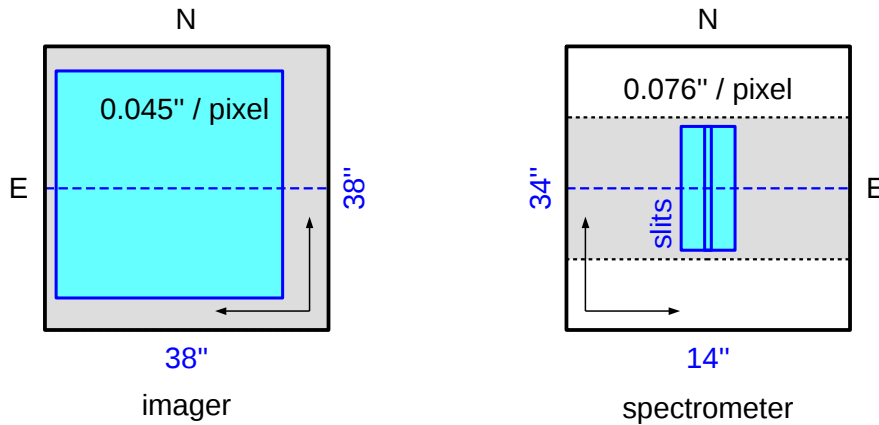


Figure 17: Field orientation and pixel scale for the imaging (SF) and the spectroscopic modes of VISIR for `TEL.ROT.OFFANGLE = 0°`. While the imaging detector follows the normal astronomical convention, the spectroscopic detector is reversed in  $x$ -direction so that East is to the right. The gray area marks the region of the detector which is typically read-out, the spectroscopy detector being windowed in  $y$ -direction. The magenta areas mark the areas illuminated by the sky – in case of the spectrometer for the very wide slit (“OPEN”). The sizes of these usable areas on sky are given in blue (see also § 3.4).

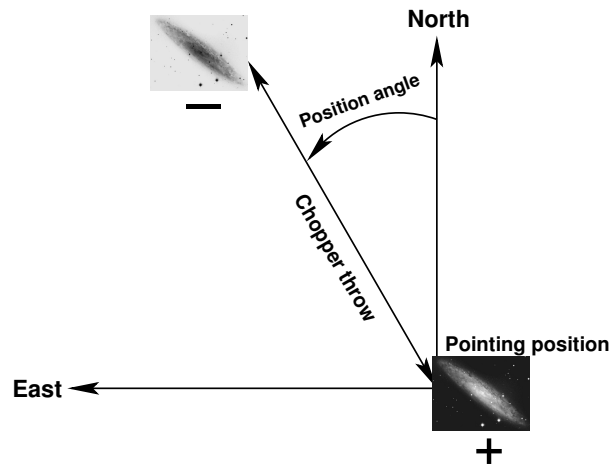


Figure 18: Definition of chopping parameters from the *telescope* point-of-view. The (chopping) position angle (`TEL.CHOP.POSANG`) is measured counter-clockwise from North to East, between  $0^\circ$  and  $360^\circ$ . The positive beam (+) is obtained when the M2 is at Chopping Position A and corresponds to the pointing position of the telescope as given in the FITS header (idle position). The negative beam (-) is obtained by moving the M2 so that it points to a position angle on the sky given by `TEL.CHOP.POSANG` and a throw of `TEL.CHOP.THROW` from the telescope pointing position (Chopping Position B). If `TEL.CHOP.POSANG = TEL.ROT.OFFANGLE`, the resulting image on the detector will appear as in one of the nodding position images illustrated in Fig. 20.

### 4.2.2 Chopping parameters

The chopping technique, as described in § 2.5, is based on beam switching using the secondary mirror of the telescope. It allows to alternatively observe a field, then another field offset from the first by a chopping distance or throw, called `TEL.CHOP.THROW`, see Fig. 18. This parameter can be set by the user. To avoid chopping inside the object it is recommended to use a chopping and nodding throw which is  $\sim 1.5$  times larger than the estimated diameter of the object in the mid-infrared. In the case of point sources and imaging, the throw is usually set to  $\sim 13''$  to ensure proper separation of the different beams. The maximum chopping throw at the VLT is  $30''$  and the minimum is  $8''$ . For chopping throws larger than  $25''$  one of the chopping throws may fall outside of the technical CCD used for the guiding. For this reason, the maximum chopping throw is limited to  $25''$ , i.e.  $8'' < \text{TEL.CHOP.THROW} < 25''$ . Chopping throws up to the maximum of  $30''$  may be allowed following a Waiver Request. In this case, the PI has to ensure that the guide probe is oriented such that both beams fall on the technical CCD. This is achieved by selecting a guide star – using the GuideCamTool – so that the two chopping positions will be aligned diagonally on the technical detector (see also § 4.4). Note that for chopping throws larger than the field-of-view (especially also if the detector is windowed), the negative beams will not be seen on the detector, and the integration times have to be adjusted accordingly.

The chopper position angle is the angle of chopping counted East of North (see Fig. 18) and specifies the direction towards which the image is offset. This causes the object to move to the opposite direction in the image obtained during the second chopping half-cycle (see also § 6.2). This parameter can be set by the observer. In order to keep the same distribution of beams on the detector for a different rotator angle (`TEL.ROT.OFFANGLE`) as in the default rotator position (see Fig. 20), then `TEL.CHOP.POSANG` must be equal to `TEL.ROT.OFFANGLE`. In particular, this is the case in spectroscopy if the observer wishes to have the 3 beams along the slit. As stated in § 3.5, the chopping frequency is not a parameter accessible to the observer, it is fixed internally to ensure the best data quality.

### 4.2.3 Nodding parameters

The nodding technique allows to switch from one field to another by offsetting the telescope by several tens of arcseconds. It allows to correct for optical path residuals that remain after chopping (§ 2).

The number of nodding cycles, `SEQ.NODNCYCLES`, is a parameter that can be modified by the observer. It strongly depends on the total integration time and should be chosen such that a nodding cycle takes about 90s, which will ensure a good removal of the sky residuals. Faster nodding will improve the removal of background residuals, especially when the object is transiting. However, the price is higher nodding overheads and hence a lower observing efficiency (see § 3.5).

In all the “AutoChopNod” templates, the nodding offset is equal to `TEL.CHOP.THROW` and cannot be modified.

In order to reach Nodding Position B, the telescope executes an offset of `TEL.CHOP.THROW`, along a position angle equal to

- $\text{PA} + 90^\circ = 360^\circ - \text{TEL.CHOP.POSANG} + 90^\circ$ , if `SEQ.CHOPNOD.DIR = PERPENDICULAR`,
- $\text{PA} + 180^\circ = 180^\circ - \text{TEL.CHOP.POSANG}$ , if `SEQ.CHOPNOD.DIR = PARALLEL`.



The resulting distribution of images on a frame is illustrated in Fig.20. In imaging, more flexibility on the nodding offsets are possible with the `VISIR_img_obs_GenericChopNod` template.

## 4.3 Target acquisition

### 4.3.1 Introduction

An observing block (OB) must start with an acquisition template. The execution of the acquisition template presets the telescope to the science target coordinates. The science target coordinates are contained in the template parameters `TEL.TARG.ALPHA` and `TEL.TARG.DELTA`. In case the science target is too faint for acquisition, the user can opt for a so-called "blind offset": first, a reference star is acquired, followed by an offset to the faint science target. The offset between reference and science target is specified by the template parameters `TEL.TARG.OFFSETALPHA` and `TEL.TARG.OFFSETDELTA`. In VISIR, the offset is defined as follows<sup>6</sup>:

$$\text{TEL.TARG.ALPHA} + \text{TEL.TARG.OFFSETALPHA} = \text{RA}_{\text{REF.STAR}},$$

$$\text{TEL.TARG.DELTA} + \text{TEL.TARG.OFFSETDELTA} = \text{DEC}_{\text{REF.STAR}}.$$

The "blind offset" is subject to two restrictions: (1) the angular separation between the reference star and the science target should be smaller than  $60''$ ; (2) it should not be used in combination with the  $0.4''$  slit.

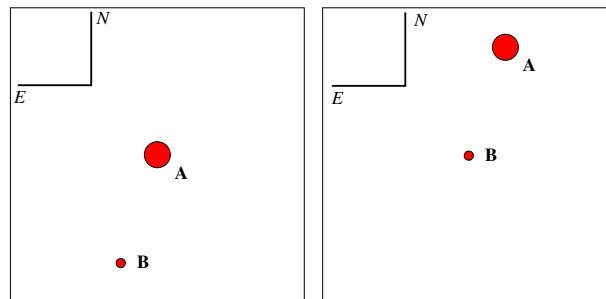


Figure 19: Blind offset in VISIR. Object A is the bright reference star, object B is the science target. Object A is acquired first. Once done, the telescope is automatically offset to object B. In this example, `TEL.TARG.OFFSETALPHA` is negative because the science target is to the east of the reference star; likewise, `TEL.TARG.OFFSETDELTA` is positive because the science target is to the south of the reference star.

### 4.3.2 Acquisition Templates

There are two acquisition templates for imaging, `VISIR_img_acq_Preset` and `VISIR_img_acq_MoveToPixel`, one for coronagraphy, `VISIR_img_acq_MoveToCoro`, and one for sparse aperture masking, `VISIR_img_acq_MoveToMask`. Two acquisition templates are also available for spectroscopy, `VISIR_spec_acq_MoveToSlit` and `VISIR_spec_acq_ImgMoveToSlit`. The latter one allows to perform spectroscopic acquisition with the imager detector and therefore offers the possibility to acquire fainter objects in a larger variety of filters. The `VISIR_spec_acq_ImgMoveToSlit`

<sup>6</sup>This convention is identical to the UVES one, but differs, from example, from the NACO one

template also allows to centre two objects in the slit by automatically calculating the angle by which the instrument has to be rotated. The observing parameters are described in § 8.

The effect of all acquisition templates is first to point the telescope so that the coordinates at the center of rotation (located at  $x, y$  on the detector) match

- the target coordinates, if no blind offset is used,
- the offset star coordinates, otherwise,

within the accuracy of the VLT pointing (see below). Once the telescope preset is done the target will fall close to pixel  $(x,y) = (430, 530)$ . The centre of the non-obscured detector is roughly at  $(x,y) = (450, 512)$ . The clear range in  $x$  is from pixel 20 to 880. For `VISIR_spec_acq_MoveToSlit`, the first acquisition images are obtained with the wide slit (14" width).

Then,

- If the target coordinates are well known, VISIR imaging modes allow to perform blind preset observations with the `VISIR_img_acq_Preset` template. In this case, no acquisition images are taken.
- The `VISIR_img_acq_MoveToPixel` and `VISIR_spec_acq_MoveToSlit` require interaction with the instrument operator or night support astronomer in order to center the target at the appropriate location on the detector. Without further indication given by the observer, the default locations are:
  - for `VISIR_img_acq_MoveToPixel` and `SEQ.CHOPNOD.DIR = PARALLEL`:  $\sim 3''$  North from the center of the detector to avoid the central-outward readout of the detector;
  - for `VISIR_img_acq_MoveToPixel` and `SEQ.CHOPNOD.DIR = PERPENDICULAR`: in the top left quadrant of the detector, at a distance equal to `TEL.CHOP.THROW/2` from the center of the detector in both X and Y;
  - for `VISIR_spec_acq_MoveToSlit`: at  $\sim 3''$  South of the center of the slit. In service mode, acquisition with the `VISIR_spec_acq_MoveToSlit` template is limited to objects brighter than 0.2 Jy.

All acquisition images are recorded and archived. Note that, *except if specifically requested in the README file*, photometric standard stars are not necessarily observed in the same filter as the acquisition filters.

As part of the execution of the `VISIR_spec_acq_MoveToSlit` template, an image used to measure the slit location is always taken and archived. In service mode, through slit images, obtained using the filter set by the `INS.FILT2.NAME` parameter, are also taken and archived so that the user can assess the correct centering of her/his object. The slit location image and the through-slit images are automatic procedures. Only the exposure time of the through-slit images can be modified by a service mode observer. Their execution time is included in the advertised execution time of the spectroscopic acquisition template.

By default, if `TEL.TARG.ALPHA` and `TEL.TARG.DELTA` contain the (accurate) coordinates of the target, the target will be located at the center of the detector, *including if the observing templates use* `SEQ.CHOPNOD.DIR = PERPENDICULAR`. In this case, in order to avoid to lose the chopnod images, it is advisable either to

- change the parameters `TEL.TARG.ALPHA` and `TEL.TARG.DELTA` so that they are offset by half the `TEL.CHOP.THROW` values, to south and west for `TEL.ROT.OFFANGLE = TEL.CHOP.POSANG = 0`, so that the target falls in the upper left quadrant of the detector;
- or use the parameters `TEL.TARG.OFFSETALPHA` and `TEL.TARG.OFFSETDELTA`: as above, the convention ‘final coordinates (RA, DEC) of the center of the field plus offsets equal initial coordinates’ is used, which translates into

$$RA + \text{TEL.TARG.OFFSETALPHA} = \text{TEL.TARG.ALPHA},$$

$$DEC + \text{TEL.TARG.OFFSETDELTA} = \text{TEL.TARG.DELTA}.$$

Therefore, if `TEL.ROT.OFFANGLE = TEL.CHOP.POSANG = 0`, `TEL.TARG.OFFSETALPHA` and `TEL.TARG.OFFSETDELTA` should be both positive in order to reproduce the scheme shown in Fig. 20. A typical value for these parameters is `TEL.CHOP.THROW/2`, where `TEL.CHOP.THROW` is the chop throw used in the subsequent templates.

If both the target and guide star coordinates are within the same astrometric systems, the pointing accuracy is limited by the relative accuracy between the coordinates of the two objects. In particular, the pointing accuracy may be affected by significant (usually unknown) proper motion of the guide star. Note that the observatory does not guarantee the accuracy of the world coordinate systems (WCS) keywords in the FITS headers.

For a successful completion of an OB, the observer has to ensure that correct target coordinates are provided for the equinox J2000.0 ideally at the epoch of the observations<sup>7</sup>. The following cases require special care:

- *imaging*: in some conditions, an error of less than 15'' in the coordinates can bring the target outside of the field;
- *spectroscopic acquisition*: in some conditions, an error of less than 7.5'' in the coordinates can bring the target outside of the wide slit used.

Errors of such scale are common in the following situations:

- *high proper-motion stars*: in particular, if the epoch of the VISIR observations is significantly different from the epoch for which the coordinates were determined.
- *point-like sources within extended objects*: such as an AGN: a number of catalogues do not provide accurate coordinates of the nucleus. Coordinates given by 2MASS are the more reliable.
- *coordinates obtained with low spatial resolution instrument*, such as MSX, etc...

For solar system objects, the J2000.0 equinox, topocentric, ICRF or FK5 coordinates at the epoch of the observations are required, as the Telescope Control System takes into account precession, nutation, annual aberration and refraction. On the contrary, the topocentric, *apparent* coordinates at the observatory, often used in other observatories, should *not* be used. Additional velocity parameters corresponding to  $\mu(\alpha) \cos \delta$  and  $\mu(\delta)$  must be given in ''/s.

---

<sup>7</sup>In particular, note that P2 only accepts coordinates for J2000.0

## 4.4 Guide stars

Guide stars are mandatory for active optics and field stabilization. Any VLT program should make sure that a guide star with a  $R = 11.0 - 13.5$  mag is available within  $7.5'$  around the object.

The VISIR field is small compared to other VLT instruments. Therefore images of a field can often appear empty in short to medium length exposures. However, objects may become visible in longer ones. Combining different exposures taken on different nights may be tricky if a proper astrometric alignment is not carried out. Since the overall astrometric accuracy of an image is actually limited by the accuracy on the coordinates of the guide star, it is strongly recommended that all OBs of a same field use the *same* guide star, in particular for faint objects.

In addition, objects within (optically) dark molecular clouds may have few or no suitable guide stars, at least in the catalogues currently used by the Telescope Control System: the UCAC3. Alternatively, some bright nebulae may saturate the region of the digital sky surveys used by the telescope operator to select guide stars. Considerable amount of telescope time will be saved if such cases are identified *before* an OB is started.

Providing the coordinates of a guide star in the acquisition template of an OB is therefore strongly recommended in a number of situations:

- observations of faint objects, hardly or not visible even after a long exposure, in particular, if this exposure has to be combined with other ones;
- observations of objects within (optically) dark molecular clouds where few suitable guide stars are expected;
- observations of objects within bright nebulae larger than the field of view accessible by the guide-probe that appeared saturated in the digital sky surveys (example: Orion);
- observations for which astrometric accuracy is important.

If chopping throws larger than  $25''$  are needed, e.g. for a very extended object, a guide star must be specified (see § 4.2.2). This guide star must be chosen such that the chopping direction is oriented diagonally on the technical CCD which is mounted on the guide probe, so that both chopping beams fall onto the detector. This is achieved by choosing a star such that the guide probe is oriented at roughly  $45^\circ$  with respect to the chopping position.

In all these cases, the use of the GuideCamTool for VISIR (see <http://www.eso.org/sci/observing/phase2/SMGuidelines/GUCT.VISIR.html>) is strongly recommended and the coordinates of a suitable guide star should be inserted in the acquisition templates. By directly interacting with P2, the GuideCamTool ensures that the correct coordinates and settings are transferred into the OB.

If `TEL.AG.GUIDESTAR` is 'CATALOGUE', a guide star from the guide star catalog will be automatically selected by the TCS. If `TEL.AG.GUIDESTAR` is 'SETUPFILE', the observer has to provide the coordinates of the GS. The coordinates of the guide star also fix the reference point for the World Coordinate System coordinates, that appear in the FITS header of the files.

In both cases, the telescope operator acknowledges the guide star. Depending on the weather conditions or if the star appears double in the guide probe, the telescope operator may have to select another guide star. Therefore, *if the observer has selected a guide star for astrometric*

*purposes* – for example, to insure the repeatability of the pointings between different OBs –, *a clear note should be given in the README file, for service mode observations, or be specifically mentioned to the night time astronomer*, in visitor mode. As stated above, the observatory does not guarantee the accuracy of the world coordinate systems (WCS) keywords in the FITS headers.

## 4.5 Brightness Limitations

There are currently no brightness limitations with VISIR. However, it is advised to observe only sources fainter than 500 Jy in N and 2500 Jy in Q to avoid detector artifacts (§ 3.4).

## 4.6 Overheads

The VLT overhead for one OB which includes active optics setting, selection of guide star, field stabilization is 6 min.

VISIR instrument configurations can be changed in a short time. For example a complete change of instrument settings takes less than 2 minutes. The total time for an image acquisition of a bright sources ( $> 1$  Jy) takes  $\sim 5$  min. for one fine acquisition iteration, or in blind preset 2 min. Spectroscopic acquisitions take longer and are strongly dependent on the source brightness: an overhead of 15 min is accounted for sources  $> 1$  Jy, while 30 min are required for sources between 0.2 and 1 Jy, respectively. Instrument overheads due to chopping and nodding duty cycle losses have been measured to be between 25 and 50 % of the observing time leading to an observing efficiency between 50 and 80% (see also §3.5). In addition, file writing times can become significant (up to 100%) for the large files created in burst mode or when all chopping half-cycles are saved. The total observing time requested by the observer must include telescope and instrument overheads and is best estimated by creating the actual OBs in the web-based P2.

## 4.7 Calibration Observations

MIR observations depend strongly on the ambient conditions such as humidity, temperature and airmass. In service mode, the science observations are interlaced by observations of calibrator stars on a timescale of 2 hours. That is, observations of photometric standards will be provided by the observatory within a time interval of two hours w.r.t. the science observations. Apart from these observations of calibrator stars, no further calibration observations are foreseen with VISIR as all other biases are removed effectively by the chopping and nodding technique (see § 2.5).

Calibrators, unless provided by the observer, are selected from the MIR spectro-photometric standard star catalog of the VLT<sup>8</sup>. This catalog is a sub-set of the radiometric all-sky network of absolutely calibrated stellar spectra by Cohen et al.<sup>9</sup>. This list is supplemented by MIR standards formerly used by TIMMI2<sup>10</sup>. At present, the standard star catalog contains 425 sources.

Continuous observations over 3 hours of the same standard star indicate that photometric stability better than 3% can be achieved with VISIR at the VLT. In order to test if a photo-

<sup>8</sup>See <http://www.eso.org/sci/facilities/paranal/instruments/visir/tools.html>.

<sup>9</sup>Cohen et al., 1999, AJ 117, 1864

<sup>10</sup>See <http://www.ls.eso.org/lasilla/Telescopes/3p6/timmi/html/stand.html>.

metric precision of the same order can be obtained, a reduced set of standard stars has been built consisting of the Cohen et al. stars which obey the following criteria:

- visibility from Paranal;
- no variability detected by Hipparcos non-variables (Var = 0 in the Hipparcos catalogue);
- absolute flux calibration errors (as reported by Cohen et al.) < 20%;
- all spectral types reported in SIMBAD no more than 1 sub-class different from that used by Cohen et al.;
- not visual binaries (as reported by SIMBAD).

This catalogue of 81 stars is also made available at <http://www.eso.org/sci/facilities/paranal/instruments/visir/tools.html>.

From this catalogue, a further selection to provide a reduced list of 12 stars has been carried out. These stars are distributed as uniformly as possible in Right Ascension, with spectral types as similar as possible. In addition, their flux in the N-band, of the order of 10Jy, is bright enough to be observable in the Q-band. At least one star in this reduced catalogue will be observed every night VISIR is in use. Note that this list could be modified without previous notice.

The photometric standard star observations can also be used to derive a PSF. However, it is not guaranteed that its S/N is sufficient for deconvolution purposes. If the observer requires a specific PSF measurement, (s)he has to provide the corresponding PSF OB.

Observations of photometric standards provided by the observatory are taken using the VISIR\_img\_cal\_AutoChopNod template (§ 6) with the following settings:

```
SEQ.TIME          180 sec for N- and 360 sec for Q-band
TEL.CHOP.POSANG   0°
TEL.CHOP.THROW    13"
SEQ.CHOPNOD.DIR   PERPENDICULAR
```

Filter INS.FILT1.NAME will be set according to the science observations.

In low resolution spectroscopy, the observatory will provide spectro-photometric observations of a telluric (K or M type) standard star in the low resolution mode, based on the same catalog as for imaging with an airmass difference no larger than 0.2 with respect to the science target. Such a calibration measurement will be performed at least once per night, per instrument configuration. More precisely the following settings of the VISIR\_spec\_cal\_LRAutoChopNod template (§ 6) will be used:

```
SEQ.TIME          180 sec
TEL.CHOP.POSANG   0°
TEL.CHOP.THROW    10"
SEQ.CHOPNOD.DIR   PARALLEL
```

The slit width INS.SLIT1.WIDTH will be adjusted to the science observation.

For coronagraphy, observers are encouraged to use calibrator stars as PSF reference stars for their Visitor Mode observations. The chopping parameters should be chosen such that the

two negative beams are not obstructed and fall on the detector ( $8'' \leq \text{TEL.CHOP.THROW} < 10''$ ). The negative beams can then be used to also flux-calibrate the coronagraphic data.

**Important note:** The observatory does **not** provide standard calibrations for VISIR high resolution spectroscopy. Thus for high resolution mode the observer has to supply his own calibration by supplying a calibration OB for each science OB. The observing time needed to execute this calibration is charged to the observer. Ideally, early type stars should be chosen. In particular, for high resolution spectroscopy, asteroids provide mostly featureless spectra on the VISIR spectral range. For service mode observations, all calibrator observations should be concatenated to their science OB.

A final recommendation concerning service mode observations is that no more than 5 filters should be grouped together in a single Observing Block. This will ensure a proper calibration of each single filter. Moreover, it is also recommended that N- and Q-band filters are not grouped together as the Q-band sensitivities can be significantly different from that in the N-band, depending on the atmospheric conditions, especially the water vapour.

## 4.8 Observing constraints and OB Classification

The *Sky Transparency* constraints used at Paranal are photometric (PHO), clear (CLR), thin (THN), and thick (THK). They originally refer to the optical band and their translation to the IR domain, and specially to the MIR, is not obvious. Also, there is some redundancy between the sky transparency and the precipitable water vapour constraints. Therefore the following scheme is applied for VISIR: OBs requiring PHO conditions will be executed and classified as “A” (fully within constraints) if the sensitivity in the corresponding band is equal or better than the nominal median value and if the conversion factor is constant within 10%. OBs requiring CLR, THN and THK conditions will be executed and classified as “A” when the sensitivity is respectively within 20%, 30% and 50% the nominal values.

Classification for VISIR observations conducted in service mode is also based on the *Precipitable Water Vapor* (PWV, see § 2.2) constraint. The PWV has a particularly strong effect in the Q-band but not so much in the N-band apart from certain spectroscopic settings. This leads to the following recommendations:

1.  $\text{PWV} < 1.5 \text{ mm}$ : Q-band imaging of faint sources & N-band spectroscopy in regions strongly affected by water vapour;
2.  $1.5 \text{ mm} \leq \text{PWV} \leq 3.5 \text{ mm}$ : Q-band bright sources and N-band spectroscopy in general;
3.  $3.5 \text{ mm} \leq \text{PWV} \leq 10 \text{ mm}$ : N-band imaging.

OBs executed with the requested PWV constraint will be classified “A”, those executed within 10% of the requested PWV value will be classified “B” (Almost within constraints) and OBs executed under PWV conditions greater than 10% of the requested PWV value will be classified “C” (out of constraints). Observations qualified as “C” will be repeated. The time required to do so will not be charged to the observer’s program. The requested PWV has to be specified during the proposal submission using the ESOFORM package in the column “Additional info” of the proposed list of targets (Box 11). The effect of different PWV values on the sensitivity for specific observations can be assessed using the VISIR ETC (see § 4.1).

For VISIR, the *lunar illumination* and *distance* constraints are not user selectable parameters. They are fixed to 1 and 30, respectively, meaning that observations can be carried out

irrespective of the lunar phase and with a minimum distance of  $30^\circ$  from the moon. Similarly, the *twilight* constraint should remain fixed at  $-30$ , meaning that the observation can be carried out up to half an hour into the twilight. The very high background from the ambient atmosphere and telescope in the mid-infrared does not change significantly from day to night or due to the presence of the moon. All background emission is removed using the chopping and nodding (see § 2.5). Therefore observations in the mid-infrared are not sensitive to the lunar phase or to the twilight, the only limitation being the telescope being able to guide using the guide star in the optical. In fact, VISIR observations are carried out preferentially during bright time (i.e. close to full moon) as observations with other instruments operating at shorter wavelengths are less efficient during this time.

The other constraints, *image quality* and *airmass*, are the same as for other instruments. Note that the image quality at the wavelength of observation – in the mid-infrared for VISIR – is typically much better than the seeing in the optical as measured by e.g. the seeing monitor (DIMM, see also § 2.3). Please consult the ETC for estimates of the image quality in a specific filter for given ambient conditions. During proposal submission (phase I) the requested *seeing* in the V-band has to be specified, while during the preparation of the OBs in phase II, the *image quality* at the wavelength of observation has to be specified. Consistency between the seeing specified at phase I and the image quality specified in phase II will be checked during the verification of the OBs. If several wavelengths are observed in one OB (e.g. several filters in an imaging OB) the image quality refers to the shortest wavelength of the observation. For other wavelength within the OB, the requested image quality then follows a linear relationship, such as the diffraction limit.

The airmass has a particular strong effect on both image quality and sensitivity in the mid-infrared. This is because of the chopping performance being somewhat airmass dependent and the total emission being dominated by the sky. Therefore, it is advised to observe at airmass  $< 1.5$ , if possible. The effect of the airmass is approximately taken into account by the ETC.

## 5 VISIR data

### 5.1 Data format and orientation

One FITS file is saved for each telescope nod position. This file is a multi-extension FITS file. At each nod position VISIR writes the following information standard:

1. a general header
2. Two averaged frames corresponding to each chop position (`DET.CHOP.CYCSUM = T`)
3. The resulting frame of (the average of chop position 1) minus (the average of chop position 2)

For regular imaging and spectroscopy only the averaged half-cycle frames are stored resulting in files with three FITS-extensions and a size of  $< 13$  MB, with the exact file size depending on the windowing of the detector.

Instead of averaging the exposure at each chop position, it is possible to store all individual chopping half-cycles by setting the half-cycle averaging flag to false (`DET.CHOP.CYCSUM = F`), resulting in files with many FITS extensions and sizes on the order of GigaBytes. Caution



is required using this mode, as this can cause large file write overheads when the DIT is small. Therefore a waiver is required if this mode is requested. For coronagraphy and sparse aperture masking on the other hand, all individual chopping half-cycles are saved by default. The exact number of extensions is then  $2 \cdot \text{CHOP.NCYCLES} + 1$ , where `CHOP.NCYCLES` is the number of chopping cycles per nodding position.

In burst mode, each file is a data cube containing hundreds of elementary frames. Only those frames useful to scientific observations are saved, meaning that all transition frames (for `DET.NDITSKIP`  $\geq 1$ ), while the M2 is moving, are discarded. The total number of files is such that the total integration time requested is reached.

For the default value of the rotator angle ( $0^\circ$ ), the frames from the imager are oriented north up and east left. Spectroscopic data are aligned vertical in the spatial and horizontal in the dispersion direction (cf. Fig. 15). For the LR and MR modes, the wavelength of the spectrum increases towards the left. For the HR and HRX modes, the short wavelength is at the top of the frame if the side *B* of the dual-grating is used, and at the bottom of the frame if the side *A* is used.

.....

Up to 200 frames per second are read for a minimum detector integration time of  $\text{DIT} = 5$  ms. Such a frame rate is too high to store all exposures for most observing programmes. One VISIR image is of size  $1024 \times 1024$ ; each pixel is coded with 4 bytes (long integer). Thus one read-out has a size of 4096 kB.

The current version of the NGC (by default) provides output files in the format of “fits-extensions” for each nodding half-cycle (each nodding position). These are structured in the following way: (i) a general long header, (ii) averages of the images obtained in each of the two chopping positions (chopping half-cycles, one “on-source” and one “off-source”), as well as (iii) a single intermediate-result image for that given nodding position with the two chopping positions subtracted from each other. Each of the three fits-extensions have their own short headers. For coronagraphy and sparse aperture masking, all individual chopping half-cycles are stored by default in separate fits-extensions, plus one additional extension with the (blindly) combined frames.

## 5.2 Pipeline

A pipeline for the reduction of the VISIR data has been developed for the main observation templates. Raw images of imaging and spectroscopic observations are recombined by the pipeline. The pipeline supports shift-and-add for sources which are clearly detected in individual frames (e.g. for data obtained using the burst mode). Spectra are extracted and calibrated in wavelength (§ 5.3) for all spectroscopic modes in low, (medium), high resolution. Sensitivity estimates, based on standard star observations, are provided both in imaging and spectroscopy (§ 4.7). The public release of the VISIR pipeline is accessible at: <http://www.eso.org/sci/software/pipelines/>.

Currently, the pipeline supports the following templates :

- VISIR\_img\_obs\_AutoChopNod
- VISIR\_img\_obs\_BurstAutoChopNod
- VISIR\_spec\_obs\_LRAutoChopNod

- VISIR\_spec\_obs\_MRAutoChopNod
- VISIR\_spec\_obs\_HRAutoChopNod
- VISIR\_spec\_obs\_HRXAutoChopNod

In mosaic (or raster) mode (VISIR\_img\_obs\_GenericChopNod) only raw frames are delivered, e.g. mapping reconstruction algorithms are not supported. Likewise, the pipeline does not support more complex data reduction methods, such as speckle interferometry, coronagraphic data reduction or the reduction of sparse aperture masking data, beyond a combination of the frames obtained using the chopping and nodding technique. A more detailed description of the pipeline capabilities are found in the VISIR Pipeline User Manual ([http://www.eso.org/sci/software/pipelines/#pipelines\\_table](http://www.eso.org/sci/software/pipelines/#pipelines_table)).

### 5.3 Spectrometer data

#### Optical distortion correction

Spectra are deformed by optical distortion and slit curvatures. The VISIR spectrometer uses curved slits to cancel the distortion of the pre-slit optics. Thus the slit projected on the sky is straight. There is an additional linear distortion in both dispersion and cross-dispersion direction of the detector.

The following algorithm corrects for this distortion in low resolution mode and is supported by the pipeline. The detector pixels in dispersion direction are along the  $x$ -axis and in cross-dispersion direction along the  $y$ -axis, respectively. The skew angle with respect to the  $x$ -axis is designated  $\Phi$  and the one with respect to the  $y$ -axis with  $\Psi$ ; the maximum curvature along  $x$  is  $\Delta$  and along  $y$  is  $\epsilon$ .

$\Phi$  is defined positive in clockwise direction and  $\Psi$  counter-clockwise;  $\Delta$  is positive by increasing  $x$  and  $\epsilon$  by decreasing  $y$ . Measured values of the distortion parameters are in the low and medium resolution mode  $\Phi = 0.52^\circ$  and  $\Psi = 1.73^\circ$ . The curvatures in the low resolution mode are  $\epsilon = -0.8$  pixels,  $\Delta = 0.0$  pixels. The center of the lower left of the detector is at (1,1). Therefore, the fix point, which is the detector center, is at (512.2, 512.2) for the  $n = 1024$  AQUARIUS pixel array.

The fix point is moved to (1,1) by:

$$f_1(x, y) = \left(x - \frac{n+1}{2}, y - \frac{n+1}{2}\right) \quad (2)$$

and the skew is corrected along the cross-dispersion:

$$f_2(x, y) = (x + y \cdot \tan(\Psi), y) \quad (3)$$

and along the dispersion direction:

$$f_3(x, y) = (x, y + x \cdot \tan(\Phi)) \quad (4)$$

The curvature is a segment of a circle with radius,  $R$  in  $x$ -direction given by:  $n = 2\sqrt{\epsilon \cdot (2R_\epsilon - \epsilon)}$  and in  $y$ -direction by:  $n = 2\sqrt{\Delta \cdot (2R_\Delta - \Delta)}$ . It is corrected along the cross-dispersion:

$$f_4(x, y) = (x, y - \text{sign}(\epsilon) \cdot (R_\epsilon - \sqrt{R_\epsilon^2 - x^2})) \quad ; \quad (\epsilon \neq 0) \quad (5)$$

and along the dispersion:

$$f_5(x, y) = (x + \text{sign}(\Delta) \cdot (R_\Delta - \sqrt{R_\Delta^2 - y^2}), y) \quad ; \quad (\Delta \neq 0) \quad (6)$$

Finally, the origin of the coordinate system is moved back from the fix point to (1,1):

$$f_6(x, y) = (x + \frac{n+1}{2}, y + \frac{n+1}{2}) \quad (7)$$

The spectral extraction is similar to the one of the TIMMI2 pipeline and described by [Siebenmorgen et al. 2004, AA 414, 123](#).

### Wavelength calibration

A first order wavelength calibration is given by the optical model of the instrument. Its precision is about  $\pm 10$  pixels for the low and medium resolution mode and  $\pm 15$  pixels for the high resolution mode. The wavelength calibration can be refined by using Fabry-Perot Etalons plates or atmospheric lines. In the VISIR FITS file, the averaged half-cycle frames, which are dominated by sky emission lines, are stored (§ 5.1). They can be used to fine-tune the wavelength calibration to sub-pixel precision by comparison with a model of the atmospheric lines. This method is used by the pipeline. More specifically, the zero-point of the wavelength calibration is obtained by cross-correlating the observed sky spectrum with a HITRAN model of the sky emission lines.

Note that the chopped frames cannot be used for calibration with atmospheric lines because the chopping process results in a near perfect cancelation of sky lines.

### Atmosphere absorption correction

The atmosphere does not uniformly absorb the MIR radiation (§ 2.1). At some wavelengths it is completely transparent, at others partly or completely opaque. Differential absorption is often corrected by dividing the extracted spectrum by a reference spectrum. This procedure may cause numerical instabilities at wavelengths close to strong sky lines that might amplify the noise.

### Photometry

Spectro-photometric calibration of low and medium resolution spectra can be achieved with the MIR standard star list provided by the Observatory (see § 4.7). For high resolution spectroscopy only calibrators known with high precision, such as, A stars or asteroids, should be considered. However, even early A stars are known to have some hydrogen absorption lines in the N- and Q-band.

## 6 Description of VISIR templates

### 6.1 Acquisition

Each OB needs to start with an acquisition template. The acquisition process is described in § 4.3.

### 6.2 Observing with the imager

#### VISIR\_img\_obs\_AutoChopNod

This template permits observing a source in imaging configuration with various sub-settings. The observer must specify the filter and the chopper throw, which can be, for the time being, in the range between  $8''$  and  $20''$ . The keyword `SEQ.CHOPNOD.DIR` is set to `PARALLEL` or `PERPENDICULAR`, which results in images as shown in Fig. 20. `PARALLEL` considers an equal nodding and chopping amplitude which are both in parallel direction. It is recommended for faint, extended sources, for which the spatial resolution is not so crucial. `PERPENDICULAR` considers an equal nodding and chopping amplitude; however in perpendicular direction. Note that while the telescope offset is in positive (East) direction, the resulting image on the detector will move to the West. This technique is recommended for point or relatively small extended ( $< 10''$ ) sources (Fig. 5).

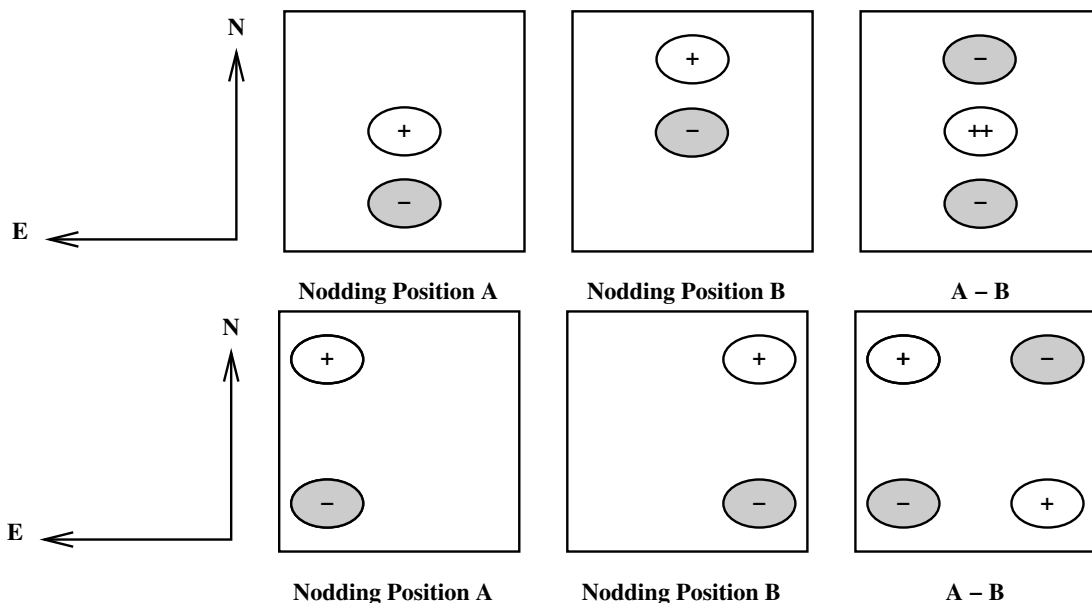


Figure 20: Schematic drawing of the content of a frame obtained with `TEL.ROT.OFFANGLE = TEL.CHOP.POSANG = 0` and `SEQ.CHOPNOD.DIR = PARALLEL` (top) and `SEQ.CHOPNOD.DIR = PERPENDICULAR` (bottom). In the individual nodding positions, the positive beams correspond to the chopper position A and the negative beams to the chopper position B. Note that the default pointing position of the telescope corresponds to the center of the detector. Within the accuracy of the telescope pointing, this location matches the nodding position A, chopper position A if `SEQ.CHOPNOD.DIR = PARALLEL`.

The keyword `SEQ.JITTER.WIDTH` allows chopping and nodding with random offsets so that a jitter pattern is carried out. This technique allows to reconstruct bad pixels. Setting the keyword `SEQ.JITTER.WIDTH` to 0, no jitter is performed and the resulting image depends on

the setting of `SEQ.CHOPNOD.DIR`. The chopping period is set by the system and the number of nodding cycles during the observations period is set by the observer with `SEQ.NODNCYCLES` (§ 3.5). The `DET.CHOP.CYCSUM` keyword specifies if the individual chopping half-cycles should be averaged (set to `TRUE`, default) or not (`FALSE`).

#### `VISIR_img_obs_BurstAutoChopNod`

The observations in burst mode are analogous to imaging with `VISIR_img_obs_AutoChopNod` but all elementary frames are saved. These can be single DIT frames or the average of a number of individual frames set by `SEQ.NAVRG`. Also the detector can be windowed to reduce file writing overheads.

#### `VISIR_img_obs_CoroChopNod`

This template is very similar to `VISIR_img_obs_AutoChopNod`, but should be used for coronagraphic observations. In this mode, however, only `PARALLEL` chopping and nodding is allowed and the list of filters is limited to those for which the coronagraphs are optimised. All chopping half-cycle frames are stored by default.

#### `VISIR_img_obs_SamAutoNod`

This template should be used for sparse aperture masking observations. The list of filters is limited to those for which include a sparse aperture mask. Also for this template, all chopping half-cycle frames are stored by default.

#### `VISIR_img_obs_GenericChopNod`

This imaging template enhances the flexibility of nodding offsets, and allows the user to specify them in a list of relative offset positions. In the most simple application, only one offset position is specified. This allows to record nodding pairs, i.e. cycle of on-off observations, using a flexible offset position. Additional jitter offsets can be specified. More than one entry in the offset list results in a freely programmable pattern of nodding pairs. Note that the integration time specified, `SEQ.TIME`, refers to the entire observation sequence. As for the normal imaging template, the time spent in a certain nodding position will depend on the number of nodding cycles, i.e. on `SEQ.NOFF`. The offset positions are calculated as the cumulative sum of offsets, i.e. are defined relative to the previous offset positions. Note that the telescope always returns to the first (reference) position, when specifying a list of offsets. This mode can be exploited to perform mosaic or raster imaging. The first reference position can then be considered as a sky observation while the offsets refer to object positions. It is recommended to offset to positions that result in observations of overlapping fields, which enhances the redundancy after image reconstruction.

An illustration of generating a raster map can be found in Fig. 21. The following parameters correspond to this setting:

```
SEQ.NOFF                3
SEQ.OFFSET1.LIST       50 15 15
SEQ.OFFSET2.LIST       50 -15 -15
SEQ.OFFSET.COORDS      SKY
```

Note that for the time being, images obtained with the `VISIR_img_obs_GenericChopNod` are not reduced by the ESO VISIR pipeline.

*Pre-imaging observations:* Since Period 76, the observatory supports a fast data release for VISIR pre-imaging observations. Pre-imaging images must be obtained either with the

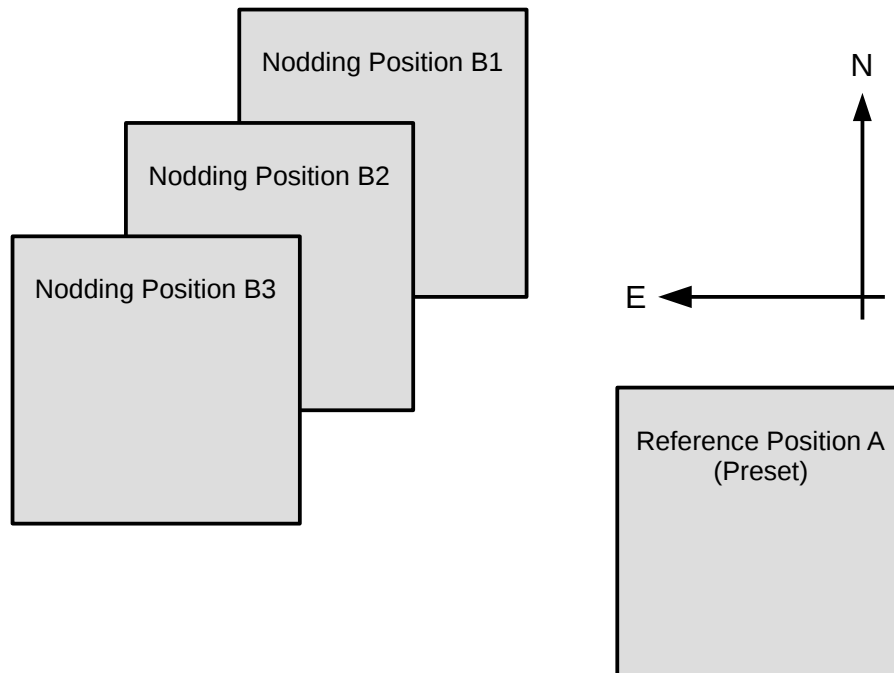


Figure 21: Illustration of generating raster maps with `VISIR_img_obs_GenericChopNod`.

`VISIR_img_obs_AutoChopNod` or `VISIR_img_obs_GenericChopNod` templates. The `SEQ.CATG` keyword must be set to `PRE-IMAGE`. In addition, the name of the OB must start with the prefix `PRE`.

### 6.3 Observing with the spectrometer

Conceptually, the same observing techniques apply for spectroscopy as well as for imaging. The default slit orientation is in the North-South direction. The length of the slit is selected by the keyword `INS.SLIT1.TYPE`: only for cross-dispersed, high resolution, observations `SHORT` must be used, otherwise `LONG` is the default setting.

A preferred observing strategy is called “nodding on the slit”, where the chopping and nodding amplitudes are small (`SEQ.CHOPNOD.DIR = PARALLEL`). Note that “nodding on the slit” requires to set the telescope rotator offset angle *and* the M2 chopping position angle to the same value (which is, in general, different from 0). This is useful to acquire two targets simultaneously in the slit.

The keyword `SEQ.JITTER.WIDTH` allows to apply random offsets *along the slit*.

More complex source geometries might require larger amplitudes, and/or `SEQ.CHOPNOD.DIR = PERPENDICULAR` in order to avoid self-cancellation.

**Low and medium resolution** The templates for low and medium resolution spectroscopy are: `VISIR_spec_obs_LRAutoChopNod` and `VISIR_spec_obs_MRAutoChopNod`, respectively. Observing parameters are: total integration time (`SEQ.TIME`), the slit width `INS.SLIT1.WIDTH`, `SEQ.CHOPNOD.DIR` and, for medium resolution, the central wavelength (`INS.GRAT1.WLEN`, see § 6.2).

#### High resolution: long-slit mode

Template for high resolution spectroscopy is `VISIR_spc_obs_HRAutoChopNod`. Three order sorting filter at 8.02, 12.81 and 17.03 $\mu\text{m}$ , `INS.FILT2.NAME = ([H2_S4],[NeII],[H2_S1])` are avail-

able. See Table 2 for the corresponding list of offered central wavelengths. Other observing parameters are: total integration time (`SEQ.TIME`), central wavelength (`INS.GRAT1.WLEN`), the slit width (`INS.SLIT1.WIDTH`) and `SEQ.CHOPNOD.DIR` (§ 6.2).

### High resolution: cross-dispersed mode

`VISIR_spc_obs_HRXAutoChopNod` is functionally similar to `VISIR_spc_obs_HRAutoChopNod`, but uses a grism for cross-dispersion and order-separation. The effective length of the spectrograph slit in this mode is limited to  $\sim 4''$ . The entire wavelength range between 7.7 and 13.3  $\mu\text{m}$  is accessible using the cross-dispersed (HRX) mode. Total integration time (`SEQ.TIME`), the slit width (`INS.SLIT1.WIDTH`) and `SEQ.CHOPNOD.DIR` are specified as usual (§ 6.2).

## 6.4 Calibration

Specific templates exist for the observations of photometric and spectro-photometric standard stars. They offer the same functionality as the corresponding science templates, but allow to monitor the sensitivity and image quality by observing standard stars, that is calibrators.

Their use is recommended to be properly recognized by the VISIR pipeline.

## 7 Checklist

This section provides advice for the preparation of the proposal (phase I) and of the Observing blocks (phase II).

### 7.1 Phase 1

It is very important that the time justification (Box 9) of the proposal contains enough information so that its feasibility can be correctly assessed. The following points must be respected:

1. the expected S/N and source brightness estimate for each object and mode must be given;
2. in particular for extended sources: does the reported S/N refer to an area of 1 arcsec<sup>2</sup> (as given by the imaging ETC), to an extent of 1 arcsec in the spatial direction (as given by the spectroscopy ETC) or to the whole spatial extent of the object?
3. in spectroscopy, does the S/N refer to one pixel in the dispersion direction (as given by the ETC) or to one resolution element?
4. in case of large throw, does the S/N take into account the fact that some beams would fall outside the detector?
5. does the overhead calculation include the time required for each preset, given that OBs should in general not be longer than 1 hour?
6. is there a guide star brighter than  $V = 13.5$  mag within a radius of 7.5 arcmin around the object?
7. the PWV constraint needs to be specified as a comment for each target in the Target List (Box 11) of the proposal. The effect of different PWV values on the sensitivity can be assessed using the ETC (see § 4.1).

### 7.2 Phase 2

1. *Acquisition:* Are the coordinates accurate in the equinox J2000.0 reference frame? For high-proper motion objects, are they valid for the epoch of the observations? For solar system objects, are they in the topocentric, ICRF or FK5, J2000.0 reference frame at the epoch of the observations?
2. *Acquisition:* If the `VISIR_img_acq_Preset` is used and the following templates have `SEQ.CHOPNOD.DIR = PERPENDICULAR`, the target will appear at the center of the detector by default, with the risk of losing 3 beams that would appear outside of the field. Either slightly change the coordinates of `TEL.TARG.ALPHA` and `TEL.TARG.DELTA`, or use `TEL.TARG.OFFSETALPHA` and `TEL.TARG.OFFSETDELTA` (see § 4.3).
3. *Acquisition:* Rather use `VISIR_img_acq_MoveToPixel` instead of `VISIR_img_acq_Preset` if the goal of the observations is to obtain accurate photometry or to identify faint structures around a bright object. This is to allow an accurate positioning of the source into



the centre of one of the detector outputs and to avoid the “bleeding”-effect of the detector (see § 3.4.6). If applicable, a note should be put into the README file specifically drawing the attention to this issue.

4. *Filters:* Be aware of the windowing of the detector for several filters, especially also when specifying the chopping parameters (see § 3.4).
5. *Acquisition:* It is strongly recommended that a guide star is selected and inserted in the acquisition template for all OBs of a same field, in particular if
  - relatively good astrometric accuracy is required;
  - the object is faint or diffuse and unlikely to be visible on short exposures;
  - the object appears in the field of a bright nebula that saturates the digitized sky survey (DSS) used by the telescope and instrument operator;
  - a chopping throw of more than 25'' is required.

The GuideCamTool (see § 4.4) can help in selecting appropriate guide stars and to insert the correct information into the OB.

6. *Calibrations:* For calibration OBs, use the appropriate VISIR\_img\_cal\_AutoChopNod or VISIR\_spc\_cal\_LR/MR/HR/HRXAutoChopNod templates.
7. *Position angle:* If the observations must be carried out at a position angle different from 0, check § 4.2.1 and § 4.2.2. In particular, it is useful to clearly indicate in the README file if TEL.CHOP.POSANG is not equal to TEL.ROT.OFFANGLE to warn the instrument operator about the non-standard configuration. In particular, in spectroscopy, TEL.CHOP.POSANG must be equal to TEL.ROT.OFFANGLE in order to have the 3 beams along the slit.
8. OB comment: specify the expected source flux density in the user comment of each OB and in the readme. This will be very beneficial in operations.
9. Constraints: Do the constraints make sense (see § 4.8)? Remember that the image quality is at the observing wavelength of the shortest wavelength setting/filter of the OB. Remember the PWV and airmass recommendations.

## 8 Appendix: VISIR template parameters

Note that the template parameters listed here only reflect the current state of the template definition. The templates are subject to change during the consolidation of the instrument status.

VISIR_img_acq_Preset.tsf			
<i>To be specified:</i>			
Parameter	Hidden	Range ( <i>Default</i> )	Label
<b>SEQ.PRESET</b>	yes	F T ( <i>T</i> )	Preset flag
<b>SEQ.PUPILTRK</b>	yes	F T ( <i>F</i> )	Pupil tracking enable
<b>TEL.AG.GUIDESTAR</b>	no	CATALOGUE      SETUPFILE NONE ( <i>CATALOGUE</i> )	Get Guide Star from
<b>TEL.GS1.ALPHA</b>	no	ra $\hat{}$	Guide star RA
<b>TEL.GS1.DELTA</b>	no	dec $\hat{}$	Guide star DEC
<b>TEL.ROT.OFFANGLE</b>	no	0..360 ( <i>0.0</i> )	Rotator on Sky (=PA on Sky)
<b>TEL.TARG.ADDVELALPHA</b>	yes	( <i>0.0</i> )	RA additional tracking velocity
<b>TEL.TARG.ADDVELDELTA</b>	yes	( <i>0.0</i> )	DEC additional tracking velocity
<b>TEL.TARG.ALPHA</b>	no	ra $\hat{}$	Alpha coordinate for the target
<b>TEL.TARG.DELTA</b>	no	dec $\hat{}$	Delta coordinate for the target
<b>TEL.TARG.EPOCH</b>	no	-2000..3000 ( <i>2000.0</i> )	Epoch
<b>TEL.TARG.EQUINOX</b>	no	-2000.0..3000.0 ( <i>2000.0</i> )	Equinox
<b>TEL.TARG.OFFSETALPHA</b>	no	( <i>0.0</i> )	RA blind offset
<b>TEL.TARG.OFFSETDELTA</b>	no	( <i>0.0</i> )	DEC blind offset
<b>TEL.TARG.PMA</b>	no	-10..10 ( <i>0.0</i> )	Proper Motion Alpha
<b>TEL.TARG.PMD</b>	no	-10..10 ( <i>0.0</i> )	Proper Motion Delta
<i>Fixed values:</i>			
Parameter	Hidden	Value	Label
<b>INS.MODE</b>	no	IMG	Instrument Mode
<b>INS.SOURCE</b>	no	SKY	Detector source
<b>TEL.TARG.TYPE</b>	no	COORDINATE	Type of given target

VISIR_img_acq_MoveToCoro.tsf			
<i>To be specified:</i>			
Parameter	Hidden	Range (Default)	Label
DET.CHOP.CYCSUM	no	F T ( <i>T</i> )	Half-Cycle Averaging flag
INS.FILT1.NAME	no	10.5_4QP 11.3_4QP 12.3_AGP 12.4_AGP ( <i>12.3_AGP</i> )	Imager Filter
INS.OPTI1.NAME	no	AGPM 4QPM_1 4QPM_2 ( <i>AGPM</i> )	Imager diaph
SEQ.CHOP.GUIDE	yes	A B BOTH ( <i>BOTH</i> )	Chopping guide window
SEQ.CHOP	yes	F T ( <i>T</i> )	Chop flag
SEQ.NOD	yes	F T ( <i>T</i> )	Nodding flag
SEQ.NODNCYCLES	no	1..100 ( <i>NODEFAULT</i> )	Number of nodding cycles.
SEQ.PFOV	yes	LF IF SF SP ( <i>SF</i> )	Pixel Field of View
SEQ.PRESET	yes	F T ( <i>T</i> )	Preset flag
SEQ.PUPILTRK	no	F T ( <i>F</i> )	Pupil tracking enable
SEQ.TIME	no	30..3600 ( <i>NODEFAULT</i> )	Total integration time (sec)
TEL.AG.GUIDESTAR	no	CATALOGUE SETUPFILE NONE ( <i>CATALOGUE</i> )	Get Guide Star from
TEL.CHOP.POSANG	no	0..360 ( <i>0</i> )	Chopping Position Angle (deg)
TEL.CHOP.THROW	no	8..30 ( <i>8</i> )	Chopping Amplitude (arcsec)
TEL.GS1.ALPHA	no	ra ( <i>)</i>	Guide star RA
TEL.GS1.DELTA	no	dec ( <i>)</i>	Guide star DEC
TEL.ROT.OFFANGLE	no	0..360 ( <i>0.0</i> )	Rotator on Sky (=-PA on Sky)
TEL.TARG.ADDVELALPHA	yes	( <i>0.0</i> )	RA additional tracking velocity
TEL.TARG.ADDVELDELTA	yes	( <i>0.0</i> )	DEC additional tracking velocity
TEL.TARG.ALPHA	no	ra ( <i>)</i>	Alpha coordinate for the target
TEL.TARG.DELTA	no	dec ( <i>)</i>	Delta coordinate for the target
TEL.TARG.EPOCH	no	-2000..3000 ( <i>2000.0</i> )	Epoch
TEL.TARG.EQUINOX	no	-2000.0..3000.0 ( <i>2000.0</i> )	Equinox
TEL.TARG.OFFSETALPHA	no	( <i>0.0</i> )	RA blind offset
TEL.TARG.OFFSETDELTA	no	( <i>0.0</i> )	DEC blind offset
TEL.TARG.PMA	no	-10..10 ( <i>0.0</i> )	Proper Motion Alpha
TEL.TARG.PMD	no	-10..10 ( <i>0.0</i> )	Proper Motion Delta
<i>Fixed values:</i>			
Parameter	Hidden	Value	Label
DPR.CATG	no	ACQUISITION	Data Prod. Categ.
DPR.TECH	no	CORONOGRAPHY	Data Prod. Tech.
DPR.TYPE	no	OBJECT	Data Prod. Type
INS.MODE	no	IMG	Instrument Mode
INS.SOURCE	no	SKY	Detector source
SEQ.CHOPNOD.DIR	no	PARALLEL	Relative Chop/Nod Direction
TEL.TARG.TYPE	no	COORDINATE	Type of given target

VISIR_img_acq_MoveToPixel.tsf			
<i>To be specified:</i>			
Parameter	Hidden	Range (Default)	Label
<b>DET.CHOP.CYCSUM</b>	no	F T ( <i>T</i> )	Half-Cycle Averaging flag
<b>INS.FILT1.NAME</b>	no	PAH1 ARIII SIV_1 SIV SIV_2 PAH2 PAH2_2 K-BAND M- BAND NEIL1 NEII NEII_2 Q1 Q2 Q3 B10.7 B11.7 B12.4 J7.9 J8.9 J9.8 J12.2 ( <i>NODEFAULT</i> )	Imager Filter
<b>SEQ.CHOP.GUIDE</b>	yes	A B BOTH ( <i>BOTH</i> )	Chopping guide window
<b>SEQ.CHOP</b>	yes	F T ( <i>T</i> )	Chop flag
<b>SEQ.CHOPNOD.DIR</b>	no	PARALLEL PERPENDICU- LAR ( <i>PERPENDICULAR</i> )	Relative Chop/Nod Direction
<b>SEQ.NOD</b>	yes	F T ( <i>T</i> )	Nodding flag
<b>SEQ.NODNCYCLES</b>	no	1..100 ( <i>NODEFAULT</i> )	Number of nodding cycles.
<b>SEQ.PFOV</b>		IF SF ( <i>SF</i> )	Pixel Field of View
<b>SEQ.PRESET</b>	yes	F T ( <i>T</i> )	Preset flag
<b>SEQ.PUPILTRK</b>	yes	F T ( <i>F</i> )	Pupil tracking enable
<b>SEQ.TIME</b>	no	30..3600 ( <i>NODEFAULT</i> )	Total integration time (sec)
<b>TEL.AG.GUIDESTAR</b>	no	CATALOGUE SETUPFILE NONE ( <i>CATALOGUE</i> )	Get Guide Star from
<b>TEL.CHOP.POSANG</b>	no	0..360 ( <i>0</i> )	Chopping Position Angle (deg)
<b>TEL.CHOP.THROW</b>	no	8..30 ( <i>8</i> )	Chopping Amplitude (arcsec)
<b>TEL.GS1.ALPHA</b>	no	ra ( <i>)</i>	Guide star RA
<b>TEL.GS1.DELTA</b>	no	dec ( <i>)</i>	Guide star DEC
<b>TEL.ROT.OFFANGLE</b>	no	0..360 ( <i>0.0</i> )	Rotator on Sky (=PA on Sky)
<b>TEL.TARG.ADDVELALPHA</b>	yes	( <i>0.0</i> )	RA additional tracking velocity
<b>TEL.TARG.ADDVELDELTA</b>	yes	( <i>0.0</i> )	DEC additional tracking velocity
<b>TEL.TARG.ALPHA</b>	no	ra ( <i>)</i>	Alpha coordinate for the target
<b>TEL.TARG.DELTA</b>	no	dec ( <i>)</i>	Delta coordinate for the target
<b>TEL.TARG.EPOCH</b>	no	-2000..3000 ( <i>2000.0</i> )	Epoch
<b>TEL.TARG.EQUINOX</b>	no	-2000.0..3000.0 ( <i>2000.0</i> )	Equinox
<b>TEL.TARG.OFFSETALPHA</b>	no	( <i>0.0</i> )	RA blind offset
<b>TEL.TARG.OFFSETDELTA</b>	no	( <i>0.0</i> )	DEC blind offset
<b>TEL.TARG.PMA</b>	no	-10..10 ( <i>0.0</i> )	Proper Motion Alpha
<b>TEL.TARG.PMD</b>	no	-10..10 ( <i>0.0</i> )	Proper Motion Delta
<i>Fixed values:</i>			
Parameter	Hidden	Value	Label
<b>DPR.CATG</b>	no	ACQUISITION	Data Prod. Categ.
<b>DPR.TECH</b>	no	IMAGE	Data Prod. Tech.
<b>DPR.TYPE</b>	no	OBJECT	Data Prod. Type
<b>INS.MODE</b>	no	IMG	Instrument Mode
<b>INS.SOURCE</b>	no	SKY	Detector source
<b>TEL.TARG.TYPE</b>	no	COORDINATE	Type of given target

VISIR_img_acq_MoveToSam.tsf			
<i>To be specified:</i>			
Parameter	Hidden	Range ( <i>Default</i> )	Label
DET.CHOP.CYCSUM	no	F T ( <i>T</i> )	Half-Cycle Averaging flag
INS.FILT1.NAME	no	10.5_SAM            11.3_SAM ( <i>10.5_SAM</i> )	Filter + SAM
SEQ.CHOP.GUIDE	yes	A B BOTH ( <i>BOTH</i> )	Chopping guide window
SEQ.CHOP	yes	F T ( <i>T</i> )	Chop flag
SEQ.CHOPNOD.DIR	no	PARALLEL    PERPENDICU- LAR ( <i>PARALLEL</i> )	Relative Chop/Nod Direction
SEQ.FILT1.NAME	no	PAH1 ARIII SIV_1 SIV SIV_2 PAH2 PAH2_2 K-BAND M- BAND NEII_1 NEII NEII_2 Q1 Q2 Q3 B10.7 B11.7 B12.4 J7.9 J8.9 J9.8 J12.2 ( <i>NEII_2</i> )	Imager Acquisition Filter
SEQ.NOD	yes	F T ( <i>T</i> )	Nodding flag
SEQ.NODNCYCLES	no	1..100 ( <i>NODEFAULT</i> )	Number of nodding cycles.
SEQ.PFOV	yes	LF IF SF SP ( <i>SF</i> )	Pixel Field of View
SEQ.PRESET	yes	F T ( <i>T</i> )	Preset flag
SEQ.TIME	no	30..3600 ( <i>NODEFAULT</i> )	Total integration time (sec)
TEL.AG.GUIDESTAR	no	CATALOGUE    SETUPFILE NONE ( <i>CATALOGUE</i> )	Get Guide Star from
TEL.CHOP.POSANG	no	0..360 ( <i>0</i> )	Chopping Position Angle (deg)
TEL.CHOP.THROW	no	8..30 ( <i>8</i> )	Chopping Amplitude (arcsec)
TEL.GS1.ALPHA	no	ra $\langle$	Guide star RA
TEL.GS1.DELTA	no	dec $\langle$	Guide star DEC
TEL.TARG.ADDVELALPHA	yes	( <i>0.0</i> )	RA additional tracking velocity
TEL.TARG.ADDVELDELTA	yes	( <i>0.0</i> )	DEC additional tracking velocity
TEL.TARG.ALPHA	no	ra $\langle$	Alpha coordinate for the target
TEL.TARG.DELTA	no	dec $\langle$	Delta coordinate for the target
TEL.TARG.EPOCH	no	-2000..3000 ( <i>2000.0</i> )	Epoch
TEL.TARG.EQUINOX	no	-2000.0..3000.0 ( <i>2000.0</i> )	Equinox
TEL.TARG.OFFSETALPHA	no	( <i>0.0</i> )	RA blind offset
TEL.TARG.OFFSETDELTA	no	( <i>0.0</i> )	DEC blind offset
TEL.TARG.PMA	no	-10..10 ( <i>0.0</i> )	Proper Motion Alpha
TEL.TARG.PMD	no	-10..10 ( <i>0.0</i> )	Proper Motion Delta
<i>Fixed values:</i>			
Parameter	Hidden	Value	Label
DPR.CATG	no	ACQUISITION	Data Prod. Categ.
DPR.TECH	no	IMAGE	Data Prod. Tech.
DPR.TYPE	no	OBJECT	Data Prod. Type
INS.MODE	no	IMG	Instrument Mode
INS.OPTI1.NAME	no	IMAGING	Imager diaph
INS.SOURCE	no	SKY	Detector source
SEQ.PUPILTRK	no	T	Pupil tracking enable
TEL.TARG.TYPE	no	COORDINATE	Type of given target

VISIR_spec_acq_MoveToSlit.tsf			
<i>To be specified:</i>			
Parameter	Hidden	Range (Default)	Label
DET.CHOP.CYCSUM	yes	F T (T)	Half-Cycle Averaging flag
INS.FILT2.NAME	no	ARIII NEII.2 (NODEFAULT)	Acquisition Filter
INS.SLIT1.TYPE	no	LONG SHORT (LONG)	Spectrometer Slit Type (long or short)
INS.SLIT1.WIDTH	no	0.40 0.75 1.00 (NODEFAULT)	Spectrometer Slit Width (arcsec)
SEQ.CHOP.GUIDE	yes	A B BOTH (BOTH)	Chopping guide window
SEQ.CHOP	yes	F T (T)	Chop flag
SEQ.CHOPNOD.DIR	no	PARALLEL PERPENDICULAR (PARALLEL)	Relative Chop/Nod Direction
SEQ.NOD	yes	F T (T)	Nodding flag
SEQ.NODNCYCLES	no	1..100 (NODEFAULT)	Number of nodding cycles.
SEQ.PRESET	yes	F T (T)	Preset flag
SEQ.PUPILTRK	yes	F T (F)	Pupil tracking enable
SEQ.TIME	no	30..3600 (NODEFAULT)	Total integration time (sec)
TEL.AG.GUIDESTAR	no	CATALOGUE SETUPFILE NONE (CATALOGUE)	Get Guide Star from
TEL.CHOP.POSANG	no	0..360 (0)	Chopping Position Angle (deg)
TEL.CHOP.THROW	no	8..30 (8)	Chopping Amplitude (arcsec)
TEL.GS1.ALPHA	no	ra ( )	Guide star RA
TEL.GS1.DELTA	no	dec ( )	Guide star DEC
TEL.ROT.OFFANGLE	no	0..360 (0.0)	Rotator on Sky (= -PA on Sky)
TEL.TARG.ADDVELALPHA	yes	(0.0)	RA additional tracking velocity
TEL.TARG.ADDVELDELTA	yes	(0.0)	DEC additional tracking velocity
TEL.TARG.ALPHA	no	ra ( )	Alpha coordinate for the target
TEL.TARG.DELTA	no	dec ( )	Delta coordinate for the target
TEL.TARG.EPOCH	no	-2000..3000 (2000.0)	Epoch
TEL.TARG.EQUINOX	no	-2000.0..3000.0 (2000.0)	Equinox
TEL.TARG.OFFSETALPHA	no	(0.0)	RA blind offset
TEL.TARG.OFFSETDELTA	no	(0.0)	DEC blind offset
TEL.TARG.PMA	no	-10..10 (0.0)	Proper Motion Alpha
TEL.TARG.PMD	no	-10..10 (0.0)	Proper Motion Delta
<i>Fixed values:</i>			
Parameter	Hidden	Value	Label
DPR.CATG	no	ACQUISITION	Data Prod. Categ.
DPR.TECH	no	IMAGE	Data Prod. Tech.
DPR.TYPE	no	OBJECT	Data Prod. Type
INS.MODE	no	SPCIMG	Instrument Mode
INS.SOURCE	no	SKY	Detector source
TEL.TARG.TYPE	no	COORDINATE	Type of given target

VISIR_spec_acq_ImgMoveToSlit.tsf			
<i>To be specified:</i>			
Parameter	Hidden	Range (Default)	Label
DET.CHOP.CYCSUM	no	F T ( <i>T</i> )	Half-Cycle Averaging flag
INS.FILT1.NAME	no	PAH1 ARIII SIV_1 SIV SIV_2 PAH2 PAH2.2 K-BAND M- BAND NEII_1 NEII NEII.2 Q1 Q2 Q3 B10.7 B11.7 B12.4 J7.9 J8.9 J9.8 J12.2 ( <i>NODEFAULT</i> )	Imager Filter
INS.FILT2.NAME	no	ARIII NEII.2 ( <i>NODEFAULT</i> )	Acquisition Filter
INS.SLIT1.TYPE	no	LONG SHORT ( <i>LONG</i> )	Spectrometer Slit Type (long or short)
INS.SLIT1.WIDTH	no	0.40 0.75 1.00 ( <i>NODEFAULT</i> )	Spectrometer Slit Width (arcsec)
SEQ.CHOP.GUIDE	yes	A B BOTH ( <i>BOTH</i> )	Chopping guide window
SEQ.CHOP	yes	F T ( <i>T</i> )	Chop flag
SEQ.CHOPNOD.DIR	no	PARALLEL PERPENDICU- LAR ( <i>PARALLEL</i> )	Relative Chop/Nod Direction
SEQ.NOD	yes	F T ( <i>T</i> )	Nodding flag
SEQ.NODNCYCLES	no	1..100 ( <i>NODEFAULT</i> )	Number of nodding cycles.
SEQ.PFOV	yes	LF IF SF ( <i>SF</i> )	Pixel Field of View
SEQ.PRESET	yes	F T ( <i>T</i> )	Preset flag
SEQ.PUPILTRK	yes	F T ( <i>F</i> )	Pupil tracking enable
SEQ.TIME	no	30..3600 ( <i>NODEFAULT</i> )	Total integration time (sec)
TEL.AG.GUIDESTAR	no	CATALOGUE SETUPFILE NONE ( <i>CATALOGUE</i> )	Get Guide Star from
TEL.CHOP.POSANG	no	0..360 ( <i>0</i> )	Chopping Position Angle (deg)
TEL.CHOP.THROW	no	8..30 ( <i>8</i> )	Chopping Amplitude (arcsec)
TEL.GS1.ALPHA	no	ra $\cap$	Guide star RA
TEL.GS1.DELTA	no	dec $\cap$	Guide star DEC
TEL.ROT.OFFANGLE	no	0..360 ( <i>0.0</i> )	Rotator on Sky (=PA on Sky)
TEL.TARG.ADDVELALPHA	yes	( <i>0.0</i> )	RA additional tracking velocity
TEL.TARG.ADDVELDELTA	yes	( <i>0.0</i> )	DEC additional tracking velocity
TEL.TARG.ALPHA	no	ra $\cap$	Alpha coordinate for the target
TEL.TARG.DELTA	no	dec $\cap$	Delta coordinate for the target
TEL.TARG.EPOCH	no	-2000..3000 ( <i>2000.0</i> )	Epoch
TEL.TARG.EQUINOX	no	-2000.0..3000.0 ( <i>2000.0</i> )	Equinox
TEL.TARG.OFFSETALPHA	no	( <i>0.0</i> )	RA blind offset
TEL.TARG.OFFSETDELTA	no	( <i>0.0</i> )	DEC blind offset
TEL.TARG.PMA	no	-10..10 ( <i>0.0</i> )	Proper Motion Alpha
TEL.TARG.PMD	no	-10..10 ( <i>0.0</i> )	Proper Motion Delta
<i>Fixed values:</i>			
Parameter	Hidden	Value	Label
DPR.CATG	no	ACQUISITION	Data Prod. Categ.
DPR.TECH	no	IMAGE	Data Prod. Tech.
DPR.TYPE	no	OBJECT	Data Prod. Type
INS.MODE	no	IMG	Instrument Mode
INS.SOURCE	no	SKY	Detector source
TEL.TARG.TYPE	no	COORDINATE	Type of given target

VISIR_img_obs_AutoChopNod.tsf			
<i>To be specified:</i>			
Parameter	Hidden	Range (Default)	Label
<b>DET.CHOP.CYCSUM</b>	no	F T ( <i>T</i> )	Half-Cycle Averaging flag
<b>INS.FILT1.NAME</b>	no	PAH1 ARIII SIV_1 SIV SIV_2 PAH2 PAH2_2 K-BAND M- BAND NEIL1 NEII NEII_2 Q1 Q2 Q3 B10.7 B11.7 B12.4 J7.9 J8.9 J9.8 J12.2 ( <i>NODEFAULT</i> )	Imager Filter
<b>SEQ.CATG</b>	no	PRE-IMAGE SCIENCE CALIB TEST ( <i>SCIENCE</i> )	Observation Category
<b>SEQ.CHOP.GUIDE</b>	yes	A B BOTH ( <i>BOTH</i> )	Chopping guide window
<b>SEQ.CHOP</b>	yes	F T ( <i>T</i> )	Chop flag
<b>SEQ.CHOPNOD.DIR</b>	no	PARALLEL PERPENDICU- LAR ( <i>PERPENDICULAR</i> )	Relative Chop/Nod Direction
<b>SEQ.JITTER.WIDTH</b>	no	0..10 ( <i>0</i> )	Random Jitter Width (arcsec)
<b>SEQ.NOD</b>	yes	F T ( <i>T</i> )	Nodding flag
<b>SEQ.NODNCYCLES</b>	no	1..100 ( <i>NODEFAULT</i> )	Number of nodding cycles.
<b>SEQ.PFOV</b>		IF SF ( <i>SF</i> )	Pixel Field of View
<b>SEQ.RETURN</b>	no	F T ( <i>T</i> )	Return to Origin
<b>SEQ.TIME</b>	no	60..3600 ( <i>NODEFAULT</i> )	Total integration time (sec)
<b>TEL.CHOP.POSANG</b>	no	0..360 ( <i>0</i> )	Chopping Position Angle (deg)
<b>TEL.CHOP.THROW</b>	no	8..30 ( <i>8</i> )	Chopping Amplitude (arcsec)
<i>Fixed values:</i>			
Parameter	Hidden	Value	Label
<b>DET.READ.CURNAME</b>	yes	ROW_HG_SRR	Detector Readout Mode
<b>DPR.CATG</b>	no	SCIENCE	Data Prod. Categ.
<b>DPR.TECH</b>	no	IMAGE	Data Prod. Tech.
<b>DPR.TYPE</b>	no	OBJECT	Data Prod. Type
<b>INS.MODE</b>	no	IMG	Instrument Mode
<b>INS.SOURCE</b>	no	SKY	Detector source



VISIR_img_obs_BurstAutoChopNod.tsf			
<i>To be specified:</i>			
Parameter	Hidden	Range (Default)	Label
<b>DET.CHOP.CYCSUM</b>	yes	F T ( <i>T</i> )	Half-Cycle Averaging flag
<b>INS.FILT1.NAME</b>	no	PAH1 ARIII SIV_1 SIV SIV_2 PAH2 PAH2.2 K-BAND M- BAND NEII_1 NEII NEII.2 Q1 Q2 Q3 B10.7 B11.7 B12.4 J7.9 J8.9 J9.8 J12.2 ( <i>NODEFAULT</i> )	Imager Filter
<b>SEQ.CATG</b>	no	PRE-IMAGE SCIENCE CALIB TEST ( <i>SCIENCE</i> )	Observation Category
<b>SEQ.CHOP.GUIDE</b>	yes	A B BOTH ( <i>BOTH</i> )	Chopping guide window
<b>SEQ.CHOP</b>	yes	F T ( <i>T</i> )	Chop flag
<b>SEQ.CHOPNOD.DIR</b>	no	PARALLEL PERPENDICU- LAR ( <i>PERPENDICULAR</i> )	Relative Chop/Nod Direction
<b>SEQ.JITTER.WIDTH</b>	no	0..10 ( <i>0</i> )	Random Jitter Width (arcsec)
<b>SEQ.NAVRG</b>	no	1..4 ( <i>1</i> )	Number of frames to be averaged
<b>SEQ.NOD</b>	yes	F T ( <i>T</i> )	Nodding flag
<b>SEQ.NODNCYCLES</b>	no	1..100 ( <i>NODEFAULT</i> )	Number of nodding cycles.
<b>SEQ.PFOV</b>		IF SF ( <i>SF</i> )	Pixel Field of View
<b>SEQ.TIME</b>	no	30..1200 ( <i>360</i> )	Total integration time (sec)
<b>SEQ.WIN.NX</b>	no	0.0..1024.0 ( <i>1024.0</i> )	Read-out window NX
<b>SEQ.WIN.NY</b>	no	0.0..1024.0 ( <i>900.0</i> )	Read-out window NY
<b>SEQ.WIN.STARTX</b>	no	1.0..1023.0 ( <i>1.0</i> )	Read-out window start-x
<b>TEL.CHOP.POSANG</b>	no	0..360 ( <i>0</i> )	Chopping Position Angle (deg)
<b>TEL.CHOP.THROW</b>	no	8..30 ( <i>8</i> )	Chopping Amplitude (arcsec)
<i>Fixed values:</i>			
Parameter	Hidden	Value	Label
<b>DET.READ.CURNAME</b>	yes	ROW_HG_SRR_BURST	Detector Readout Mode
<b>DPR.CATG</b>	no	SCIENCE	Data Prod. Categ.
<b>DPR.TECH</b>	no	IMAGE,BURST	Data Prod. Tech.
<b>DPR.TYPE</b>	no	OBJECT	Data Prod. Type
<b>INS.MODE</b>	no	IMG	Instrument Mode
<b>INS.SOURCE</b>	no	SKY	Detector source
<b>SEQ.RETURN</b>	no	T	Return to Origin

VISIR_img_obs_CoroChopNod.tsf			
<i>To be specified:</i>			
Parameter	Hidden	Range (Default)	Label
<b>DET.CHOP.CYCSUM</b>	no	F T ( <i>F</i> )	Half-Cycle Averaging flag
<b>INS.FILT1.NAME</b>	no	10.5_4QP 11.3_4QP 12.3_AGP 12.4_AGP ( <i>12.3_AGP</i> )	Imager Filter
<b>INS.OPT11.NAME</b>	no	AGPM 4QPM_1 4QPM_2 ( <i>AGPM</i> )	Imager diaph
<b>SEQ.CATG</b>	no	PRE-IMAGE SCIENCE CALIB TEST ( <i>SCIENCE</i> )	Observation Category
<b>SEQ.CHOP.GUIDE</b>	yes	A B BOTH ( <i>BOTH</i> )	Chopping guide window
<b>SEQ.CHOP</b>	yes	F T ( <i>T</i> )	Chop flag
<b>SEQ.NOD</b>	yes	F T ( <i>T</i> )	Nodding flag
<b>SEQ.NODNCYCLES</b>	no	1..100 ( <i>NODEFAULT</i> )	Number of nodding cycles.
<b>SEQ.PFOV</b>	yes	LF IF SF SP ( <i>SF</i> )	Pixel Field of View
<b>SEQ.RETURN</b>	no	F T ( <i>T</i> )	Return to Origin
<b>SEQ.TIME</b>	no	60..3600 ( <i>NODEFAULT</i> )	Total integration time (sec)
<b>TEL.CHOP.POSANG</b>	no	0..360 ( <i>0</i> )	Chopping Position Angle (deg)
<b>TEL.CHOP.THROW</b>	no	8..30 ( <i>8</i> )	Chopping Amplitude (arcsec)
<i>Fixed values:</i>			
Parameter	Hidden	Value	Label
<b>DET.READ.CURNAME</b>	yes	ROW_HG_SRR	Detector Readout Mode
<b>DPR.CATG</b>	no	SCIENCE	Data Prod. Categ.
<b>DPR.TECH</b>	no	CORONOGRAPHY	Data Prod. Tech.
<b>DPR.TYPE</b>	no	OBJECT	Data Prod. Type
<b>INS.MODE</b>	no	IMG	Instrument Mode
<b>INS.SOURCE</b>	no	SKY	Detector source
<b>SEQ.CHOPNOD.DIR</b>	no	PARALLEL	Relative Chop/Nod Direction
<b>SEQ.JITTER.WIDTH</b>	no	0	Random Jitter Width (arcsec)

VISIR_img_obs_GenericChopNod.tsf			
<i>To be specified:</i>			
Parameter	Hidden	Range (Default)	Label
<b>DET.CHOP.CYCSUM</b>	no	F T ( <i>T</i> )	Half-Cycle Averaging flag
<b>INS.FILT1.NAME</b>	no	PAH1 ARIII SIV_1 SIV SIV_2 PAH2 PAH2.2 K-BAND M- BAND NEII_1 NEII NEII.2 Q1 Q2 Q3 B10.7 B11.7 B12.4 J7.9 J8.9 J9.8 J12.2 ( <i>NODEFAULT</i> )	Imager Filter
<b>SEQ.CATG</b>	no	PRE-IMAGE SCIENCE CALIB TEST ( <i>SCIENCE</i> )	Observation Category
<b>SEQ.CHOP.GUIDE</b>	yes	A B BOTH ( <i>BOTH</i> )	Chopping guide window
<b>SEQ.CHOP</b>	yes	F T ( <i>T</i> )	Chop flag
<b>SEQ.NOD</b>	yes	F T ( <i>T</i> )	Nodding flag
<b>SEQ.NOFF</b>	no	1..100 ( <i>NODEFAULT</i> )	Number of offset positions
<b>SEQ.OFFSET.COORDS</b>	no	SKY DETECTOR ( <i>NODE- FAULT</i> )	Offset coordinates
<b>SEQ.OFFSET1.LIST</b>	no	( <i>NODEFAULT</i> )	List of offsets in RA or X
<b>SEQ.OFFSET2.LIST</b>	no	( <i>NODEFAULT</i> )	List of offsets in DEC or Y
<b>SEQ.PFOV</b>		IF SF ( <i>SF</i> )	Pixel Field of View
<b>SEQ.RETURN</b>	no	F T ( <i>T</i> )	Return to Origin
<b>SEQ.TIME</b>	no	30..3600 ( <i>NODEFAULT</i> )	Total integration time (sec)
<b>TEL.CHOP.POSANG</b>	no	0..360 ( <i>0</i> )	Chopping Position Angle (deg)
<b>TEL.CHOP.THROW</b>	no	8..30 ( <i>8</i> )	Chopping Amplitude (arcsec)
<i>Fixed values:</i>			
Parameter	Hidden	Value	Label
<b>DET.READ.CURNAME</b>	yes	ROW_HG_SRR	Detector Readout Mode
<b>DPR.CATG</b>	no	SCIENCE	Data Prod. Categ.
<b>DPR.TECH</b>	no	IMAGE,RASTER	Data Prod. Tech.
<b>DPR.TYPE</b>	no	OBJECT	Data Prod. Type
<b>INS.MODE</b>	no	IMG	Instrument Mode
<b>INS.SOURCE</b>	no	SKY	Detector source
<b>SEQ.JITTER.WIDTH</b>	no	0	Random Jitter Width (arcsec)

VISIR_img_obs_SamAutoNod.tsf			
<i>To be specified:</i>			
Parameter	Hidden	Range (Default)	Label
<b>DET.CHOP.CYCSUM</b>	no	F T ( <i>F</i> )	Half-Cycle Averaging flag
<b>INS.FILT1.NAME</b>	no	10.5_SAM                      11.3_SAM ( <i>10.5_SAM</i> )	Filter + SAM
<b>SEQ.CATG</b>	no	PRE-IMAGE SCIENCE CALIB TEST ( <i>SCIENCE</i> )	Observation Category
<b>SEQ.CHOP.GUIDE</b>	yes	A B BOTH ( <i>BOTH</i> )	Chopping guide window
<b>SEQ.CHOP</b>	yes	F T ( <i>T</i> )	Chop flag
<b>SEQ.CHOPNOD.DIR</b>	no	PARALLEL    PERPENDICU- LAR ( <i>PARALLEL</i> )	Relative Chop/Nod Direction
<b>SEQ.JITTER.WIDTH</b>	no	0..10 ( <i>0</i> )	Random Jitter Width (arcsec)
<b>SEQ.NOD</b>	yes	F T ( <i>T</i> )	Nodding flag
<b>SEQ.NODNCYCLES</b>	no	1..100 ( <i>NODEFAULT</i> )	Number of nodding cycles.
<b>SEQ.PFOV</b>	yes	LF IF SF SP ( <i>SF</i> )	Pixel Field of View
<b>SEQ.RETURN</b>	no	F T ( <i>T</i> )	Return to Origin
<b>SEQ.TIME</b>	no	60..3600 ( <i>NODEFAULT</i> )	Total integration time (sec)
<b>TEL.CHOP.POSANG</b>	no	0..360 ( <i>0</i> )	Chopping Position Angle (deg)
<b>TEL.CHOP.THROW</b>	no	8..30 ( <i>8</i> )	Chopping Amplitude (arcsec)
<i>Fixed values:</i>			
Parameter	Hidden	Value	Label
<b>DET.READ.CURNAME</b>	yes	ROW_HG_SRR	Detector Readout Mode
<b>DPR.CATG</b>	no	SCIENCE	Data Prod. Categ.
<b>DPR.TECH</b>	no	SAM	Data Prod. Tech.
<b>DPR.TYPE</b>	no	OBJECT	Data Prod. Type
<b>INS.MODE</b>	no	IMG	Instrument Mode
<b>INS.OPTI1.NAME</b>	no	IMAGING	Imager diaph
<b>INS.OPTI2.NAME</b>	no	TMA_SF	Imager tma
<b>INS.SOURCE</b>	no	SKY	Detector source

<b>VISIR_spec_obs_HRAutoChopNod.tsf</b>			
<i>To be specified:</i>			
Parameter	Hidden	Range (Default)	Label
<b>INS.FILT2.NAME</b>	no	NEIL2 H2S.1 H2S.4 ( <i>NEIL2</i> )	Spectrometer Filter
<b>INS.GRAT1.WLEN</b>	no	7.5..28.0 ( <i>NODEFAULT</i> )	Spectrometer Wavelength (microns)
<b>SEQ.CATG</b>	no	SCIENCE CALIB TEST ( <i>SCIENCE</i> )	Observation Category
<b>SEQ.CHOP.GUIDE</b>	yes	A B BOTH ( <i>BOTH</i> )	Chopping guide window
<b>SEQ.CHOP</b>	yes	F T ( <i>T</i> )	Chop flag
<b>SEQ.CHOPNOD.DIR</b>	no	PARALLEL PERPENDICULAR ( <i>PARALLEL</i> )	Relative Chop/Nod Direction
<b>SEQ.JITTER.WIDTH</b>	no	0..10 ( <i>0</i> )	Random Jitter Width (arcsec)
<b>SEQ.NOD</b>	yes	F T ( <i>T</i> )	Nodding flag
<b>SEQ.NODNCYCLES</b>	no	1..100 ( <i>NODEFAULT</i> )	Number of nodding cycles.
<b>SEQ.RETURN</b>	no	F T ( <i>T</i> )	Return to Origin
<b>SEQ.TIME</b>	no	180..3600 ( <i>NODEFAULT</i> )	Total integration time (sec)
<b>TEL.CHOP.POSANG</b>	no	0..360 ( <i>0</i> )	Chopping Position Angle (deg)
<b>TEL.CHOP.THROW</b>	no	8..30 ( <i>8</i> )	Chopping Amplitude (arcsec)
<i>Fixed values:</i>			
Parameter	Hidden	Value	Label
<b>DET.CHOP.CYCSUM</b>	no	F	Half-Cycle Averaging flag
<b>DET.READ.CURNAME</b>	yes	ROW_HG_CDS	Detector Readout Mode
<b>DPR.CATG</b>	no	SCIENCE	Data Prod. Categ.
<b>DPR.TECH</b>	no	SPECTRUM	Data Prod. Tech.
<b>DPR.TYPE</b>	no	OBJECT	Data Prod. Type
<b>INS.MODE</b>	no	SPC	Instrument Mode
<b>INS.RESOL</b>	no	HRS	Spectrometer Resolution
<b>INS.SOURCE</b>	no	SKY	Detector source

VISIR_spec_obs_HRXAutoChopNod.tsf			
<i>To be specified:</i>			
Parameter	Hidden	Range (Default)	Label
<b>INS.GRAT1.WLEN</b>	no	7.5..28.0 ( <i>NODEFAULT</i> )	Spectrometer Wavelength (microns)
<b>SEQ.CATG</b>	no	SCIENCE CALIB TEST ( <i>SCIENCE</i> )	Observation Category
<b>SEQ.CHOP.GUIDE</b>	yes	A B BOTH ( <i>BOTH</i> )	Chopping guide window
<b>SEQ.CHOP</b>	yes	F T ( <i>T</i> )	Chop flag
<b>SEQ.CHOPNOD.DIR</b>	no	PARALLEL PERPENDICULAR ( <i>PARALLEL</i> )	Relative Chop/Nod Direction
<b>SEQ.JITTER.WIDTH</b>	no	0..10 ( <i>0</i> )	Random Jitter Width (arcsec)
<b>SEQ.NOD</b>	yes	F T ( <i>T</i> )	Nodding flag
<b>SEQ.NODNCYCLES</b>	no	1..100 ( <i>NODEFAULT</i> )	Number of nodding cycles.
<b>SEQ.RETURN</b>	no	F T ( <i>T</i> )	Return to Origin
<b>SEQ.TIME</b>	no	180..3600 ( <i>NODEFAULT</i> )	Total integration time (sec)
<b>TEL.CHOP.POSANG</b>	no	0..360 ( <i>0</i> )	Chopping Position Angle (deg)
<b>TEL.CHOP.THROW</b>	no	8..30 ( <i>8</i> )	Chopping Amplitude (arcsec)
<i>Fixed values:</i>			
Parameter	Hidden	Value	Label
<b>DET.CHOP.CYCSUM</b>	no	F	Half-Cycle Averaging flag
<b>DET.READ.CURNAME</b>	yes	ROW_HG_CDS	Detector Readout Mode
<b>DPR.CATG</b>	no	SCIENCE	Data Prod. Categ.
<b>DPR.TECH</b>	no	ECHELLE	Data Prod. Tech.
<b>DPR.TYPE</b>	no	OBJECT	Data Prod. Type
<b>INS.MODE</b>	no	SPC	Instrument Mode
<b>INS.RESOL</b>	no	HRX	Spectrometer Resolution
<b>INS.SOURCE</b>	no	SKY	Detector source

VISIR_spec_obs_LRAutoChopNod.tsf			
<i>To be specified:</i>			
Parameter	Hidden	Range (Default)	Label
<b>DET.CHOP.CYCSUM</b>	no	F T ( <i>T</i> )	Half-Cycle Averaging flag
<b>SEQ.CATG</b>	no	SCIENCE CALIB TEST ( <i>SCIENCE</i> )	Observation Category
<b>SEQ.CHOP.GUIDE</b>	yes	A B BOTH ( <i>BOTH</i> )	Chopping guide window
<b>SEQ.CHOP</b>	yes	F T ( <i>T</i> )	Chop flag
<b>SEQ.CHOPNOD.DIR</b>	no	PARALLEL PERPENDICULAR ( <i>PARALLEL</i> )	Relative Chop/Nod Direction
<b>SEQ.JITTER.WIDTH</b>	no	0..10 ( <i>0</i> )	Random Jitter Width (arcsec)
<b>SEQ.NOD</b>	yes	F T ( <i>T</i> )	Nodding flag
<b>SEQ.NODNCYCLES</b>	no	1..100 ( <i>NODEFAULT</i> )	Number of nodding cycles.
<b>SEQ.RETURN</b>	no	F T ( <i>T</i> )	Return to Origin
<b>SEQ.TIME</b>	no	180..3600 ( <i>NODEFAULT</i> )	Total integration time (sec)
<b>TEL.CHOP.POSANG</b>	no	0..360 ( <i>0</i> )	Chopping Position Angle (deg)
<b>TEL.CHOP.THROW</b>	no	8..30 ( <i>8</i> )	Chopping Amplitude (arcsec)
<i>Fixed values:</i>			
Parameter	Hidden	Value	Label
<b>DET.READ.CURNAME</b>	yes	ROW_HG_SRR	Detector Readout Mode
<b>DPR.CATG</b>	no	SCIENCE	Data Prod. Categ.
<b>DPR.TECH</b>	no	SPECTRUM	Data Prod. Tech.
<b>DPR.TYPE</b>	no	OBJECT	Data Prod. Type
<b>INS.FILT2.NAME</b>	no	OPEN	Spectrometer Filter
<b>INS.MODE</b>	no	SPC	Instrument Mode
<b>INS.RESOL</b>	no	LRP	Spectrometer Resolution
<b>INS.SOURCE</b>	no	SKY	Detector source

VISIR_img_cal_AutoChopNod.tsf			
<i>To be specified:</i>			
Parameter	Hidden	Range (Default)	Label
<b>DET.CHOP.CYCSUM</b>	no	F T ( <i>T</i> )	Half-Cycle Averaging flag
<b>INS.FILT1.NAME</b>	no	PAH1 ARIII SIV_1 SIV SIV_2 PAH2 PAH2_2 K-BAND M- BAND NEIL1 NEII NEII_2 Q1 Q2 Q3 B10.7 B11.7 B12.4 J7.9 J8.9 J9.8 J12.2 ( <i>NODEFAULT</i> )	Imager Filter
<b>SEQ.CATG</b>	no	PRE-IMAGE SCIENCE CALIB TEST ( <i>CALIB</i> )	Observation Category
<b>SEQ.CHOP.GUIDE</b>	yes	A B BOTH ( <i>BOTH</i> )	Chopping guide window
<b>SEQ.CHOP</b>	yes	F T ( <i>T</i> )	Chop flag
<b>SEQ.CHOPNOD.DIR</b>	no	PARALLEL PERPENDICU- LAR ( <i>PERPENDICULAR</i> )	Relative Chop/Nod Direction
<b>SEQ.JITTER.WIDTH</b>	no	0..10 ( <i>0</i> )	Random Jitter Width (arcsec)
<b>SEQ.NOD</b>	yes	F T ( <i>T</i> )	Nodding flag
<b>SEQ.NODNCYCLES</b>	no	1..100 ( <i>NODEFAULT</i> )	Number of nodding cycles.
<b>SEQ.PFOV</b>		IF SF ( <i>SF</i> )	Pixel Field of View
<b>SEQ.RETURN</b>	no	F T ( <i>T</i> )	Return to Origin
<b>SEQ.TIME</b>	no	60..3600 ( <i>NODEFAULT</i> )	Total integration time (sec)
<b>TEL.CHOP.POSANG</b>	no	0..360 ( <i>0</i> )	Chopping Position Angle (deg)
<b>TEL.CHOP.THROW</b>	no	8..30 ( <i>8</i> )	Chopping Amplitude (arcsec)
<i>Fixed values:</i>			
Parameter	Hidden	Value	Label
<b>DET.READ.CURNAME</b>	yes	ROW_HG_SRR	Detector Readout Mode
<b>DPR.CATG</b>	no	CALIB	Data Prod. Categ.
<b>DPR.TECH</b>	no	IMAGE	Data Prod. Tech.
<b>DPR.TYPE</b>	no	STD	Data Prod. Type
<b>INS.MODE</b>	no	IMG	Instrument Mode
<b>INS.SOURCE</b>	no	SKY	Detector source



VISIR_img_cal_BurstAutoChopNod.tsf			
<i>To be specified:</i>			
Parameter	Hidden	Range (Default)	Label
<b>DET.CHOP.CYCSUM</b>	yes	F T ( <i>T</i> )	Half-Cycle Averaging flag
<b>INS.FILT1.NAME</b>	no	PAH1 ARIII SIV_1 SIV SIV_2 PAH2 PAH2.2 K-BAND M- BAND NEII_1 NEII NEII.2 Q1 Q2 Q3 B10.7 B11.7 B12.4 J7.9 J8.9 J9.8 J12.2 ( <i>NODEFAULT</i> )	Imager Filter
<b>SEQ.CATG</b>	no	PRE-IMAGE SCIENCE CALIB TEST ( <i>CALIB</i> )	Observation Category
<b>SEQ.CHOP.GUIDE</b>	yes	A B BOTH ( <i>BOTH</i> )	Chopping guide window
<b>SEQ.CHOP</b>	yes	F T ( <i>T</i> )	Chop flag
<b>SEQ.CHOPNOD.DIR</b>	no	PARALLEL PERPENDICU- LAR ( <i>PERPENDICULAR</i> )	Relative Chop/Nod Direction
<b>SEQ.JITTER.WIDTH</b>	no	0..10 ( <i>0</i> )	Random Jitter Width (arcsec)
<b>SEQ.NAVRG</b>	no	1..4 ( <i>1</i> )	Number of frames to be averaged
<b>SEQ.NOD</b>	yes	F T ( <i>T</i> )	Nodding flag
<b>SEQ.NODNCYCLES</b>	no	1..100 ( <i>NODEFAULT</i> )	Number of nodding cycles.
<b>SEQ.PFOV</b>		IF SF ( <i>SF</i> )	Pixel Field of View
<b>SEQ.TIME</b>	no	30..1200 ( <i>360</i> )	Total integration time (sec)
<b>SEQ.WIN.NX</b>	no	0.0..1024.0 ( <i>1024.0</i> )	Read-out window NX
<b>SEQ.WIN.NY</b>	no	0.0..1024.0 ( <i>900.0</i> )	Read-out window NY
<b>SEQ.WIN.STARTX</b>	no	1.0..1023.0 ( <i>1.0</i> )	Read-out window start-x
<b>TEL.CHOP.POSANG</b>	no	0..360 ( <i>0</i> )	Chopping Position Angle (deg)
<b>TEL.CHOP.THROW</b>	no	8..30 ( <i>8</i> )	Chopping Amplitude (arcsec)
<i>Fixed values:</i>			
Parameter	Hidden	Value	Label
<b>DET.READ.CURNAME</b>	yes	ROW_HG_SRR_BURST	Detector Readout Mode
<b>DPR.CATG</b>	no	CALIB	Data Prod. Categ.
<b>DPR.TECH</b>	no	IMAGE,BURST	Data Prod. Tech.
<b>DPR.TYPE</b>	no	STD	Data Prod. Type
<b>INS.MODE</b>	no	IMG	Instrument Mode
<b>INS.SOURCE</b>	no	SKY	Detector source
<b>SEQ.RETURN</b>	no	T	Return to Origin

VISIR_img_cal_CoroChopNod.tsf			
<i>To be specified:</i>			
Parameter	Hidden	Range (Default)	Label
<b>DET.CHOP.CYCSUM</b>	no	F T ( <i>F</i> )	Half-Cycle Averaging flag
<b>INS.FILT1.NAME</b>	no	10.5_4QP 11.3_4QP 12.3_AGP 12.4_AGP ( <i>12_3_AGP</i> )	Imager Filter
<b>INS.OPT11.NAME</b>	no	AGPM 4QPM_1 4QPM_2 ( <i>AGPM</i> )	Imager diaph
<b>SEQ.CATG</b>	no	PRE-IMAGE SCIENCE CALIB TEST ( <i>CALIB</i> )	Observation Category
<b>SEQ.CHOP.GUIDE</b>	yes	A B BOTH ( <i>BOTH</i> )	Chopping guide window
<b>SEQ.CHOP</b>	yes	F T ( <i>T</i> )	Chop flag
<b>SEQ.NOD</b>	yes	F T ( <i>T</i> )	Nodding flag
<b>SEQ.NODNCYCLES</b>	no	1..100 ( <i>NODEFAULT</i> )	Number of nodding cycles.
<b>SEQ.PFOV</b>	yes	LF IF SF SP ( <i>SF</i> )	Pixel Field of View
<b>SEQ.RETURN</b>	no	F T ( <i>T</i> )	Return to Origin
<b>SEQ.TIME</b>	no	60..3600 ( <i>NODEFAULT</i> )	Total integration time (sec)
<b>TEL.CHOP.POSANG</b>	no	0..360 ( <i>0</i> )	Chopping Position Angle (deg)
<b>TEL.CHOP.THROW</b>	no	8..30 ( <i>8</i> )	Chopping Amplitude (arcsec)
<i>Fixed values:</i>			
Parameter	Hidden	Value	Label
<b>DET.READ.CURNAME</b>	yes	ROW_HG_SRR	Detector Readout Mode
<b>DPR.CATG</b>	no	CALIB	Data Prod. Categ.
<b>DPR.TECH</b>	no	CORONOGRAPHY	Data Prod. Tech.
<b>DPR.TYPE</b>	no	STD	Data Prod. Type
<b>INS.MODE</b>	no	IMG	Instrument Mode
<b>INS.SOURCE</b>	no	SKY	Detector source
<b>SEQ.CHOPNOD.DIR</b>	no	PARALLEL	Relative Chop/Nod Direction
<b>SEQ.JITTER.WIDTH</b>	no	0	Random Jitter Width (arcsec)

VISIR_img_cal_SamAutoNod.tsf			
<i>To be specified:</i>			
Parameter	Hidden	Range (Default)	Label
<b>DET.CHOP.CYCSUM</b>	no	F T ( <i>F</i> )	Half-Cycle Averaging flag
<b>INS.FILT1.NAME</b>	no	10.5_SAM            11.3_SAM ( <i>10.5_SAM</i> )	Filter + SAM
<b>SEQ.CATG</b>	no	PRE-IMAGE SCIENCE CALIB TEST ( <i>CALIB</i> )	Observation Category
<b>SEQ.CHOP.GUIDE</b>	yes	A B BOTH ( <i>BOTH</i> )	Chopping guide window
<b>SEQ.CHOP</b>	yes	F T ( <i>T</i> )	Chop flag
<b>SEQ.CHOPNOD.DIR</b>	no	PARALLEL    PERPENDICU- LAR ( <i>PARALLEL</i> )	Relative Chop/Nod Direction
<b>SEQ.JITTER.WIDTH</b>	no	0..10 ( <i>0</i> )	Random Jitter Width (arcsec)
<b>SEQ.NOD</b>	yes	F T ( <i>T</i> )	Nodding flag
<b>SEQ.NODNCYCLES</b>	no	1..100 ( <i>NODEFAULT</i> )	Number of nodding cycles.
<b>SEQ.PFOV</b>	yes	LF IF SF SP ( <i>SF</i> )	Pixel Field of View
<b>SEQ.RETURN</b>	no	F T ( <i>T</i> )	Return to Origin
<b>SEQ.TIME</b>	no	60..3600 ( <i>NODEFAULT</i> )	Total integration time (sec)
<b>TEL.CHOP.POSANG</b>	no	0..360 ( <i>0</i> )	Chopping Position Angle (deg)
<b>TEL.CHOP.THROW</b>	no	8..30 ( <i>8</i> )	Chopping Amplitude (arcsec)
<i>Fixed values:</i>			
Parameter	Hidden	Value	Label
<b>DET.READ.CURNAME</b>	yes	ROW_HG_SRR	Detector Readout Mode
<b>DPR.CATG</b>	no	CALIB	Data Prod. Categ.
<b>DPR.TECH</b>	no	SAM	Data Prod. Tech.
<b>DPR.TYPE</b>	no	STD	Data Prod. Type
<b>INS.MODE</b>	no	IMG	Instrument Mode
<b>INS.OPTI1.NAME</b>	no	IMAGING	Imager diaph
<b>INS.OPTI2.NAME</b>	no	TMA_SF	Imager tma
<b>INS.SOURCE</b>	no	SKY	Detector source

VISIR_spec_cal_HRAutoChopNod.tsf			
<i>To be specified:</i>			
Parameter	Hidden	Range (Default)	Label
<b>INS.FILT2.NAME</b>	no	NEII.2 H2S.1 H2S.4 ( <i>NEII.2</i> )	Spectrometer Filter
<b>INS.GRAT1.WLEN</b>	no	7.5..28.0 ( <i>NODEFAULT</i> )	Spectrometer Wavelength (microns)
<b>SEQ.CATG</b>	no	SCIENCE CALIB TEST ( <i>CALIB</i> )	Observation Category
<b>SEQ.CHOP.GUIDE</b>	yes	A B BOTH ( <i>BOTH</i> )	Chopping guide window
<b>SEQ.CHOP</b>	yes	F T ( <i>T</i> )	Chop flag
<b>SEQ.CHOPNOD.DIR</b>	no	PARALLEL PERPENDICULAR ( <i>PARALLEL</i> )	Relative Chop/Nod Direction
<b>SEQ.JITTER.WIDTH</b>	no	0..10 ( <i>0</i> )	Random Jitter Width (arcsec)
<b>SEQ.NOD</b>	yes	F T ( <i>T</i> )	Nodding flag
<b>SEQ.NODNCYCLES</b>	no	1..100 ( <i>NODEFAULT</i> )	Number of nodding cycles.
<b>SEQ.RETURN</b>	no	F T ( <i>T</i> )	Return to Origin
<b>SEQ.TIME</b>	no	30..3600 ( <i>NODEFAULT</i> )	Total integration time (sec)
<b>TEL.CHOP.POSANG</b>	no	0..360 ( <i>0</i> )	Chopping Position Angle (deg)
<b>TEL.CHOP.THROW</b>	no	8..30 ( <i>8</i> )	Chopping Amplitude (arcsec)
<i>Fixed values:</i>			
Parameter	Hidden	Value	Label
<b>DET.CHOP.CYCSUM</b>	no	F	Half-Cycle Averaging flag
<b>DET.READ.CURNAME</b>	yes	ROW_HG_CDS	Detector Readout Mode
<b>DPR.CATG</b>	no	CALIB	Data Prod. Categ.
<b>DPR.TECH</b>	no	SPECTRUM	Data Prod. Tech.
<b>DPR.TYPE</b>	no	STD	Data Prod. Type
<b>INS.MODE</b>	no	SPC	Instrument Mode
<b>INS.RESOL</b>	no	HRS	Spectrometer Resolution
<b>INS.SOURCE</b>	no	SKY	Detector source

VISIR_spec_cal_HRXAutoChopNod.tsf			
<i>To be specified:</i>			
Parameter	Hidden	Range (Default)	Label
<b>INS.GRAT1.WLEN</b>	no	7.5..28.0 ( <i>NODEFAULT</i> )	Spectrometer Wavelength (microns)
<b>SEQ.CATG</b>	no	SCIENCE CALIB TEST ( <i>CALIB</i> )	Observation Category
<b>SEQ.CHOP.GUIDE</b>	yes	A B BOTH ( <i>BOTH</i> )	Chopping guide window
<b>SEQ.CHOP</b>	yes	F T ( <i>T</i> )	Chop flag
<b>SEQ.CHOPNOD.DIR</b>	no	PARALLEL PERPENDICULAR ( <i>PARALLEL</i> )	Relative Chop/Nod Direction
<b>SEQ.JITTER.WIDTH</b>	no	0..10 ( <i>0</i> )	Random Jitter Width (arcsec)
<b>SEQ.NOD</b>	yes	F T ( <i>T</i> )	Nodding flag
<b>SEQ.NODNCYCLES</b>	no	1..100 ( <i>NODEFAULT</i> )	Number of nodding cycles.
<b>SEQ.RETURN</b>	no	F T ( <i>T</i> )	Return to Origin
<b>SEQ.TIME</b>	no	30..3600 ( <i>NODEFAULT</i> )	Total integration time (sec)
<b>TEL.CHOP.POSANG</b>	no	0..360 ( <i>0</i> )	Chopping Position Angle (deg)
<b>TEL.CHOP.THROW</b>	no	8..30 ( <i>8</i> )	Chopping Amplitude (arcsec)
<i>Fixed values:</i>			
Parameter	Hidden	Value	Label
<b>DET.CHOP.CYCSUM</b>	no	F	Half-Cycle Averaging flag
<b>DET.READ.CURNAME</b>	yes	ROW_HG_CDS	Detector Readout Mode
<b>DPR.CATG</b>	no	CALIB	Data Prod. Categ.
<b>DPR.TECH</b>	no	ECHELLE	Data Prod. Tech.
<b>DPR.TYPE</b>	no	STD	Data Prod. Type
<b>INS.MODE</b>	no	SPC	Instrument Mode
<b>INS.RESOL</b>	no	HRX	Spectrometer Resolution
<b>INS.SOURCE</b>	no	SKY	Detector source

VISIR_spec_cal_LRAutoChopNod.tsf			
<i>To be specified:</i>			
Parameter	Hidden	Range (Default)	Label
<b>DET.CHOP.CYCSUM</b>	no	F T ( <i>T</i> )	Half-Cycle Averaging flag
<b>SEQ.CATG</b>	no	SCIENCE CALIB TEST ( <i>CALIB</i> )	Observation Category
<b>SEQ.CHOP.GUIDE</b>	yes	A B BOTH ( <i>BOTH</i> )	Chopping guide window
<b>SEQ.CHOP</b>	yes	F T ( <i>T</i> )	Chop flag
<b>SEQ.CHOPNOD.DIR</b>	no	PARALLEL PERPENDICU- LAR ( <i>PARALLEL</i> )	Relative Chop/Nod Direction
<b>SEQ.JITTER.WIDTH</b>	no	0..10 ( <i>0</i> )	Random Jitter Width (arcsec)
<b>SEQ.NOD</b>	yes	F T ( <i>T</i> )	Nodding flag
<b>SEQ.NODNCYCLES</b>	no	1..100 ( <i>NODEFAULT</i> )	Number of nodding cycles.
<b>SEQ.RETURN</b>	no	F T ( <i>T</i> )	Return to Origin
<b>SEQ.TIME</b>	no	30..3600 ( <i>NODEFAULT</i> )	Total integration time (sec)
<b>TEL.CHOP.POSANG</b>	no	0..360 ( <i>0</i> )	Chopping Position Angle (deg)
<b>TEL.CHOP.THROW</b>	no	8..30 ( <i>8</i> )	Chopping Amplitude (arcsec)
<i>Fixed values:</i>			
Parameter	Hidden	Value	Label
<b>DET.READ.CURNAME</b>	yes	ROW_HG_SRR	Detector Readout Mode
<b>DPR.CATG</b>	no	CALIB	Data Prod. Categ.
<b>DPR.TECH</b>	no	SPECTRUM	Data Prod. Tech.
<b>DPR.TYPE</b>	no	STD	Data Prod. Type
<b>INS.FILT2.NAME</b>	no	OPEN	Spectrometer Filter
<b>INS.MODE</b>	no	SPC	Instrument Mode
<b>INS.RESOL</b>	no	LRP	Spectrometer Resolution
<b>INS.SOURCE</b>	no	SKY	Detector source

## 9 Appendix: Filter transmission curves

The filter transmission has been measured using a Fourier Transform Spectrometer, at a temperature of 35 K for filters manufactured by the company READING. Their absolute transmission curves are displayed in Fig. 22. They are also available in digital form at <http://www.eso.org/sci/facilities/paranal/instruments/visir/inst.html>. The other filters, manufactured by OCLI, have been measured using the WCU and wavelength scans with the monochromator. Note that for these filters, the transmission curves are normalized to 1, see Fig. 19.

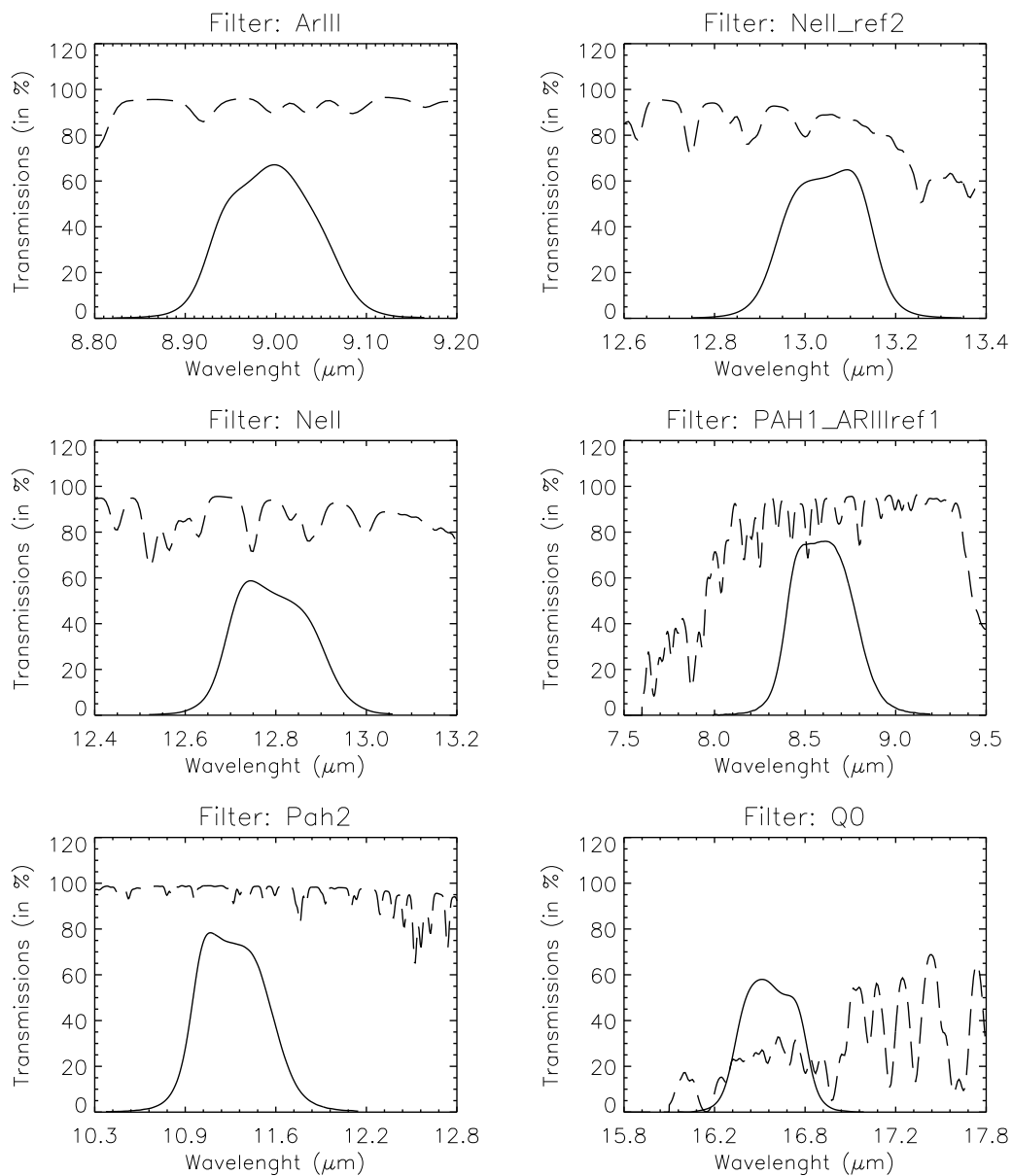


Figure 22: Transmission curves of VISIR imager filters, manufactured by READING. Overplotted (dashed) is the atmospheric transmission at low resolution. The absolute transmission values are given, expressed in percent.

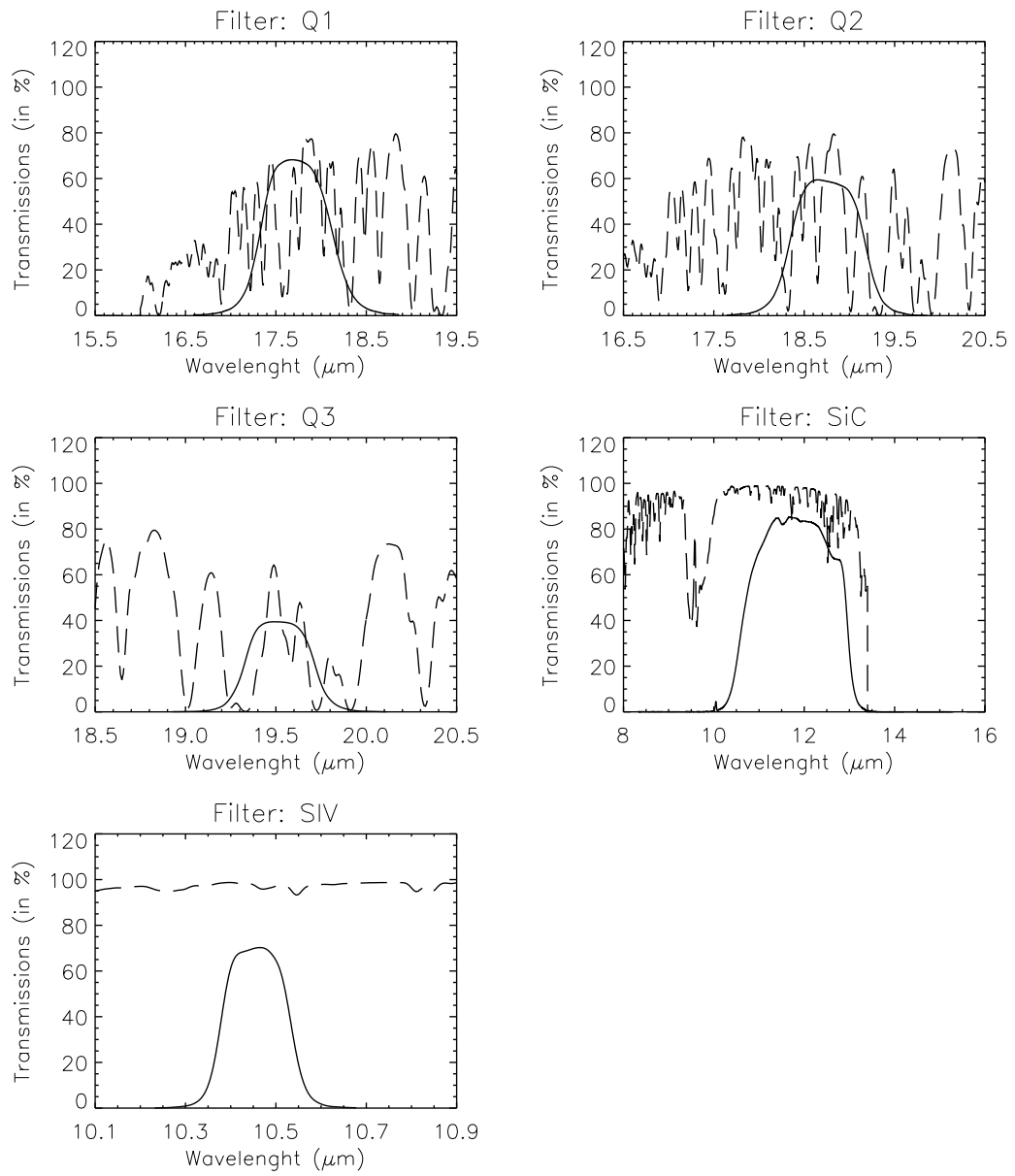


Figure 18: – continued.



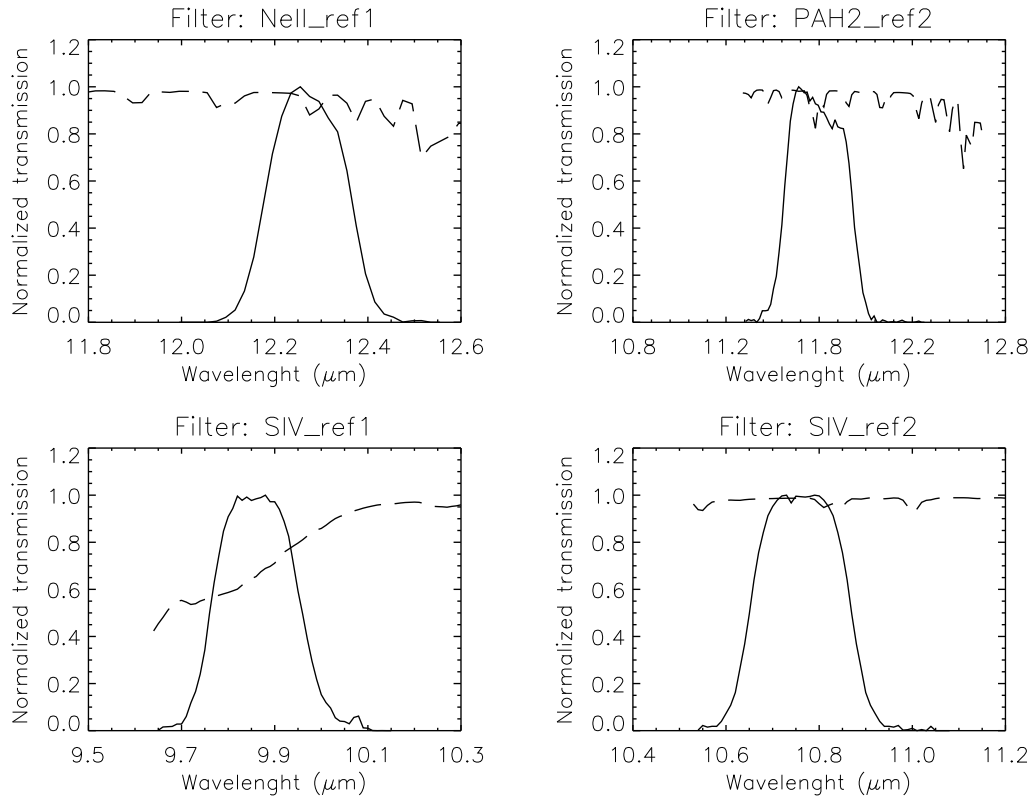


Figure 19: Transmission curves of VISIR imager filters, manufactured by OCLI. Overplotted (dashed) is the atmospheric transmission at low resolution. Only relative transmissions have been determined; their values are normalized so that their peak transmission is equal to 1.

## 10 Appendix: Sensitivities in various spectroscopic settings

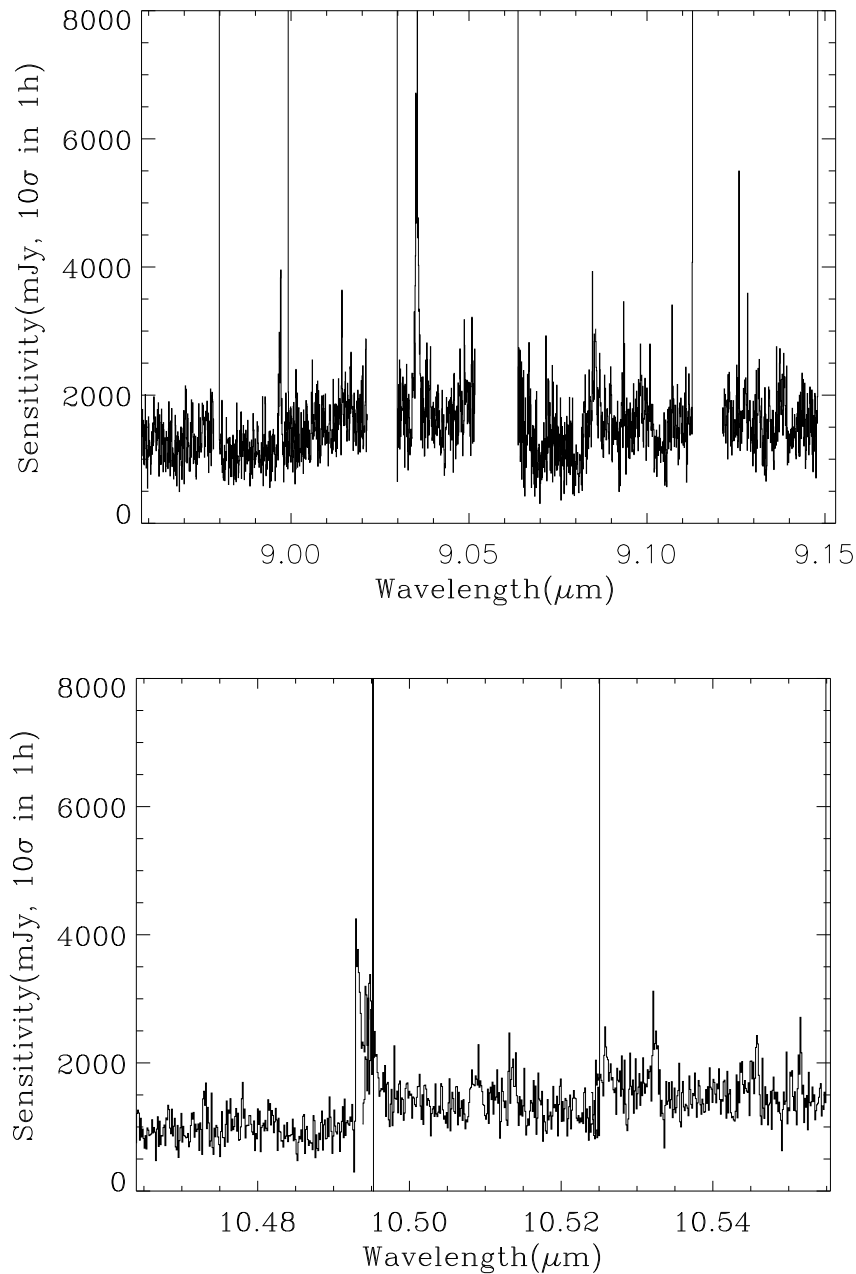


Figure 20: Observed sensitivity measured for the old DRS detector as a function of wavelength for high resolution mode (I). Offered sensitivity is typically a factor of 2 larger and still valid until new measurements are available.

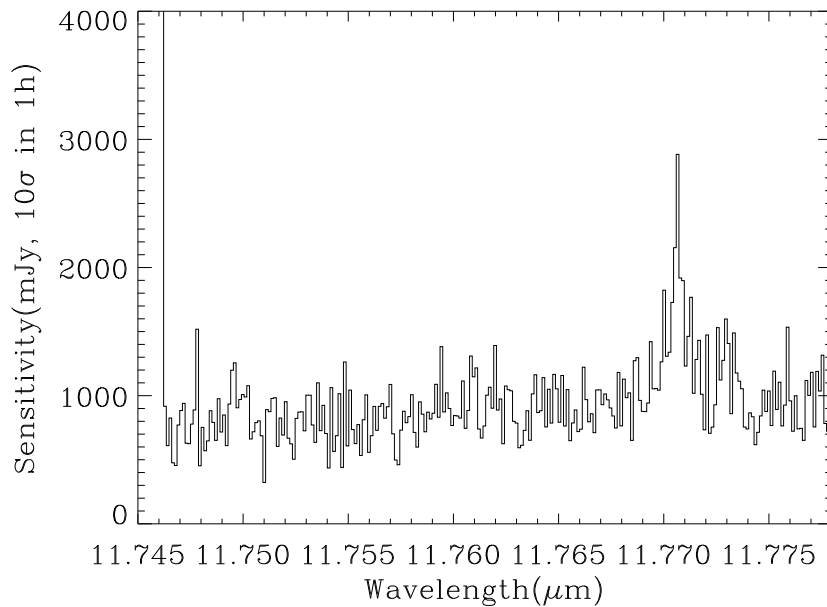
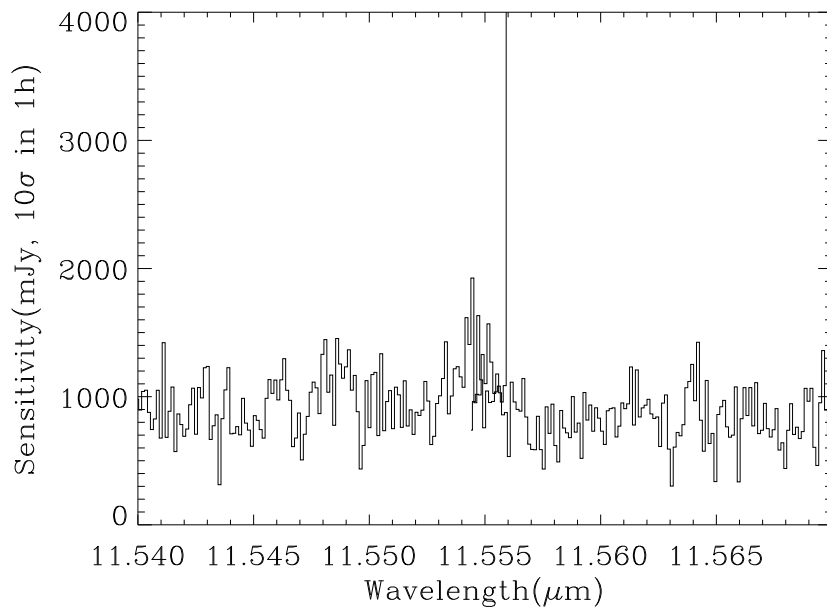


Figure 21: Observed sensitivity measured for the old DRS detector as a function of wavelength for high resolution mode (II). Offered sensitivity is typically a factor of 2 larger and still valid until new measurements are available.

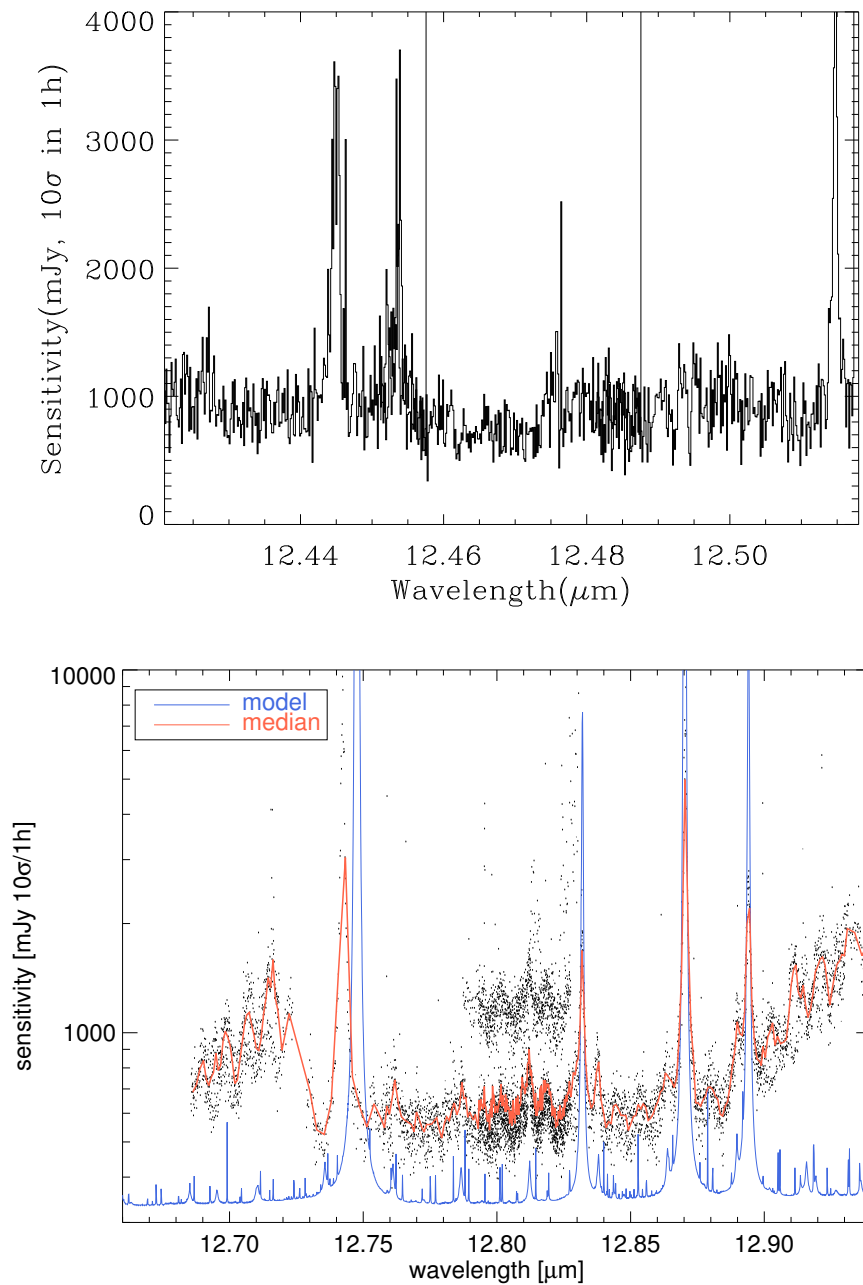


Figure 22: Observed sensitivity measured for the old DRS detector as a function of wavelength for high resolution mode (III). Offered sensitivity is typically a factor of 2 larger and still valid until new measurements are available. *Bottom:* Observed sensitivities obtained on various nights, compared with the theoretical model curves, corresponding to BLIP.

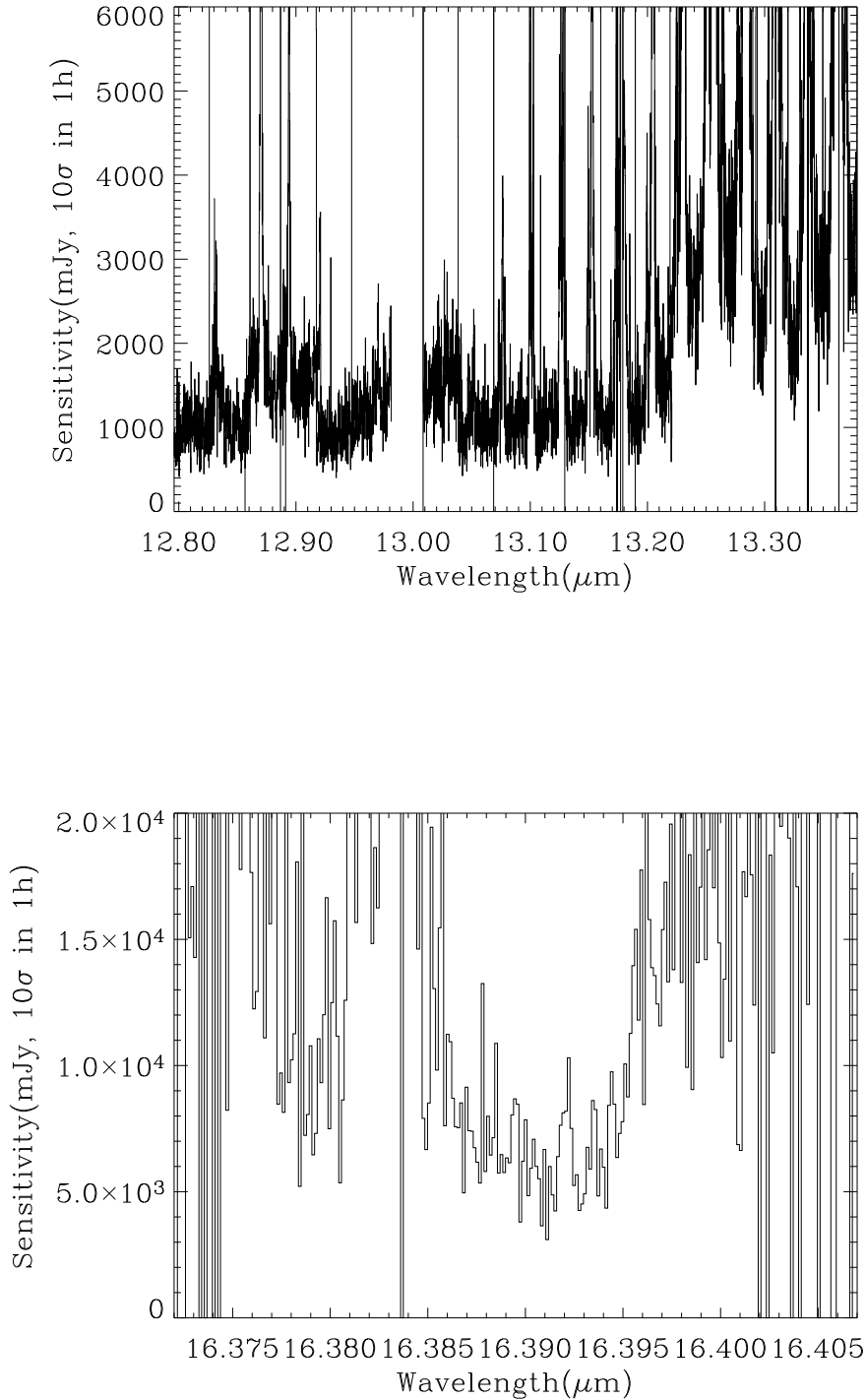


Figure 23: Observed sensitivity measured for the old DRS detector as a function of wavelength for high resolution mode (IV). Offered sensitivity is typically a factor of 2 larger and still valid until new measurements are available. *Top*: Sensitivities over an extended region encompassing the observed wavelength of [NeII] up to  $z \approx 0.038$ .

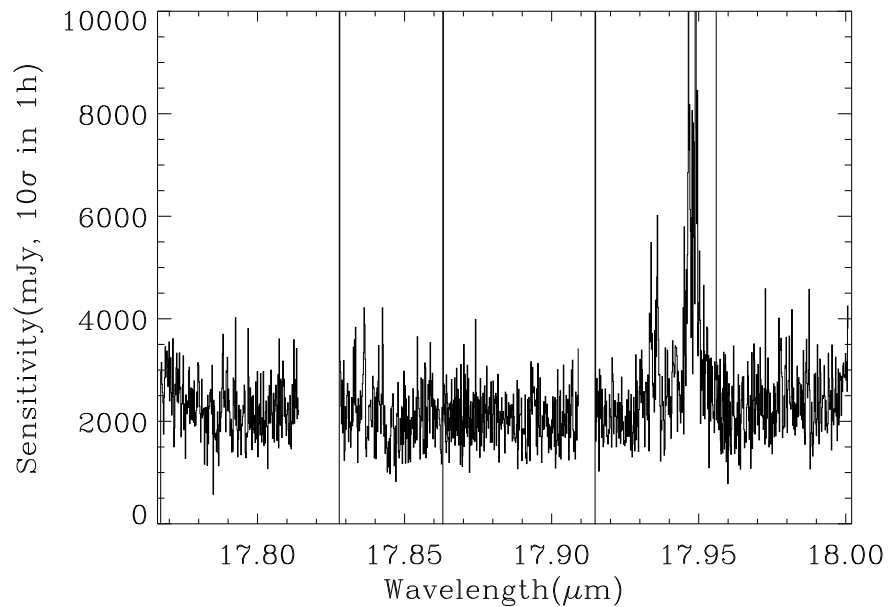
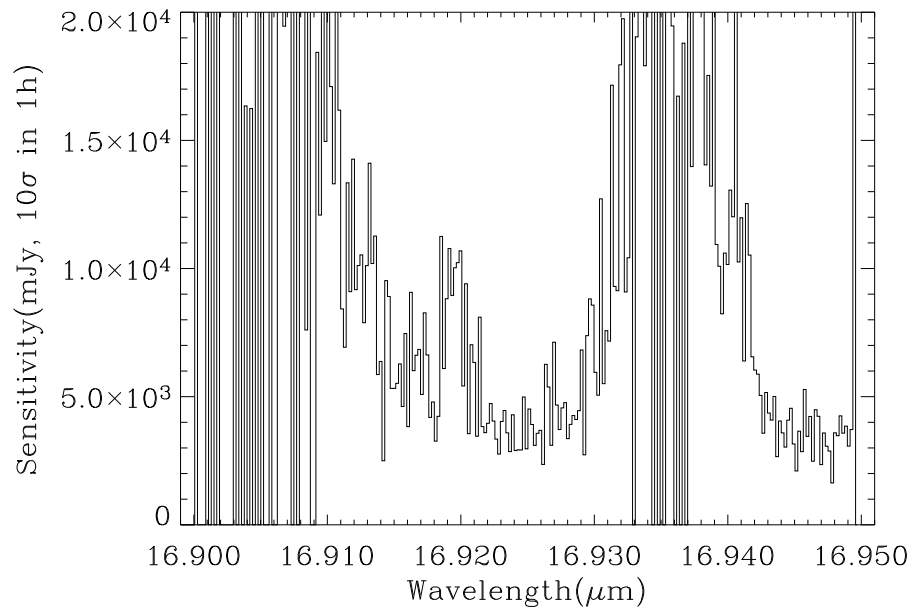


Figure 24: Observed sensitivity measured for the old DRS detector as a function of wavelength for high resolution mode (V). Offered sensitivity is typically a factor of 2 larger and still valid until new measurements are available.

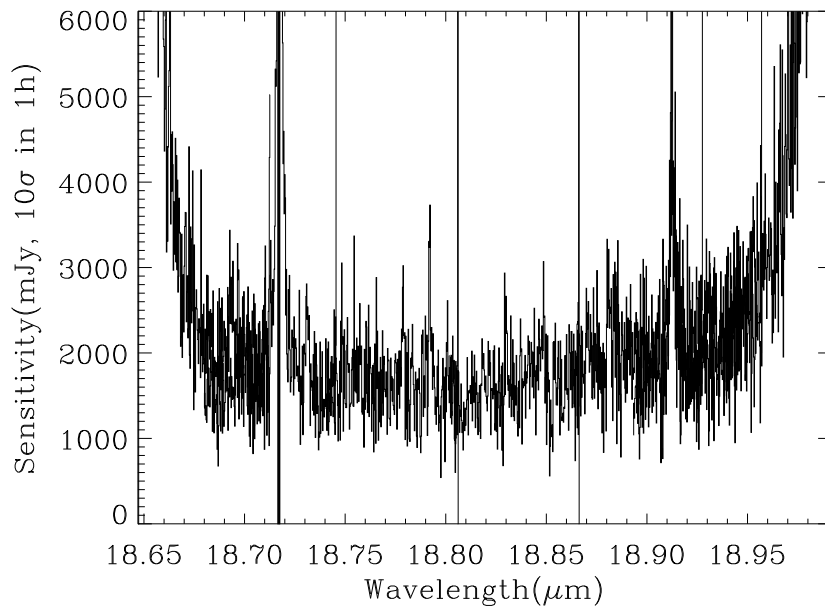
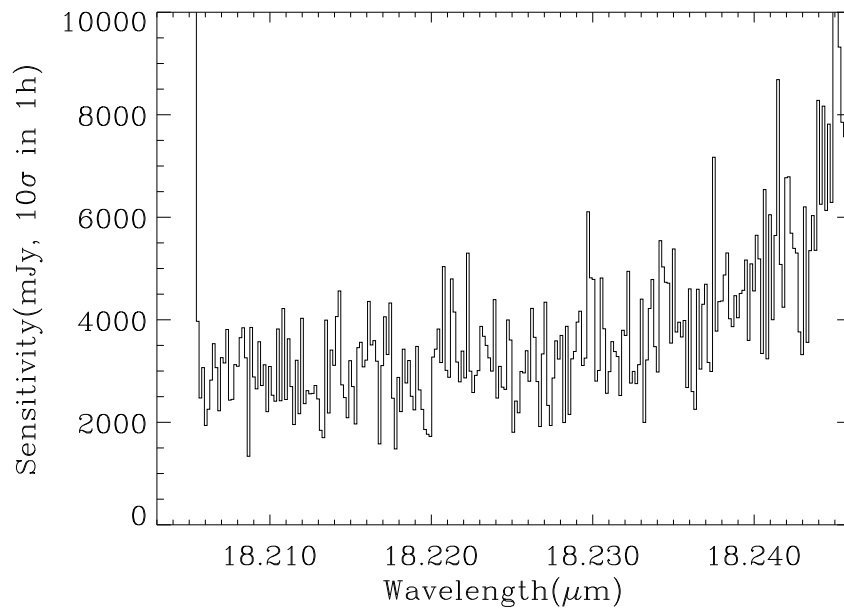


Figure 25: Observed sensitivity measured for the old DRS detector as a function of wavelength for high resolution mode (VI). Offered sensitivity is typically a factor of 2 larger and valid until new measurements are available.

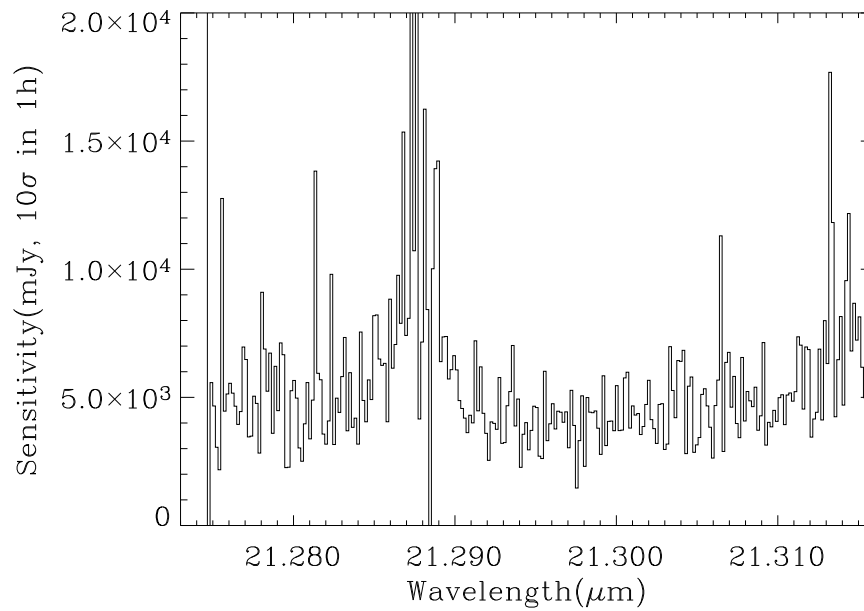


Figure 26: Observed sensitivity measured for the old DRS detector as a function of wavelength for high resolution mode (VII). Offered sensitivity is typically a factor of 2 larger and still valid until new measurements are available.